Superiority of ear skin for DNA immunization in mouse tumor models

Dissertation

Submitted to the Faculty of Biosciences

of The Ruprecht-Karls-Universität Heidelberg, Germany

for the Degree of

Doctor of Natural Sciences

Presented by

Jing Ni

Oral examination at September 17th 2008

This thesis was written in the Tumor Immunology of German Cancer Research Centre (DKFZ, Heidelberg, Germany) in the duration period of October 2005 to July 2008 under the supervision of Prof. Dr. Volker Schirrmacher.

1st Supervisor: Prof. Dr. Volker Schirrmacher, Tumor Immunology of German Cancer Research Centre (Division of Cellular Immunology)

2nd Supervisor: Prof. Dr. Michael Wink, Institute of Pharmacy and Molecular Biotechnology at the University of Heidelberg (Department of Biology)

I herewith declare that I wrote this PhD thesis independently under supervision and used no other sources and aids than those indicated

…… ……

Date **Signature**

For my little girl

Nicole

"Immunization ranks among the most important health advances of the 20th century. With the exception of safe drinking water, vaccinology has more effectively reduced mortality than any other modality."

"Extraordinary advances in biotechnology make DNA vaccines the most promising area of vaccinology."

James Mark Simmerman

http://findarticles.com/p/articles/mi_qa3958/is_200201/ai_n9053796/pg_1

"Tumor antigens are being rapidly revealed, and can be expressed on cell surface or more commonly, as peptides in association with the major histocompatibility complex class I (or II) molecules. DNA vaccines can be designed to activate antibody and /or T-cell responses, providing focused immune attack on selected antigens."

"DNA vaccines offer a precise but flexible strategy for delivering antigens to the immune system, and additional sequences encoding molecules to manipulate outcome can be included."

Jason Rice et al.

Nat Rev Cancer 2008, 8: 108-20

Table of Contents

Acknowledgements

I feel very lucky to work on this project. It is interesting and promising for DNA vaccine development. I would like to give my great gratitude to my supervisor, **Professor Volker Schirrmacher**. He gave me the chance to work on this project, led me step by step to get into it, and gave me a lot of support and encouragement. I learned from him not only how to do research, but also the attitude to science. He is a respectable scientist. I need to learn from him for my whole life.

I want to thank **Professor Michael Wink**, to be my second supervisor and to evaluate my thesis. I also thank **Dr. Philipp Beckhove** and **Dr. Martin Müller** for reading my thesis and to be the examiners for my oral examination.

Dr. Philippe Fournier introduced me to this project, and offered me a lot of help for experimental design and new information acquirement.

It is an unforgettable and precious period working in the Division **D010**. I want to thank first **Annette Anold**, our technician, who helped me a lot for DNA preparation, real-time PCR as well as other routine lab work. I very much appreciate also her friendship. I worked together with **Britta Nolte** on the electroporation part of this project. Without her, I could not have finished many big experiments with more than 15 groups and more than 120 mice. I am very lucky to have had her, a good friend, working together with me for those laborious experiments. I thank **Dr. Philipp Beckhove** for giving me suggestions for experimental design; **Andreas Griesbach** for the introduction of DNA intra-ear pinna injection; **Holger Wilden** for introduction of real-time PCR; **Christina Pfirschke** for introduction to the cryostat; **Mariana Bucur** for introduction of X-gal staining and preparation of cell lysates. I appreciate the help and cooperation from all members in **D010 and D011**. I will miss the coffee room and those impressive trips.

I specially thank my best friend, **Yingzi Ge,** for the introduction of FACS, ^{51}Cr release assay, and discussions about interesting topics.

I would also like to thank the following people in Tumor Immunology: **Professor Günter Hämmerling** for providing the CD11c-DTR-tg mice, the CMV-Ruc vector and the BAC clone RP24-78I2 vector; **Dr. Gerhard Moldenhauer** for providing the DA3-EpCAM cell line and anti-EpCAM antibodies; **Dr. Frank Momburg** for providing the human EpCAM gene; **Dr. Natalio Garbi** for introduction of the FACS CantoII system; **Dr. Dominik Djandji** and **Carmen Henrich** for introduction of the IVIS100 in vivo imaging system; **Dr. Adelheid Cerwenka** and **Ioanna Galani** for discussions of experiments and provision of RAG2$^{-/-}$ and RAG2$^{-/-}$IFNAR$^{-/-}$ mice.

I also thank the people who work in the **Animal Care Facilities**. I also give my great respect to those experimental **mice** that were sacrificed for scientific research.

I thank **Professor Kenneth L. Rock** (Department of Pathology, University of Massachusetts, USA) for providing the DC2.4 cell line.

This project has been performed partially within the frame of the project **MOLEDA** (acronym standing for Molecular Optimization of Laser / Electrotransfer DNA Administration into muscle and skin for gene therapy) sponsored by the European Commission during the research program FP6. We thank **Professor Daniel Scherman** (Institut National de la Santé et de la Recherche Médicale, Paris, France) for providing the CMV-luc vector.

I appreciate the **DAAD-Helmholtz scholarship** to support me for the 3-year study.

I had wonderful experiences to work in **DKFZ** because of the great scientific atmosphere and facilities. The cooperation between different divisions is very helpful.

It is a short time for me although I have been in Heidelberg for almost 3 years. Besides my interesting work, I also have some **good friends**. I give my gratitude to them for sharing great time with me. They are always the treasure in my heart. Especially, I thank Hong and Xin for the great friendship.

Last but not least, I want to give my deep appreciation and love to **my family**: my husband, **Yi**, for all his love, support, encouragement and good discussions for my project. It would have been hard for me to go through the tough part of the project without him; my mother-in-law, **Meiying**, who understands and supports me a lot for my study, and takes care of my daughter so that I could finish this PhD; my daughter, **Nicole**, brings me unimaginable hope and happiness; I ask **my parents** to forgive me for not seeing them for 3 years. My family is the most important part in my life.

Jing Ni
16 July, 2008

Contributions

The work including EP-improved antigen expression, humoral & cellular immune responses and prophylactic anti-tumor effect described in Part 4.4 was conducted together with **Britta Nolte** for her Master thesis.

Abstract

DNA vaccination can induce antibodies, helper T cell responses, CTL responses, and protective immunity in various animal models for infectious diseases and cancers. However, naked DNA immunization is still inefficient in large animals and human.

I demonstrate in this thesis: i) that the site of DNA vaccine application is important; ii) that a viral DNA sequence can augment anti-tumor effects; iii) that electroporation improves anti-tumor immunity; and iv) that dendritic cells are essential and sufficient for antigen presentation in ear pinna DNA immunization.

Intra-ear pinna (ie) DNA injection led to earlier and stronger antigen expression compared to intradermal injection at the flank skin (id). The ie site was superior to the id site also with regard to induction of humoral and cellular immune responses.

To improve the anti-tumor effect of the DNA vaccines, an immunostimulating sequence coding for hemagglutinin-neuraminidase (HN) of Newcastle disease virus (NDV) was introduced as an adjuvant. HN expression in cells was demonstrated to induce IFN-α production, lymphocyte binding activity as well as anti-tumor activity. By combining this adjuvant with ie TAA (tumor associated antigen) DNA immunization, prophylactic and therapeutic anti-tumor immunity was improved in mouse tumor models. The tumor lines expressed either a surrogate tumor antigen beta-galactosidase (β-gal), or a TAA, human epithelial cell adhesion molecule (EpCAM). Improvements of the anti-tumor activity might be due to the observed increase of Th1 responses, anti-tumor CTL activity and innate immune reactivity, as well as due to down-regulated suppressive factors such as TGF-β and level of myeloid derived suppressor cells (MDSCs).

To further improve the ie DNA immunization strategy, it was combined with electroporation (EP). Such DNA EP led to clear-cut improvements of humoral and cellular immune responses when applied ie. The effects in the ear pinna were superior to id DNA EP. In both prophylactic (β-gal as a TAA) and therapeutic (human EpCAM as a TAA) tumor models, DNA EP was demonstrated to increase anti-tumor activity significantly compared to DNA immunization without EP.

I was able to identify a short DC-specific CD11c promoter sequence of 700-bp. Upon introduction into the DNA vaccine, such vector was found to induce similar anti-tumor immunity as a DNA vector driven by the CMV promoter although the latter led to much stronger antigen expression. This observation suggests that DCs are sufficient for antigen presentation of ear pinna DNA immunization.

Thus, DNA vaccines encoding xenogeneic TAAs were particularly effective when applied to the ear pinna and induced protective and therapeutic anti-tumor immunity in mouse tumor models. The combination with HN as an adjuvant or with electroporation further augmented the anti-tumor effects. Studies on the mechanisms revealed that DCs in the ear pinna are essential for the immunization effect.

Zusammenfassung

Ziel der Arbeit war es, herauszufinden wie man eine DNS Vakzine, die für ein Tumorantigen kodiert, so optimieren kann, dass sie in Maus Tumormodellen zu einer protektiven anti-Tumor Immunantwort führt. Es konnten mehrere wichtige Parameter herausgearbeitet werden, die für eine effektive Immunantwort entscheidend sind: 1. Die Injektionsstelle der Vakzine. Die Haut der Ohrmuschel stellte sich als optimal heraus und war anderen Injektionsorten überlegen. 2. Durch Einführung einer viralen Nukleotidsequence in den DNS Vektor ließ sich die Immunogenität der anti-tumoralen Vakzine weiter steigern. 3. Durch zusätzliche Elektroporation der Injektionsstelle ließ sich eine weitere Steigerung des Immunisierungseffektes erreichen. 4. Was den Mechanismus der Ohrmuschelhaut-Immunisierung betrifft, so konnte gezeigt werden, dass hierfür Dendritische Zellen entscheidend wichtig sind.

Immunisierungen in der Ohrmuschel (ie) der Maus führten zu einer früheren und stärkeren Antigenexpression im Vergleich zur intradermalen (id) Inokulation in der Flanke. ie Immunisierungen führten im Vergleich zu id Immunisierungen auch zu einer stärkeren humoralen und zellulären spezifischen Immunantwort.

Die virale Nukleotidsequence, die einen zusätzlichen Adjuvans Effekt ausübte kodierte für Hämagglutinin-Neuraminidase (HN) Protein des Newcastle-Disease Virus. HN Expression in transfizierten Zellen regte die Produktion von Interferon alpha in anderen Zellen an, und führte zu einer verbesserten Bindung von Lymphozyten. Durch Kombination von HN und Tumorantigen konnte bei ie Immunisierungen in Maus Tumormodellen sowohl in einem prophylaktischen wie auch in einem therapeutischen Immunisierungsprotokoll durch DNS Immunisierung protektive anti-Tumor Immunität erzeugt werden. Die transfizierten Tumorlinien exprimierten wie die DNS Vektoren entweder bakterielle ß-Galaktosidase als Surrogat Tumorantigen oder humanes EpCAM als natürliches Tumorantigen. Die optimierten Immunisierungsprotokolle führten zu erhöhten Th1 und zytotoxischen T Zell Antworten , sowie erhöhter natürlicher Immunität und verminderter suppressiver Faktoren with TGF-ß und Level von MDSC Zellen.

Durch Elektroporation konnte der DNS Immunisierungseffekt ie weiter gesteigert werden. Das drückte sich auch in einer Verbesserung des anti-tumoralen Effektes aus.

Es konnte gezeigt werden, dass selektive Expression des Vektor vermittelten Tumorantigens in Dendritischen Zellen (DZ) mit Hilfe eines DZ-spezifischen Promoters (CD11c, eine neue 700 Basenpaar Sequenz) ausreichend für den anti-Tumor Effekt war, obwohl der Gesamt-Antigen-Expressionslevel in der Ohrmuschel viel geringer war als bei Verwendung des CMV Promoters. Wurden DZ in CD11c-Diphtheria Toxin (DT) Rezeptor transgenen Mäusen durch Einsatz von DT eliminiert, so ließ sich ie keine anti-tumorale Immunität mehr erzeugen. DZ in der Ohrmuschel sind also essentiell und ausreichend für den DNS vermittelten Immunisierungseffekt.

List of Abbreviations

β-gal	beta-galactosidase
Ab	antibody
Ag	antigen
APC	Allophycocyanin (conjugate of Ab for FACS)
APCs	antigen presenting cells
bp	Base pair
CMV	cytomegalovirus
CTL	cytotoxic T lymphocyte
d	day
DCs	dendritic cells
DE	DA3-EpCAM
DMEM	Dulbecco's Modified Eagle's Medium
DMSO	Dimethyl sulfoxide
DNA	Deoxyribonucleic acid
dNTP	Deoxynucleoside triphosphate
dsRNA	Double-stranded RNA
EDTA	Ethylene diamine tetraacetic acid
EGFP	Enhanced green fluorescence protein
ELISA	Enzyme-linked Immunosorbent Assay
EpCAM	epithelial cell adhesion molecule
FACS	Fluorescence-activated cell sorting (flow cytometry)
FCS	Fetal calf serum
FITC	Fluorescein isothiocyanate
GM-CSF	Granulocyte macrophage colony-stimulating factor
h	hour
HA	hemagglutinin
HAd	Hemadsorption
HIV	Human immunodeficiency virus
HLA	Human leukocyte antigen
HN	hemagglutinin-neuraminidase
HPV	Human Papillomavirus

HU	Hemagglutination unit
id	intradermally
ie	intra-ear pinna
IFN	interferon
IL	interlukin
im	intramuscularly
ip	intraperitoneally
LCs	Langerhans cells
MDSCs	Myeloid derived suppressor cells
min	minute
NA	neuraminidase
NDV	Newcastle disease virus
NK	Natural Killer
NOD/SCID	nonobese diabetic/severe combined immunodeficient
PBMCs	Peripheral blood mononuclear cells
PBS	Phosphate buffered saline
PCR	Polymerase chain reaction
PE	Phycoerythrin
PI	Propidium iodide
PKR	Protein kinase PKR
RLU	relative light unit
RNA	Ribonucleic acid
ROI	region of interest
s	second
SARS	Severe acute respiratory syndrome
sc	subcutaneously
SD	Standard deviation
SEM	Standard error of the mean
SRBC	sheep red blood cells
TAA	Tumor associated antigen
TGF	transforming growth factor

TMB	tetramethylbenzidine
TNF-α	Tumor necrosis factor-alpha
TRAIL	tumor necrosis factor-related apoptosis-inducing ligand
wt	wild-type
w/v	Weight per volume
WHO	World Health Oganization

1 Introduction

1.1 Vaccine

1.1.1 The development of vaccine

A vaccine is a preparation which is used to improve immunity to a particular disease. As early as in the 10th century, variolation (Early form of vaccination in which part of the lesions produced by smallpox was used to try and trigger immunity to the disease) was practiced in China to protect against a lethal smallpox infection. 200 years ago, the concept of vaccination was proven by Edward Jenner who used cowpox inoculation to prevent smallpox infection. The work of Louis Pasteur on chicken cholera (1880) opened the way to vaccine development in the laboratory (1). Over the last century, the development and widespread use of vaccines against different infectious diseases have been a great triumph of medical science (2-4). Vaccines for some infectious diseases are routinely inoculated to children and special adult populations with high risk of infection (5). More than nine million deaths could be prevented annually by using vaccines against a few important infectious diseases such as pneumonia, meningitis, diarrheal diseases, tuberculosis, malaria, and schistosomiasis (2, 6-10). According to a CDC (Centers for Disease Control and Prevention) report, the following vaccines (Table 1.1) are available to prevent diseases.

Table 1.1 Vaccine-Preventable Diseases

Anthrax	Lyme disease	Rotavirus
Cervical Cancer	Measles	Rubella
Diphtheria	Meningococcal	Shingles (Herpes Zoster)
Hepatitis A	Monkeypox	Smallpox
Hepatitis B	Mumps	Tetanus
Haemophilus influenzae type b (Hib)	Pertussis	Typhoid
Human Papillomavirus (HPV)	Pneumococcal	Tuberculosis (TB)
Influenza (Flu)	Polio	Varicella (Chickenpox)
Japanese encephalitis (JE)	Rabies	Yellow Fever

Traditional vaccination aims at the prevention of a specific infectious disease by delivering an immunogenic antigen derived from the surface of the infectious agent, resulting in immunity against the foreign organism replicating and establishing an infection (3). There are four types of traditional vaccines: 1) killed microorganisms; 2) attenuated microorganisms; 3) toxoid (inactivated toxic compounds); 4) subunit vaccines. Most currently used vaccines are based on these technologies. A number of innovative vaccines with promising aspects are also in development and in use (Table 1.2) including both prophylactic and therapeutic vaccines (1). Different to a traditional prophylactic vaccine which prevents occurrence of an infection, a therapeutic vaccine can limit or eradicate an already present and established infectious agent or condition (3, 11-13).

Table 1.2 New strategies for vaccine development

Strategy	Example
Live recombinants	Dengue virus, parainfluenza virus, Mycobacterium tuberculosis
Recombinant protein production	Hepatitis B surface antigen, pertussis toxin, Borrelia burgdorferi outer surface protein A
Replication-defective particles	Human papillomavirus, herpes simplex virus
Alphavirus replicons	HIV, hemorrhagic fever agents
Naked DNA plasmid	Hepatitis B virus
Recombinant vectors	Cytomegalovirus, human immunodeficiency virus
Prime-boost with DNA/vectors	Human immunodeficiency virus, malaria
Reverse genetics	Influenza virus, parainfluenza virus, respiratory syncytial virus
Peptides	Cancer
T cell receptor	Multiple sclerosis

1.1.2 Vaccine and immune responses

In order to be effective, vaccines should be designed to elicit appropriate protective immunological effects. Understanding protective mechanisms (the molecular processes involved in the immunological recognition of microbial antigens and in the differentiation of cells that mediate effector mechanisms) is useful for the design of new vaccines against diseases for which an empirical approach to vaccine development has failed (2).

A hallmark of the immune system is its ability to remember an encounter with a pathogen for several decades, even for a whole lifetime (14, 15). This fundamental property of the immune system is the basis for vaccination. The goal of a successful vaccine is to induce long-term protective immunity against a given pathogen. The process of induction of adaptive immunity by vaccines is shown in Figure 1.1. After vaccination, foreign antigens are produced by somatic cells. Antigen presenting cells (APCs) can express directly (direct-presentation) or take up (cross-presentation) foreign antigens and migrate to draining lymph nodes. There they induce activation and proliferation of naive CD8 cytotoxic T lymphocyte (CTL) and CD4 T helper cells (Th) in a MHC class I and class II restricted manner, respectively. There are two subsets of CD4 T cells: Th1 and Th2. Th1 cells are crucial for activation of macrophages, for proliferation of CD8 T cells by producing IL-2 and IFN-γ, and for up-regulation of MHC class I molecules on target cells. Th2 cells are most effective as helper cells for B cell responses that lead to antibody production (16-18).

For most viral and bacterial infections, primary protection is mediated by a humoral immune response (antibody production) (19). For intracellular infections such as *Mycobacterium tuberculosis, Leishmaniamajor,* and other parasites, protection is mostly mediated by cellular immunity (20-22). For some diseases, e.g. human immunodeficiency virus (HIV) infection, herpes, and malaria, both humoral and cellular responses are required (23-28). Exogenous antigens provided by killed/inactivated pathogens, recombinant protein, or protein derived from live vaccines are taken up by APCs by phagocytosis or pinocytosis and presented by MHC class II molecules to stimulate CD4 T cells, which can help generate effective antibody responses. In contrast, MHC class I molecules associate with antigens synthesized within the cytoplasm of the cell. Live or DNA vaccines involve this endogenous pathway of antigen processing and presentation. They also involve "cross-presentation", a mechanism in which exogenous antigen is taken up by professional APCs (DCs) and processed similar to the endogenous pathway leading to expression of MHC I-antigen peptide-complexes at their cell surface (29, 30).

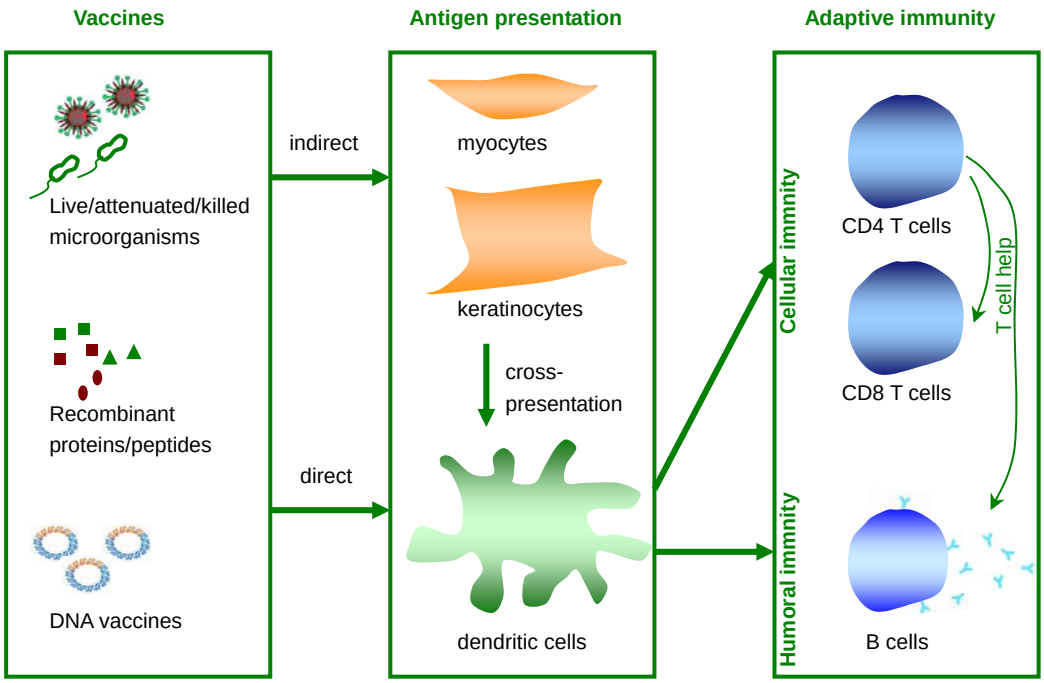

Figure 1.1 Vaccine-induced adaptive immunity.

Vaccines can be taken up by myocytes (im immunization) or keratinocytes (id immunization) in which case antigen will be cross-presented by APCs (mostly DCs). If vaccines are taken up by DCs (distributed in most tissues), antigen will be presented directly to naïve T cells in draining lymph nodes to induce adaptive immunity. CD4 and CD8 T cells will be activated and proliferate. TH1 CD4 cells can further activate macrophage and CD8 T cells. B cells can induce antibodies by the help of TH2 CD4 cells.

1.1.3 DNA vaccine

Observations in the early 1990s that plasmid DNA could directly transfect animal cells *in vivo* (31) initiated the use of DNA plasmids encoding antigenic proteins to induce immune responses by direct injection into animals (32). This novel method is considered to be one of the most important discoveries in the history of vaccine development (33, 34).

DNA vaccines consist of a bacterial plasmid with a strong viral promoter, the gene of interest, a polyadenylation/ transcriptional termination sequence, an antibiotic resistance gene and several CpG motifs (Figure 1.2). The plasmid is grown in bacteria (E. coli), purified, dissolved in a saline solution, and then simply injected into the host (35). The DNA plasmid is taken up by host cells where the encoded protein is made. It is demonstrated now that DNA vaccination can induce antibodies, helper T cell responses, CTL responses, and protective immunity in various animal models for different infectious diseases and cancers (29, 36).

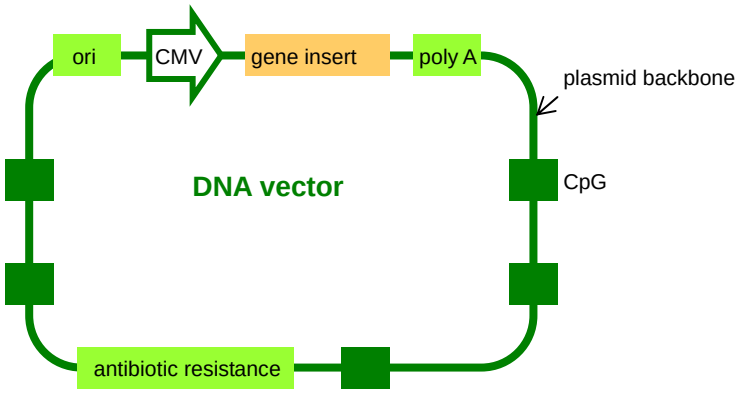

Figure 1.2 The basic requirements of a DNA vector.

A bacterial plasmid contains a viral promoter. CMV (Cytomegalovirus) promoter is the most commonly used promoter which is strong and universally active for most tissues. A DNA vaccine vector further contains a gene insert for an antigen, a poly A transcriptional termination sequence, an antibiotic resistance gene and several CpG motifs

DNA vaccination provides several appealing advantages over conventional vaccines. Because of the simplicity of altering constructs or of mixing different plasmids, DNA vaccines have been used to explore the effect of various vaccination conditions such as the use of different forms of an antigen (secreted and membrane-bound), the effect of different intracellular targeting signals for a protein, and the effects of coexpressed cytokines. The intracellular synthesis of a plasmid protein results in the antigen likely to be folded in its natural conformation, correctly glycosylated, and with normal post-translational modifications (30, 37), which favor the induction of efficient immune responses. In contrast to killed microorganisms, subunits or recombinant proteins/peptides, DNA vaccines effectively induce both humoral and cellular immune responses. They are especially promising for induction of cellular immunity which is less efficient in protein/peptide vaccinated animals. In addition, DNA vectors are easy to be manufactured, transported and stored. They are also safer than live and attenuated vaccines with their possibility to revert into virulence (29, 33).

Table 1.3 Advantage/Disadvantage of DNA vaccine

Advantage	Disadvantage
Express native protein antigens *in vivo*	Risk of integration into host genome
Efficient humoral and cellular responses	Inefficient in large animals
Specially efficient CD8 T cell responses	
Long-term immunity	
Convenient construction	
Versatile combination of several epitopes	
Efficient manufacturing	
Easy transportation and storage	
Low cost	
Safer than live/attenuated microorganisms	

1.1.4 Improvement of DNA vaccine

Performance of gene-based vaccines will have to stand the test of evaluation in human subjects. Although it has been proven in many disease models that naked DNA vaccines are sufficient to induce protective immunity, in large animals and for human application it is still difficult to achieve high efficiency (29, 38). Therefore, it is necessary to improve the vaccination strategy.

1.1.4.1 Delivery methods

The influences of dose, volume, site and method of delivery of DNA vaccines are known to be critical for the induction of immune response. New delivery methods have proven to be superior to naked DNA injection. These include gene-gun, electroporation, tattooing, lipid/liposome (also as adjuvants) and viral carriers (vectors) together with different injection routes e.g. intramuscular (im), intradermal (id), subcutaneous (sc), intravenous (iv), intranasal (in) and intra-ear pinna (ie) (39-41). Electronic pulse dependent strategies of application are most commonly applied to skin because of its richness in immune cells. Different delivery methods are listed and compared in Table 1.4. Among them, electroporation (EP) appears to provide a desirable balance of safety, efficiency, and cost effectiveness. It uses electrical pulses to create pores in cell membranes. It can be applied directly to tumor, muscle, skin, or mucosal tissue and enhances intracellular delivery of DNA plasmids by 1,000 times or

more (42-44). Compared to gene gun immunization which might skew immune responses towards Th2 (45, 46), EP is efficient to induce privileged Th1 responses (43, 47, 48).

Table 1.4 Comparison of DNA delivery methods*

Delivery methods	Advantage/Disadvantage				
	Simplicity	DNA dose	Safety	Efficiency	Cost
Naked DNA injection	++++	-	+++	+	++++
Gene gun	+	++++	++	+++	+
Electroporation	+++	+++	+++	+++	++++
Tattooing	++	+++	+++	+++	++
Lipid/liposome	++	++	++	++	+
Viral carriers	-	++	-	++++	-

- no advantage; + low advantage; ++ middle advantage; +++ high advantage; ++++ excellent advantage
* outline information from reference 29, 39-48

1.1.4.2 Adjuvants

Adjuvants are components that enhance the specific immune responses against co-inoculated antigens, both for the magnitude and duration of immune responses (49). The nature of the adjuvant can determine the particular type of immune response, which may be skewed toward cytotoxic T cell (CTL) responses, antibody responses, or particular classes of T helper (Th) responses and antibody isotypes (50). Adjuvants such as lipid/liposome, CpG motifs, coexpression of immunostimulating molecules as well as many other adjuvants have been shown to be efficient to improve DNA vaccination effects (Table 1.5) (29, 40, 51-54). Obviously, DNA fusion gene vaccines (coexpression of immunomodulatory molecules such as cytokines, co-stimulatory molecules or chemokines) are an attractive means of modulating an antigen-specific immune response without the use of potentially toxic chemical adjuvants (55-57).

Table 1.5 Adjuvants for DNA vaccines

Category	Classification	Examples	References
Genetic adjuvants	Costimulatory molecules	CD80, CD86, CD40L, CD54, LFA-3, L-selectin, CTLA4	(29, 56, 58-60)
	Cytokines	IL-1, IL-2, IL-4, IL-5, IL-6, IL-7, IL-8, IL-10, IL-12, IL-15, IL-18, TNF, GM-CSF, TGF-β, IFN-γ, IFN-α	
	Chemokines	TCA-3, RANTES, MIP1-a	(61, 62)
	CpG motifs	Phosphorothioate synthetic ODNs	(63, 64)
	Complement	C3d	(65)
	Heat shock protein	Hsp70	(66)
	Apoptosis inducer	Fas, Caspase	(67)
	Transcriptional factors	IRFs	(68)
Conventional adjuvants	Mineral salts	Aluminum phosphate, Aluminum hydorxide	(60, 69)
	Bacteria-derived adjuvants	Monophosphoryl lipid A, Cholera toxin, Muramyl peptides	
	Lipid particles	Cationic liposomes, Mannan-coated liposomes*	
	Emulsifier-based adjuvants	QS-21**	
	Synthetic adjuvants	Ubenimex***	

* Mannose is a carbohydrate moiety that coats the surfaces of many infectious agents including viruses, bacteria, yeasts, and protozoans. Several immune systems use carbohydrates as activators.
** QS-21 is a highly purified triterpene glycoside saponin isolated from the bark of the Quillaja saponaria Molina tree.
*** Ubenimex (UBX; ((2S,3R)-3-amino-2-hydroxy-4-phenyl-butyryl-L-leucine), an immunomodulator which has been used for immunotherapy of cancer, is a small molecular weight aminopeptidase inhibitor isolated from a culture filtrate of Streptomyces olivoreticuli.
Abbreviations: IL, Interleukin; TNF, tumor necrosis factor; GM-CSF, granulocyte monocyte colony stimulating factor; TGF, transforming growth factor; IFN, interferon; TCA, T cell activator; RANTES, regulated upon activation, normal T cell expressed and secreted; MIP, Macrophage inflammatory protein; Hsp, heat shock protein; IRF, interferon regulatory factor.

1.1.5 Functions of dendritic cells in DNA vaccine

A key event that triggers the immune response is when the immune system ‘‘senses’’ the vaccine or microbe. DCs are the pivotal APCs to present antigens to T and B cells and to modulate the strength, quality, and persistence of the adaptive immune response (70). DCs are distributed in almost all tissues. Local inflammation induced by DNA vaccination can recruit DCs as well as other immune cells to the injection site (e.g. im DNA immunization). Efficiency of antigen presentation might be improved by id DNA vaccination because skin is a DC-rich tissue containing both epidermal Langerhans cells (LCs) and dermal DCs (71, 72).

Peripheral immature DCs are in a highly pinocytic state and express low-levels of MHC and costimulatory molecules. After DNA uptake, these DCs are stimulated vigorously by CpG motifs and proinflammatory cytokines. They synthesize and process the DNA encoded antigen for presentation at the cell surface and then migrate to draining lymph nodes where they can efficiently activate antigen-specific naïve T cells. During this migratory process, DCs undergo maturation with MHC and costimulatory molecules being up-regulated. During this period of activation and antigen (MHC-peptide) presentation, communication with CD4 cells induces the ability of the DCs to activate naïve CD8 cells and also induces the establishment of memory CD4 T cells. These are potentially capable of long-life existence without repeated antigenic stimulation (37). DCs are capable of processing antigen via the classical pathways: endogenous antigens via the proteasome into the MHC class I compartment; exogenous antigens via the endocytic lysosomes into the MHC class II compartment. DCs also possess alternative pathways of antigen processing and can route exogenous antigen into the MHC class I pathway through a mechanism known as cross-priming (29, 35, 37).

1.1.6 DNA immunization to ear pinna

Muscle was the first site to be tested for DNA injection (31). By targeting the body’s natural defense system, the skin, intradermal DNA immunization attempts to produce an immunologically efficacious response (32, 42). DNA vaccines provide DNA for protein expression in a variety of cells, including keratinocytes, Langerhans cells (LC),

and dendritic cells (DC), which are located in the two main areas of the skin, the epidermis and the dermis (42). After maturation, the LC, which are found mainly in the epidermis, and the dermal DC, which are found mainly in the dermis, can migrate to local lymph nodes where presentation of antigens to T cells can occur and initiate a variety of immunological responses (30, 73). In mouse models, id injection is usually applied to abdominal or flank skin, sometimes to ear skin when separation of skin cells is needed. Interestingly, in our previous studies with the highly metastatic lymphoma ESb tumor inoculation, it was shown that the ear pinna is a privileged site (compared to sc tumor inoculation) for the induction of antitumor immunity, preventing the outgrowth of an otherwise lethal dose of tumor cells (74). Further studies then have corroborated the superiority of intra-pinna DNA vaccination to induce strong immune responses compared to im and id (flank) DNA immunization (75, 76). One of the advantages might be the special structure of ear pinna which contains two layers of epidermis and dermis with more professional APCs within a certain area. In this thesis, I tried to further analyze and improve this strategy for application in mouse tumor models.

1.2 Cancer therapy

Cancer is the general name for a group of more than 100 diseases in which cells in a part of the body begin to grow out of control. In USA, a total of 1,444,920 new cancer cases and 559,650 deaths from cancer are reported in 2007 (77). Research of efficient cancer therapy is highly important to save people's life. In the U.S. and other developed countries, cancer is presently responsible for about 25% of all deaths. On a yearly basis, 0.5% of the population is diagnosed with cancer (Wikipedia information).

1.2.1 Traditional cancer therapy

Cancer can be treated by traditional methods such as surgery, chemotherapy, and radiation therapy, as well as by new strategies such as targeted therapy (including antibodies, peptides, photodynamic therapy), immunotherapy (including cytokines, adoptive transfer of immune cells, gene therapy and cancer vaccines), virus-based therapy, hormonal therapy, and angiogenesis inhibitors. The choice of therapy depends upon the location and grade of the tumor and the stage of the disease, as well as the general state of the patient (performance status).

Surgery is one of the basic strategies to cure cancer if the solid tumor can be completely removed. This is the case if the tumor has no metastases and if its removal does not damage vital organs such as the brain or the liver. However, if the tumor cannot be completely removed, other treatment methods have to be applied as well. One of these methods is radiation therapy, the use of ionizing radiation to kill cancer cells. Radiation therapy works by damaging the DNA of cells and since cancer cells generally proliferate more and have acquired defects in the DNA damage repair, they are more susceptible to radiation-induced DNA damage than normal, non-malignant cells. Another important way to treat cancer is chemotherapy, the use of drugs that interfere with cell division in different ways. Most forms of chemotherapy target all rapidly dividing cells and are not specific for cancer cells. Since most chemotherapeutic drugs target all proliferating cells, normal replicating cells of the body such as bone marrow cells, intestinal cells or cells of hair follicles are also killed. This can lead to side-effects such as immunosuppression, diarrhea or hair loss.

Primary solid tumors can often be treated successfully with surgical resection, chemotherapy or radiation; however, these therapies are mostly ineffective against metastatic spreading. Therefore, other new strategies are necessary to be applied. In general, the most successful treatment for cancer can be achieved by a combination of different strategies. For example, chemotherapy and radiation therapy are commonly used after surgical removal of the primary tumor to target residual tumor cells and possible metastases in the body. Other strategies are also needed, especially for tumors resistant to chemotherapy and radiation, as well as for late-phase patients (Information is obtained from NCI (National Cancer Institute) website).

1.2.2 Cancer immunotherapy

Cancer immunotherapy is a more precisely targeted therapy. The primary goal of this strategy is to direct immune responses to tumors that either are ignored by the immune system or are actively suppressing the immune system (78, 79). This might be fulfilled by stimulating the patients' own immune system or transferring immune components to the patients. Different immunotherapeutic strategies (Table 1.6) are studied and combined to improve the traditional methods.

Most cancer vaccines are applied in a therapeutic setting. They are intended to treat existing cancer rather than to prevent it (80, 81). The cancer patient would initially undergo surgery to remove most of the primary tumor. Vaccination would then be undertaken to generate a specific immune response capable of clearing any residual cancer, thus preventing relapse (81-83) and extending the period of remission or survival in the patient.

Table 1.6 Strategies of cancer immunotherapy

Cancer immunotherapy	Clinical application and clinical trials	References
Cytokines	IL-2, IL-12, IFN-α, IFN-γ, GM-CSF,	NCI website**
Antibodies	trastuzumab (anti-Her2/neu) rituximab (anti-CD20) Alemtuzumab (anti-CD52) Lym-1 (anti-HLA-DR) Bevacizumab (anti-VEGF) Cetuximab (anti-EGFR) Tarceva (anti-EGFR-TK1) Iressa (anti-EGFR-TK1) Thalidomide (anti-TNF-α)	
Radioimmunotherapy*	Zevalin (anti-CD20-^{111}In/^{90}Y) Bexxar (anti-CD20-^{131}I)	
Adoptive transfer of immune cells	Antigen specific autologous T cells Genetically modified T cells	
Gene therapy	Advexin (Ad-P53) MetXia-P450 (retrovirus-based vector) Ad.HSVtk/ganciclovir (adenovirus-based vector)	
Cancer vaccines	Tumor cell vaccines Dendritic cell vaccines Synthetic proteins	

* Monoclonal antibodies against tumor antigens can also be coupled to radioactive isotopes.
Abbreviation: VEGF, vascular endothelial growth factor; EGFR, epidermal growth factor receptor; TK, thymidine kinase; Ad, adenovirus.
** NCI website: http://www.cancer.gov/cancertopics/treatment/types-of-treatment

1.3 Newcastle Disease Virus (NDV)

Newcastle disease virus (NDV) is an avian RNA virus of the genus paramyxoviridae. Newcastle disease is highly contagious in domestic poultry and wild birds featured by gastro-intestinal, respiratory and nervous signs. Human infections have been reported with flu-like symptoms and conjunctivitis (84).

1.3.1 Application of NDV for Cancer therapy

NDV preferentially replicates in tumor cells and can effectively kill tumors in animal models. With regard to human application, NDV selectively kills human tumor cells with limited toxicity to normal cells. Therefore, NDV has been used in cancer therapy for more than 40 years (85-91). Although the virus also binds to normal cells, these cells normally resist viral replication. Three major strategies are in clinical development now: 1) Oncolysates (extracts of cancer cells that are infected with lytic viruses); 2) whole cell vaccines (NDV infected autologous tumor cells); 3) Systemic application of oncolytic strains of NDV to patients. Clinical anti-tumor immunotherapy with these strategies showed improvement of survival (92-96). NDV induced tumor destruction involves several mechanisms: 1) inducing necrosis or oncolysis by their excessive replication; 2) inducing programmed cell death (apoptosis); 3) stimulating anti-tumor immune responses. Upon replication in infected cells, double-strand viral RNA (dsRNA) is produced in the cytoplasma which, via interaction with PKR, induces an interferon (IFN) response in the infected cells. The interferon response represents an early host defense reaction that occurs prior to the onset of adaptive immune responses (84, 86, 87).

In addition, recombinant NDV could be used in vector-based vaccines encoding a pathogen antigen. Such vectors were shown competent to lead to pathogen antigen expression and to induce anti-pathogen immunity. The following characters enable NDV to be used as a good vector: highly attenuated in primates, antigenic distinction from human pathogens, stability to accommodate foreign sequences, easy production and low incidence of recombination. This vector is especially efficient by intranasal immunization to protect respiratory infection because of the respiratory tropism. Intranasal inoculation with recombinant NDV vector expressing influenza virus

hemagglutinin or respiratory syncytial virus fusion protein induced sufficient antibody responses to protect against virus infection (97-101). DiNapoli et al reported promising neutralizing antibody production by using recombinant NDV vector encoding SARS-CoV (severe acute respiratory syndrome-associated coronavirus) spike S glycoprotein (100).

1.3.2 Functional study of NDV molecules

NDV is a membrane-enveloped virus of roughly spherical structure with 150 to 300 nm in diameter. It contains a non-segmented, negative sense and single stranded RNA genome of 15-kb size. The NDV genome codes for the following six genes (Figure 1.2): nucleocapsid protein (NP), phosphoprotein (P), matrix protein (M), fusion protein (F), hemagglutinin-neuraminidase (HN) and large protein (L) (84).

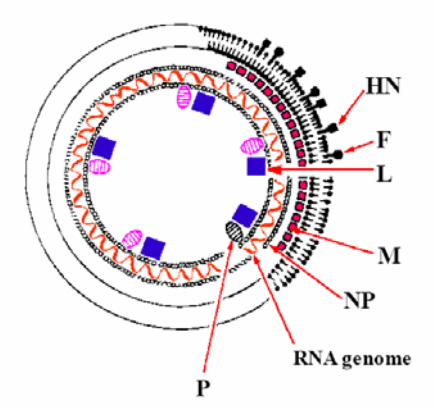

Figure 1.3 The structure of NDV virus particle.

NDV virus particle contains a negative-sense, single-stranded, non-segmented RNA genome encoding six genes: NP (nucleocapsid protein), P (phosphoprotein), M (matrix protein), F (fusion protein), HN (hemagglutinin-neuraminidase) and L (large protein).
Image is obtained from: http://www.microbiologybytes.com/virology/Paramyxoviruses.html

The surface protein HN is anchored in the viral envelope and it is indispensable for the attachment of the virus to the cell surface receptors as well as release of virus from the cells (102, 103). The F protein, which is also anchored in the viral envelope, mediates the fusion of the viral envelope with the host cell membrane and thereby enables the entry of the viral capsid (104). The M protein is located between the viral capsid and the envelope and is important for the generation and packaging of viral RNA as well as for the assembly of new virus particles. The nucleocapsid consists of three viral proteins that form a complex with the RNA genome. About 2,200-2,600

subunits of the NP protein form the nucleocapsid. A complex of the NP, the L and the P protein are involved in the transcription of the RNA genome. The L protein is an RNA-dependent RNA polymerase that is active only in a complex with the NP and the P protein (105, 106).

The HN molecule is a 74-kDa membrane type II glycoprotein which has both hemagglutinin (HA) and neuraminidase (NA) activity. HN is crucial in mediating the attachment of the virus to host cell receptors, as well as the attachment of infected cells to other cells. HN expression *in vitro* by DNA transfection induced lymphocyte binding activity. *In vitro* studies also showed induction of IFN-α and TRAIL (tumor necrosis factor-related apoptosis-inducing ligand) in human PBMCs (peripheral blood mononuclear cells) by HN (107-109). It is not clear which receptors are involved in the HN induced IFN-α response. Interestingly, it was reported that influenza HA can enhance lysis of virus-infected target cells by NK cells, and can directly activate NK cells via triggering the NKp44 and NKp46 receptor (110-113). These studies all indicate that HN is an immunostimulating molecule.

Aims of this thesis

Aims: To improve the intra-ear pinna DNA vaccination strategy by adjuvant viral DNA sequences and by electroporation in mouse tumor models.

Naked DNA vaccine based on xenogeneic tumor associated antigens (TAAs) is an appealing strategy for anti-tumor immunotherapy for many reasons, but the efficiency of such a procedure may need improvements.

We focused on the following issues and studied the anti-tumor effects in mouse tumor models:

1) Studying an optimal site for vaccine application: Comparison of different sites (ear and flank) of skin.

2) Studying adjuvant DNA sequence effects on DNA vaccine activity: Focus on viral HN from NDV.

3) Studying influence of electroporation (EP) on vaccination efficiency: Comparison of EP applied to different sites, including ear pinna.

4) Studying a possible role of dendritic cells (DCs) in ie DNA vaccination to elucidate mechanism of action: This should be achieved by targeting DCs with a short CD11c promoter *in vivo*.

By analyzing these issues above, it was intended to finally optimize and test new ways for efficient anti-tumor DNA vaccination.

Materials and Methods

3.1 Equipment

Axioplan2/AxioCam	Zeiss, Jena, Germany
Binocular microscope	Zeiss, Jena, Germany
Biological safety cabinet	Baker, Sanford, USA
Cell culture incubator	Labotec, Göttingen, Germany
Cell homogeniser Ultra-Turrax T25	Werke, Staufen, Germany
Centrifuge *Biofuge fresco*	Heraeus, Hanau, Germany
Centrifuge *Megafuge 2.0R*	Heraeus, Hanau, Germany
Duolumat LB9507 luminometer	Berthold, Bad Wildbad, Germany
Elgen1000 Electroporation system	Inovio, San Diego, USA
ELISA reader	Perkin-Elmer,Überlingen,Germany
Flow cytometer *FACSCalibur*	BD, Heidelberg, Germany
Flow cytometer *FACSCantoII*	BD, Heidelberg, Germany
Freezer -20 °C	Liebherr, Biberach an der Riss, Germany
Freezer -80 °C Thermo	Fisher Scientific, Karlsruhe, Germany
Glass pipettes	Hirschmann, Eberstadt, Germany
Glassware	Schott, Mainz, Germany
Heatable magnetic stirrer	Heidolph Instruments, Schwabach, Germany
Heat block	Grant Instruments, Cambridgeshire, UK
IVIS100 *in vivo* imaging system	XENOGEN, Alameda, USA
Microwave oven	Bosch, Heidelberg, Germany
Nucleofector I electroporation device	Amaxa, Cologne, Germany
Neubauer cell counting chamber	B.Braun, Melsungen, Germany
pH meter	Wissenschaftliche Technische, Weilheim, Germany
Pipettes (2-1000 µL)	Eppendorf, Hamburg, Germany

Pipetting aid *Pipetboy acu*	INTEGRA Biosciences, Fernwald, Germany
Photometer *GeneQuant pro*	Amersham Biosciences, Freiburg, Germany
Power supply for electrophoresis	Pharmacia, Freiburg, Germany
PTC-200 Peltier Thermal Cycler	MJ Research, Waltham, USA
Quartz cuvette	Hellma; Fa. Migge, Heidelberg, Germany
Shaker *Mixer 5432*	Eppendorf, Hamburg, Germany
Shaker *Reax 2000*	Heidolph Instruments, Schwabach, Germany
Table centrifuge	WiFug, Sweden
Water baths	Grant Instruments, Cambridgeshire, UK

3.2 Molecular biological methods

3.2.1 Buffers and solutions

TAE, 50×	Tris base 242 g/L $Na_2EDTA•2H_2O$ 37.2 g/L glacial acetic acid 57.1 mL/L in ddH_2O, pH 8.5, RT
LB, 10×	Bacto-Tryptone 100 g/L Bacto-yeast extract 50 g/L NaCl 100 g/L in ddH_2O, pH 7.0, autoclave, 4^oC

3.2.2 Preparation of DNA from bacteria

Plasmid DNA used for cloning was purified by QIAprep Spin Miniprep Kit (QIAGEN) according to the manufacturer's instruction (QIAGEN, www.qiagen.com, QIAprep Miniprep Handbook as at Dec 2006).

Plasmid DNA used for *in vitro* transfection was purified by EndoFree Plasmid Maxi Kit (QIAGEN) according to the manufacturer's instruction (QIAGEN, www.qiagen.com, Endofree Plasmid Purification Handbook as at Nov 2005).

Plasmid DNA used for DNA immunization was purified by EndoFree Plasmid Giga Kit (QIAGEN) according to the manufacturer's instruction (QIAGEN, www.qiagen.com, Endofree Plasmid Purification Handbook as at Nov 2005).

3.2.3 Cloning of DNA vectors

3.2.3.1 Preparation of DNA fragments by enzyme-cutting

Fragment DNA was acquired by enzyme-cutting with the following protocol:

Components	For checking (20μL)	For gel purification (50μL)
10×reaction buffer	2 μL	5 μL
100×BSA*	o.2 μL	0.5 μL
Enzyme 1**	0.3 μL	3 μL
Enzyme 2**	0.3 μL	3 μL
DNA	0.5 μg	4 μg
ddH_2O	to 20 μL	to 50 μL

* include if required

** all restriction endonucleases were purchased from NEW ENGLAND BioLabs; digestion was performed according to the manufacturer's protocol; buffer for double digestion depends on if there is a universal reaction buffer for the 2 enzymes; if not, digestion should be made one by one;

3.2.3.2 Preparation of DNA fragments by PCR

PCR was performed with Platinum *Pfx* DNA Polymerase (Invitrogen) following the protocol below by using a PTC-200 Peltier Thermal Cycler (MJ Research):

Components	For checking (20μL)	For gel purification (50μL)
10 × *Pfx* buffer	2 μL	5 μL
10mM dNTP	0.6 μL	1.5 μL
50mM $MgSO_4$	0.4 μL	1 μL
10 × enhancer*	1~4 μL	2.5~10 μL
Pfx DNA polymerase	2 μL	5 μL
10μM Primer 1	0.3 μL	3 μL
10μM Primer 2	0.3 μL	3 μL
Template DNA	10pg~200ng	10pg~200ng
ddH_2O	to 20 μL	to 50 μL

* use more enhancer for problematic PCR

PCR general procedure:

Steps	Temperature & Time	Cycle
1	94°C, 2 min	1
2	94 °C, 15 s	35
	56 °C, 30 s*	
	60°C, 1 min/1 kb	
3	4°C	forever

* Other annealing temperature was applied when this procedure did not work.

Primer sequence

Name	Sequence 5'-3'	Enzymes
JN1	CTCGAGGGAGGTGGTGGATCCATGTGTTTACTTTGACCAAC	XhoI
JN2	GGGCCCTTATTTTTGACACCAGACCAACTG	ApaI
JN3	GTTTAAACAACATG GACCGCGCAGTTAGCC	PmeI
JN4	CGCCTAGGTACCAACATGGACCGCGCAGTTAGCC	AvrII, KpnI
JN5	CGATGCATGTCGACTGGCCAGCTGGCAGCGTAAGACTC	NsiI, SalI
JN6	CGGGATCCACTAGTGGTTATTTTCCACC	BamHI
JN7	CGGCATGCGTCGACTTATGGCCAGCTGGCAGCGTAAG	SphI, SalI
JN8	GCTAGCGAGCTCACGCGTAATGACTAATCCACTGAATG	NheI, SacI, MluI
JN9	GCTAGCACGCGTGAGCTCAGCTCAAGTGCTACTTCCCC	NheI, MluI, SacI
JN10	GCTAGCGAGCTCACGCGTTAGCACCCCAGTTCTTTGCTG	NheI, SacI, MluI
JN11	GCTAGCGAGCTCACGCGTGGCCTGCTGTCCAGTGGACT	NheI, SacI, MluI
JN12	GCTAGCGAGCTCACGCGTAGTCTGTCCATCCACCCTGGG	NheI, SacI, MluI
JN13	AAGCTTCTCGAGATCTGACTGGAGAACAGAAGCAGGC	XhoI, BglII
JN14	CGACGCGTCCGGCGAACGTGGCGAGAA	MluI
JN15	CGACGCGTCAAGGCCTGAGACGACA	MluI
JN16	CGACGCGTTGCTTAGCCATTTTAGACC	MluI
JN17	CGACGCGTTATGTTGAGCAAATGACTAATC	MluI
JN18	CGAGATCTTGAGCAACTTGGAGACAGC	BglII
JN19	CGGGTACCTATAGATAGCCCCTCGCAACC	KpnI
JN20	CGACGCGTTTCATTCATTCAGTGGATTAGTCA	MluI
JN21	CGGGTACCCGCCACACCCGCTCCTAACAT	KpnI
JN22	CGACGCGTCATAACCCAGAGATCAGAGTAAAA	MluI
JN23	CGACGCGTCTGCCCAGCCCACCCCTCTA	MluI
JN24	CGACGCGTTTGCCCCTGCTGCCCTGATT	MluI
JN25	CGGGTACC GGGGCCCTACACAAAACCATCC	KpnI
JN26	CGGATCCGAATTCATGGAAGACGCCAAAAACAT	BamHI, EcoRI
JN27	CGGATCCGAATTCTTACACGGCGATCTTTCCGC	BamHI, EcoRI
JN28	CGCTGCAGATGGAAGACGCCAAAAACAT	PstI
JN29	CGGGATCCGAATTCAGCTCAAGTGCTACTTCCCC	BamHI, EcoRI
PF229	GCTCAGCCCCTTATGGCCAGCTGGCAGCGTAAG	BlpI

PCR fragments were purified by QIAquick PCR purification Kit (QIAGEN) according to the manufacturer's instruction (Qiagen, www.qiagen.com, QIAquick Spin Handbook as at July 2002).

3.2.3.3 Extraction of DNA fragments from the gel

For the extraction of DNA from agarose gels the QIAquick Gel Extraction Kit (QIAGEN) was used according to the manufacturer's instructions (QIAGEN, www.qiagen.com, QIAquick Spin Handbook as at July 2002).

3.2.3.4 Commercial and ready-to-use plasmids

Code	Name	Encoding gene	Company	Author
1003	pTandem1	IRES	Novagen	
1005	pBK-SFV-HN	NDV HN		Jinyang Zeng
1008	pCMVβ	lacZ	Clontech	
1009	pGL3-Basic	Firefly luciferase	promega	
1016	pcDNA3.1/Hygro		Invitrogen	
1026	pCMV SPORT-βgal	lacZ	Invitrogen	
1078	pCMV-Ruc-GFP	Renilla luciferase		Günter Hämmerling
1083	CD11c-PR3562-GCDLA	Murine CD11c promoter Region: -1~-4046		
1084	pCMV-luc	Firefly luciferase		Daniel Scherman
1118	pSPORT6-EpCAM	Human EpCAM		Frank Momburg
1136	pkeratin14-luc	Firefly luciferase		Daniel Scherman
1142	pfascin-luc	Firefly luciferase		
	pCMV-GFP	EGFP		Yi Ni
	pmax-GFP	EGFP	Amaxa	

3.2.3.4 Cloning strategies

Code	Name	Fragment	Vector	Enzymes
1061	pTandem1-HN	HN (PCR: PF229+JN3)	1009	BlpI, PmeI
1067	pSPORT-HN-lacZ	HN (PCR: JN4+JN5)	1026	AvrII, SalI
1068	pSPORT-lacZ-IRES-HN	IRES-HN (PCR: JN6+JN7)	1026	BamHI, XhoI
1072	pSPORT	lacZ cut out	1026	SalI, XhoI
1073	pSPORT-HN	HN (PCR: JN4+JN7)	1026	AvrII, SalI/XhoI
1108	pCD11c488-luc	CD11c-24~-511* (JN17+JN18)	1003	BglII, MluI
1109	pCD11c500-luc	CD11c-1~-500* (JN8+JN13)	1003	BglII, MluI
1110	pCD11c700-luc	CD11c-1~-700* (JN9+JN13)	1003	BglII, MluI
1111	pCD11c1082-luc	CD11c-24~-1105* (JN16+JN18)	1003	BglII, MluI
1112	pCD11c2425-luc	CD11c-24~-2448* (JN15+JN18)	1003	BglII, MluI
1113	pCD11c3695-luc	CD11c-24~-3383* (JN14+JN18)	1003	BglII, MluI
1119	pCMV-EpCAM	Human EpCAM (cut from 1118)	1009	EcoRV, NotI
1120	pCMV-EpCAM-IRES-HN	Human EpCAM (cut from 1118)	1061	EcoRV, NotI
1132	pcDNA3-luc-hygro	Luciferase (cut from 1003)	1016	HindIII, XbaI
1139	pCD11c1105-luc	CD11c-1~-601* (cut from 1110)	1111	ApaI, BglII
1140	pCD11c2448-luc	CD11c-99~-2448* (cut from 1112)	1110	ApaI, MluI
1141	pCD11c3383-luc	CD11c-99~-2881* (cut from 1113)	1110	ApaI
1144	pCD11c5534-luc	CD11c -2272~-5534* (JN19+JN23)	1141	KpnI, NheI
1145	pGL3-Basic-m1	NotI mutation	1003	Klenow treated
1146	pGL3-Basic-m2	BamHI mutation	1003	Klenow treated
1147	pGL3-Basic-m3	NotI and BamHI mutation	1145	Klenow treated
1148	pGL3-Basic-MCS1	NotI and BamHI mutation, MCS fragment**	1147	HindIII, XbaI
1149	pGL3-Basic-MCS2	NotI and BamHI mutation, MCS fragment***	1147	NheI, XhoI
1150	pcDNA3-EpCAM-hygro	Human EpCAM (cut from 1118)	1016	EcoRV, NotI
1151	pCD11c700-EpCAM	Human EpCAM (cut from 1150)	1110	HindIII, XbaI
1152	pCD11c700-GFP	EGFP (cut from pCMV-GFP)	1110	HindIII, XbaI
1153	pCD11c700-lacZ	CD11c-1~-700* (JN29+JN13)	1008	EcoRI, XhoI

* position in murine CD11c promoter region
** MCS (multiple cloning sites) from pcDNA3.1/Zeo+ between HindIII and XbaI
*** MCS (multiple cloning sites) from pcDNA3.1/Zeo+ between NheI and XhoI

DNA Template for PCR

Fragment	Template
HN	Plasmid 1005
IRES-HN	Plasmid 1061
CD11c -1~-3383	Plasmid 1083
CD11c -2272~-5534	BAC RP24-78I2

DNA fragments were inserted into linearized vectors by T4 DNA ligase (Invitrogen) following the manufacturer's protocol. Ligation reactions were inactivated at 65^{o}C for 10 min and transformed to One Shot Top10 Competent Cells (Invitrogen) following the manufacturer's protocol. Problematic ligations (large DNA fragments or blunt ends) were transformed to XL10-Gold Ultracompetent Cells (Stratagene) following the manufacturer's protocol.

3.2.4 Determination of nucleic acid concentration

The plasmid DNA/total RNA concentration in a sample was determined photometrically via the absorbance at 260 nm (A260) using the following formula: concentration of DNA/RNA sample [μg/mL] = ε×A260×dilution factor with ε double-stranded DNA = 50, ε single-stranded DNA and ε RNA = 40. The ratio A260/A280 was taken as a measure of the purity of a sample.

3.3 Cell biological methods

3.3.1 Buffers and solutions

PBS	NaCl 8 g/L KCl 0.2 g/L KH_2PO_4 0.2 g/L Na_2HPO_4•12 H_2O 2.85 g/L in ddH_2O, pH 7.2, autoclave, 4°C
Freezing medium	DMSO 10% (v/v) FCS 40% (v/v) Complete medium 50% (v/v) prepared freshly before use
Trypsin/EDTA	trypsin 0.5 g/L EDTA 0.2 g/L in sterile PBS, storage at 4°C
Trypan blue solution	trypan blue 0.16% (w/v) NaCl 0.9% (w/v) NaN_3 0.1% (w/v) in ddH_2O, filtered (0.45 μm), 4°C
ACK lysis buffer	NH_4Cl 8.3 g/L $KHCO_3$ 1 g/L EDTA 0.037 g/L in ddH_2O, pH 7.2~7.4, autoclave, 4°C
Tissue digestion buffer	Collagenase Type IV 5g/L DNase I 50,000 U/L FCS 1% in PBS, prepared freshly before use
Fix buffer for X-gal staining	2 % formaldehyde 2 % gluteraldehyde in PBS, 4°C
X-gal dilution buffer	$K_4Fe(CN)_6$•3H_2O 5mM $K_3Fe(CN)_6$ 5mM $MgCl_2$ 2mM in PBS, 4°C, protected from light
X-gal stock solution	X-gal 40g/L in DMF, -20°C, protected from light

3.3.2 Cell culture methods

3.3.2.1 Culture of cell lines

All cell lines were grown at 37°C in a cell incubator in a 5% carbon dioxide/100% humidity atmosphere. Complete medium was supplemented with 100 U/mL penicillin and 100 µg/mL streptomycin, 2 mM L-glutamine, 25 mM HEPES, as well as 10% FCS (BIOCHROM, AG, heat inactivated at 56°C for 1 h).

Most adherent cells were detached from the surface of the cell culture flasks with the help of a trypsin/EDTA solution. Before the detachment the growth medium was removed and the cells were washed by the careful addition and subsequent removal of 10~20 mL PBS. Then 40 µL trypsin/EDTA solution per square centimeter surface was added and the cells were kept for 5-10 min at 37°C in a cell incubator. When the cells were detached they were washed in 10-20 mL growth medium to inactivate the trypsin/EDTA and used for further experiments

DC2.4 is a dendritic cell line which becomes suspended after confluence. No treatment with trypsin/EDTA was applied to this cell line. Medium needs to be changed every day for confluent cells. Suspended cells could be planted to a new flask.

List of medium for different cell line

Name	Origin	Medium	Other supplements
B16	Murine melanoma	complete RPMI1640	
BHK 21	Hamster kidney fibroblast	complete GMEM	0.1mM neAA* 1.0mM SP*
CT26	Murine colon carcinoma	complete DMEM	
CT26EP	Murine colon carcinoma	complete DMEM	
DA3	Murine mammary carcinoma	complete RPMI1640	50μM 2-ME*
DA3-EpCAM	Murine mammary carcinoma	complete RPMI1640	50μM 2-ME
DC2.4	Murine dendritic cells	complete RPMI1640	50μM 2-ME
Eb-lacZ	Murine lymphoma	complete RPMI1640	50μM 2-ME
ESb-lacZ	Murine lymphoma	complete RPMI1640	50μM 2-ME
LTK-HK	Murine fibroblast	complete DMEM	
MCF-7	Human breast adenocarcinoma	complete DMEM	
NIH 3T3	Murine fibroblastoma	complete RPMI1640	
P815	Murine blastocytoma	complete RPMI1640	50 μM 2-ME
RAW264	Murine macrophage-like cells	complete DMEM	
RMA-S	Murine lymphoma	complete RPMI1640	

*neAA: non-essential amino acids; SP: sodium pyruvate; 2-ME: β-Mercaptoethanol

3.3.2.2 Freezing and thawing of cells

In order to freeze mammalian cells, 1×10^6 to 1×10^7 cells were suspended in 1 mL freezing medium and transferred immediately to -80°C. After one week at -80°C, the cells were transferred to liquid nitrogen (-196°C).

In order to thaw cells, 37°C warm growth medium was added to the frozen cells with a Pasteur pipette. One washing step was performed in 10 mL growth medium (250 g, 5 min.) to remove the DMSO. After that the cells were seeded in fresh medium in a cell culture flask.

3.3.2.3 Determination of cell number and viability

Cells were counted with the help of a hemocytometer (Neubauer cell counting chamber, depth 0.1 μL) and an optical microscope. To distinguish live and dead cells,

trypan blue was added to the cell suspension in different dilutions ranging from 1:2 up to 1:10. Trypan blue stains only dead cells. The suspension was diluted enough so that the cells did not overlap each other on the counting grid. Cells that overlapped the top or left ruling of a large square were counted, whereas cells overlapping the bottom or right ruling were not counted. At least 100 living cells were counted for each sample in order to produce a statistically significant count. The cell number was calculated using the following formula:

$$\text{Cells } [\text{mL}^{-1}] = \frac{\text{Total cell count}}{\text{Number of counted large squares}} \times \text{Dilution factor} \times 10^4$$

The viability of a cell population could be determined by calculating the percentage of living cells.

3.3.3 Preparation of human PBMC

The human PBMC used in the experiments were prepared from buffy coats, a fraction of a centrifuged blood sample that contains most of the leukocytes. LeucoSep centrifuge tubes were filled with 15 mL Ficoll solution and centrifuged shortly (250 g, 1 min.). The buffy coat was diluted 1:4 in serum-free RPMI1640 and loaded onto the prepared LeucoSep tubes with 35 mL volume per tube. The tubes were centrifuged (800 g, 20 min., no brake), leading to an interphase enriched in PBMC between the Ficoll solution and the plasma. This interphase was collected with a Pasteur pipette and washed with serum-free RPMI1640 (PAA) (800 g, 10 min.). Two more washing steps with serum-free RPMI1640 followed (250 g, 5 min. and 100 g, 5 min.). The cell pellet was resuspended in PBS and filtered with a cell strainer (40 μm).

3.3.4 Generation of dendritic cells from murine bone marrow

To prepare bone marrow cells, mice were sacrificed by CO_2 inhalation and the fur was sterilized with 70% ethanol. All the following steps were carried out under sterile conditions in a tissue culture hood. Femora and tibiae from female BALB/c mice, 8–12 wk, were removed and stripped of muscles and tendons. After soaking the bones in 70% ethanol for 2 min and rinsing in complete RPMI1640 medium, both ends were cut with scissors and the marrow was flushed with medium using a 27-gauge needle.

Cell clusters were dissociated by repeated pipetting. After washing twice in medium (300 g, 10 min), bone-marrow cells were counted and used in the subsequent experiments.

For generation of dendritic cells, the cell pellet was resuspended in medium supplemented with 2000 U/mL recombinant mouse GM-CSF (BD 554586) to reach a cell density of 1×10^6/ml. Transfer the cells into 24-well plates (1 ml/well) and incubate them in a 37°C incubator with a 5% CO_2 atmosphere. To yield a high number of functional dendritic cells it is necessary to maintain a sufficient level of GM-CSF. Fresh medium containing GM-CSF should be added every second day. On day 2, carefully remove 700 µL of the cell medium from each well and replace it by fresh plating medium, to maintain an appropriate GM-CSF concentration. Remove and discard the cell medium completely on day 3. Wash the cells carefully with 500 µL per well using medium to remove residual non adherent cells and add 1 ml per well fresh medium containing GM-CSF. Incubate the cells at 37°C in an incubator with 5% CO_2 atmosphere. Harvest the immature dendritic cells on day 6 by collecting non adherent cells and loosely adherent cells or mature cells as described below. To release loosely adherent cells, wash off the cells thoroughly by pipetting them with medium. Discard adherent cells.

3.3.5 Transfection of mammalian cells with jetPEI

To transfect mammalian cells with plasmid DNA, the cationic polymer transfection reagent jetPEI (PolyPlus, for B16, BHK 21, CT26, DA3, NIH 3T3 cell lines) or jetPEI-macrophage (PolyPlus, for RAW264 cell line) was used according to the manufacturer's instructions (www.polyplus-transfection.com, *In vitro* Transfection Protocol,). The transfections were usually carried out on a 96- to 24-well scale.

3.3.6 Transfection of mammalian cells with Lipofectamine 2000

To transfect DC2.4 cells with plasmid DNA, the cationic lipid formulation transfection reagent Lipofectamine 2000 was used according to the manufacturer's instructions (www.invitrogen.com, Lipofectamine 2000 Reagent, 11, July, 2006). The transfections were usually carried out on a 96- to 24-well scale.

3.3.7 Transfection of dendritic cells with Nucleofector device

To transfect murine BMDC cells with plasmid DNA, the Mouse Dendritic Cell Nucleofector Kit (Amaxa) was used according to the manufacturer's instructions (www.Amaxa.com, Optimized protocol, DPA-1012 Vs. 02-2008) with a Nucleofector I electroporation device (Amaxa). The transfections were usually carried out on a 12-well scale according to the manufacturer's instructions.

3.3.8 Stable transfection of mammalian cells with jetPEI and CombiMag

To construct cell lines with stable gene expression, CT26, DA3 and DE cells were transfected with plasmid DNA (pcDNA3-EpCAM-hygro for CT26, pcDNA3-luc-hygro for DA3 and DE) by using jetPEI (PolyPlus) combined with CombiMag (OZ BIOSCIENCES) according to the manufacturer's instructions (www.ozbiosciences.com, Magnetofection: PolyMag & CombiMag INSTRUCTION MANUAL). The transfections were carried out on a 6-well plate. 48 h after the transfection, cells were splitted to 2× 60mm Petri dish. Since day 3, 200μg/mL hygromycin was added to the medium. Medium was changed every 2 days until single clones were detectable.

Single clones of cells were transferred to a 96-well plate

1) For CT26: simply put a tip in the colony and transfer to fresh medium
2) For DA3 and DE: with a sterile steel cloning ring, the colony was treated with Trypsin/EDTA and then transfered to fresh medium

Single clones were further analyzed for stable gene expression (EpCAM expression by FACS for pcDNA3-EpCAM-hygro transfection, luciferase expression for pcDNA3-luc-hygro transfection).

3.3.9 *In vitro* promoter activity

For *in vitro* promoter activity analysis, cells were transfected with DNA vectors encoding firefly luciferase driven by different promoters, or pGL3-Basic (negative control) and CMV-luc (positive control). A vector CMV-Ruc encoding renilla luciferase was used for co-transfection to control the transfection efficiency. Promoter activity is expressed relative to the luciferase activity produced by the promoterless plasmid, pGL3-Basic, after correction for transfection efficiency by renilla luciferase.

Transfections were made by triplicate, and repeated for 3 times.

3.3.10 *In vitro* luciferase assay

3.3.10.1 Firefly luciferase assay

Single clone cells from stable pcDNA3-luc-hygro transfected cells (DA3 and DE) were lysed (Passive lysis buffer, Promega: 20µL/well for 96-well plate, 100µL/well for 24-well plate) and analyzed for luciferase expression with the Luciferase Assay System (Promega) according to the manufacturer's instructions (www.promega.com, Luciferase Assay System, Protocol Vs 6/06) by using a Duolumat LB9507 luminometer (Berthold).

3.3.10.2 Firefly/Renilla dual luciferase assay

Cells (transfected with both firefly and renilla luciferase DNA) after 24 h transfection were lysed (Passive lysis buffer, Promega: 20µL/well for 96-well plate, 100µL/well for 24-well plate) and analyzed for firefly/renilla luciferase activity with the Dual-Luciferase Reporter Assay System (Promega) according to the manufacturer's instructions (www.promega.com, Dual-Luciferase Reporter Assay System, Protocol Vs 8/06) by using a Duolumat LB9507 luminometer (Berthold).

3.3.11 X-gal staining

X-gal staining is a method to visualize β-galactosidase (β-gal) expression (encoded by lacZ gene), through hydrolysis of X-gal (5-bromo-4-chloro-3-indoyl-β-D-galactopyranoside) which yields a blue precipitate. Briefly, cells were planted (for adherent cells) or centrifuged (for suspended cells) in a 24-well plate. Media were removed. Cells were washed twice by PBS and fixed 10 min at RT with Fix buffer. After 2 times washes, cells were stained in X-gal staining buffer (dilute X-gal stock solution 1:40 in X-gal dilution buffer) in a cell culture incubator for 3-12h. Longer incubation may produce unspecific staining. Cells with successful staining were then washed twice by PBS and photographed under a microscope.

3.3.12 FDG staining

Fluorescein di-D-galactopyranoside (FDG, molecular weight = 657, F1179, Invitrogen) is a fluorogenic substrate for β-gal. Non-fluorescent FDG is sequentially hydrolyzed by the β-gal enzyme, first to fluoresce in monogalactoside (FMG) and then to highly fluorescent fluorescein (Figure 3.1). Low levels of β-gal activity are readily detectable with FDG due to the superior spectral characteristics of fluorescein. These characteristics enable β-gal activity to be measured in single cells using FDG.

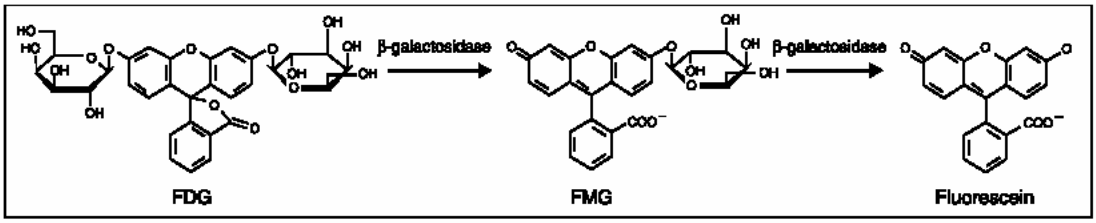

Figure 3.1 Sequential hydrolysis of FDG to FMG and fluorescein by β-galactosidase.

1) Flow Cytometric Analysis of Mammalian Cells

Cells were assayed for β-galactosidase activity 24 h after transfection with lacZ DNA in 6-well plate.

Prepare a 20 mM FDG stock solution (FDG dissolved in dimethylsulfoxide (DMSO)) and store at -20^{o}C, protected from light. Dilute this stock 10-fold into sterile deionized water and prewarm at 37°C for 10 min. Mix the diluted FDG solution with an equal volume of cell suspension in growth medium (1×10^{6} cells in 100μl) and incubate 1 minute at 37°C. The resulting hypotonic solution will permeabilize the cells, allowing the FDG to enter. After 1 minute, stop the FDG loading by adding at least 10-fold (1.8mL) ice cold staining medium(1μg/mL propidium iodide, 4% FCS, 10mM HEPES in PBS). Maintain the sample on ice until analysis.

2) Fluorometric Assays

Cells were assayed for β-galactosidase activity 24 h after transfection with lacZ DNA in 96-well microplate (black, light protected).

Following aspiration of the medium for each well, wash the cells once with PBS and

add 100μL lysis buffer (0.03% Triton X-100 in 100 mM HEPES, pH 7.8, containing 10 mM KCl, 1 mM $MgSO_4$) incubated at 50°C for 45 min. Cool plate to RT, and add 10 μL 100 μM FDG. Incubate the plate at 37°C for 3 min, and then measure the fluorescein signal with a microplate fluorimeter (Model 7620, Cambridge Technology Inc.

3.4 Immunobiological methods

3.4.1 Buffers and solutions

ELISA coating buffer	$NaHCO_3$ 10 mM pH 9.6
FACS buffer	NaN_3 0.1% FCS 5% (v/v) in PBS, 4°C

3.4.2 ELISA (Enzyme-linked Immunosorbent Assay)

Enzyme-linked Immunosorbent Assay (ELISA) combine the specificity of antibodies with the sensitivity of simple enzyme assays, by using antibodies or antigens coupled to an easily-assayed enzyme. ELISA can provide a useful measurement of antigen or antibody concentration. There are two main variations on this method: The ELISA can be used to detect the presence of antigens that are recognized by an antibody or it can be used to test for antibodies that recognize an antigen. Usually, an ELISA is a five-step procedure: 1) coat the microtiter plate wells with antigen; 2) block all unbound sites to prevent false positive results; 3) add antibody to the wells; 4) add anti-mouse IgG conjugated to an enzyme; 5) reaction of a substrate with the enzyme to produce a colored product, thus indicating a positive reaction.

3.4.2.1 β-gal ELISA

To determine mouse serum anti-β-gal antibodies (IgG+M, IgG1 and IgG2a), an β-gal ELISA was performed as the following steps:

Immunoabsorbant ELISA-plates (flexible, 96 well, flat bottom, Becton Dickinson) were coated with purified β-gal protein (SIGMA, 25µg/mL, 50µL/well) overnight at 4 °C in a humid chamber. After five washing steps with PBS, 200 µL/well of PBS-2% milk were used for blocking for 2 h at room temperature (RT). After five washing steps with PBS-Tween 20 (0.05%), 50µL/well of samples (diluted in PBS-2% milk) were added to the wells and incubated for 2 h at RT. After 5 washings with PBS-Tween 20 (0.05%), detection antibodies IgG+M-HRP (Dianova 1:5000),

IgG1-HRP (1:2000) and IgG2a-HRP (1:2000) were added with 50µL/well and incubated for 2 h at RT. After the washing steps with PBS-Tween 20, tetramethylbenzidine (TMB) substrate (KPL) was used for colour detection (50µL/well). After incubation for 20 min at RT (protected from light), the reaction was stopped with 50µL/well 2N H_2SO_4. The colour reaction was read at 450 nm within 30 minutes of stopping reaction.

3.4.2.2 Mouse IFN-γ and IL-4 ELISA

High Sensitivity ELISA Ready-SET-Go (eBioscience) Kits for mouse IFN-γ and mouse IL-4 were used in accordance with the manufacturer's protocol (www.ebioscience.com).

3.4.2.3 Human IFN-α ELISA

BHK21 cells (3.5×10^4/well, seeding 24 h before transfection in 24-well plate) were transfected with DNA (0.4µg/sample) encoding HN and/or lacZ gene. 48 h later, freshly prepared human PBMC were tested as responder cells to produce IFN-α by overnight incubation at 37°C with transient transfected BHK21 cells in 24-well plates. They were incubated at a final concentration of 2.5×10^6/mL in a total volume of 0.4 ml/well. As positive controls, PBMC were incubated with NDV or LTK-HN (a stable transfectant with HN expression). Cell supernatants were collected, centrifuged to remove cells, and stored at -20°C before testing IFN-α content by ELISA. Human IFN-α instant ELISA Kit (Bender MedSystems) was used according to the manufacturer's instructions (www.bendermedsystems.com).

3.4.2.4 Mouse IFN-α ELISA

Immunoabsorbant ELISA-plates were coated with the first antibody Rat anti-mouse IFN-α monoclonal antibody RMMA1 (1:2000 in PBS, 50µL/well, PBL), 4°C overnight or RT 3 h. After 3 washing steps with PBS-Tween 20 (0.05%), 200 µL/well of PBS-1% BSA were used for blocking for 30min at 37°C. After 3 washing steps with PBS-Tween 20 (0.05%), 50µL/well of samples (diluted in PBS- 0.05% Tween 20-1% BSA) were added to the wells and incubated for 2 h at RT. After 4 washings

with PBS-Tween 20 (0.05%), the second antibody Rabbit anti-mouse IFN-α polyclonal antibody (1:5000 in PBS-0.05% Tween 20-1% BSA, 50µL/well, PBL) was added with 50µL/well and incubated for 2 h at RT. After the washing steps with PBS-Tween 20, the third antibody Peroxidase-conjugated $F(ab)_2$ Donkey anti-Rabbit IgG(H+L) (1:4000 in PBS-0.05% Tween 20-1% BSA, 50µL/well, Jackson Immunoresearch) was added with 50µL/well and incubated for 1 h at RT. After the washing steps with PBS-Tween 20, tetramethylbenzidine (TMB) substrate (KPL) was used for colour detection (50µL/well). After incubation for 20 min~1 h at RT (protected from light), the reaction was stopped with 50µL/well 2N H_2SO_4. The colour reaction was read at 450 nm within 30 minutes of stopping reaction. Standard IFN-α4 (20,000IU/mL stock concentration) was gifted by Professor Rainer Zawatzky (German Cancer Research Center).

3.4.2.5 TGF-β ELISA

Mouse serum TGF-β was analyzed with 1:60 dilutions by DuoSet ELISA Development kit mouse TGF-β1 (R&D Systems) according to the manufacturer's protocol (www.RnDSystems.com).

3.4.2.6 IL-10 ELISA

Mouse serum IL-10 was analyzed with 1:2 dilutions by BD OptiEIA Mouse IL-10 ELISA Set (BD Biosciences) according to the manufacturer's protocol (www.bdbioscience.com).

3.4.3 ^{51}Cr release assay

The classical method to analyse the cell-dependent cytotoxicity is based on the release of radioactive chromium from dead cells. At the beginning of this experiment the target cells were incubated in a [^{51}Cr]-containing medium for one and a half hours, to get the chromium isotope into the cytoplasm (cytosol). There it binds covalently at proteins and accumulates in the cells. After that a washing step is needed to remove unbound [^{51}Cr]. The labelled target cells were co-cultured with the cytotoxic effector cells for four hours. After short centrifugation of the cells, the supernatants were

carefully removed and by means of a γ-counter the radioactivity could be quantified. The higher the amount of [^{51}Cr] released into the culture supernatant (percent specific cytotoxicity), the more target cells have been killed by the effector cells. Negative controls eliminate the CTL and measure spontaneous release of [^{51}Cr] from the target cells. Positive controls use detergent to lyse target cells and determine maximum [^{51}Cr] release. Percent specific cytotoxicity is calculated by the formula:

[(experimental cpm - spontaneous cpm)/(maximum cpm - spontaneous cpm)]×100.

To test the specific cytotoxicity induced by DNA vaccines in the mice, 2 weeks after DNA immunization, 5×10^7 spleen cells were re-stimulated *in vitro* for 5 days in RPMI medium containing 10% FCS and 0.5 μg/ml TPHPARIGL in 10 mL volume. Supernatant was collected at day 2 for IFN-γ ELISA and day 5 for IL-4 ELISA. Re-stimulated spleen cells were used as the effector cells for their cytotoxic activity in a standard 4 h ^{51}Cr release assay. ^{51}Cr-labeled P13.1 (lacZ$^+$) and P815 (lacZ$^-$) cells was used as the specific and unspecific target cells respectively. Target cells (2×10^6) were labeled with 100μCi Na^{51}CrO$_4$* for 90 min at 37°C. The target cells were washed 3 times in complete medium and resuspended at 5000 cells/100μL/well in a 96-well round-bottomed plate (Corning). Effector cells were added to the target cells (100μL/well) at various effector to target (E:T, 100:1, 50:1, 25:1, 12:1) ratios. 1% SDS was used as the positive control for maximum release. Complete medium was used as the negative control for spontaneous release. The plate was centrifuged (500 rpm, 3 min) and incubated for 4 h at 37°C. After the incubation, the plate was centrifuged again (1000 rpm, 3 min), and 100μl of supernatant were transferred to a γ-counter tube and sealed with wax. The amount of ^{51}Cr released was measured in a γ-counter (COBRA Packard) and the percentage of lysis was calculated from the formula showed before. The ^{51}Cr-release was read on a γ-counter.

* dose is dependent upon the age of the ^{51}Cr
1st week → 200 μL
2nd week → 250 μL
3rd week → 300 μL

3.4.4 Flow cytometry

For staining of primary mouse cells, 0.5~1 x 10^6 cells were washed twice with FACS

buffer (centrifugation at 4°C, 10 min, 1400rpm) and incubated with 10% Fc block (2.4G2 supernatant, gifted by Dr Adelheid Cerwenka) for 10 min on ice to block Fc receptors. Subsequently, the primary antibodies were added and cells were further incubated for 30 min on ice. For second antibodies or biotinylated antibodies, cells were washed twice with FACS buffer and stained with conjugated second antibodies or streptavidin for 30 min on ice. After staining, cells were washed twice and resuspended in 100~200 µL FACS buffer. Propidium iodide (PI, 1µg/mL) or 7-AAD (2.5µg/mL) was added 10 min before FACS acquisition to exclude dead cells. Viable cells (5×10^4~5×10^5) were acquired with the CellQuest software on a FACS*Calibur* (BD Biosciences) or with the FACSDiva software on a FACS*CantoII* (BD Biosciences) if PE-Cy7/APC-Cy7 was used.

For staining of cell lines, 0.5~1 x 10^6 cells were washed twice with FACS buffer (centrifugation at 4°C 5 min, 1200rpm) and incubated with the primary antibodies for 30 min on ice. For second antibodies or biotinylated antibodies, cells were washed twice with FACS buffer and stained with conjugated second antibodies or streptavidin for 30 min on ice. After staining, cells were washed twice and resuspended in 100~200 µL FACS buffer. Propidium iodide (PI, 1µg/mL) was added 10 min before FACS acquisition to exclude dead cells. Viable cells (5×10^4~5×10^5) were acquired with the CellQuest software on a FACS*Calibur* (BD Biosciences).

For anti-human and mouse EpCAM antibody analysis, 4×10^5 MCF-7 (overexpression of human EpCAM) and DA3 (overexpression of mouse EpCAM) cells were used respectively. Mouse sera were diluted as 1:100 in FACS buffer and stained for 30 min on ice. Cells were washed twice with FACS buffer and stained with conjugated second antibodies for 30 min on ice. After staining, cells were washed twice and resuspended in 100~200 µL FACS buffer. Propidium iodide (PI, 1µg/mL) was added 10 min before FACS acquisition to exclude dead cells. Viable cells (5×10^4~5×10^5) were analyzed with the CellQuest software on a FACS*Calibur* (BD Biosciences).

FlowJo software (Tree Star, San Carlon, CA) was used to analyze FACS data. Data were expressed as dot plots or histograms.

List of antibodies for FACS staining:

Antigen-label	**Isotype & Clone**	**Cat. No. or Author**	**Dilution**
Human EpCAM	Mouse IgG1, HEA125	Dr. Gerhard Moldenhauer,	1:100
Mouse EpCAM	Rat IgG2a, κ, G8.8,	Dr. Gerhard Moldenhauer	1:100
NDV HN	Mouse IgG2a, HN.B	Annette Arnold	1:100
CD3e-APC	Hamster IgG1, κ, 145-2C11	BD 553066	1:100
CD4-PE	Rat IgG2a, κ, RM4-5	BD 553049	1:100
CD8a-APC-Cy7	Rat IgG2a, κ, 53-6.7	BD 557654	1:100
CD11b-APC	Rat IgG2b, κ, M1/70	BD 553312	1:100
CD11c-PE	Hamster IgG1, λ2, HL3	BD 557401	1:100
CD45.2-FITC	Mouse IgG2a, κ, 104	BD 553772	1:100
CD45.2-PerCP-Cy5.5	Mouse IgG2a, κ, 104	BD 552950	1:100
CD49b-FITC (Pan-NK)	Rat IgM, κ, DX5	BD 553858	1:100
CD80-PE	Hamster IgG2, κ, 16-10A1		1:100
CD86-PE	Rat IgG2a, κ, GL1	BD 553692	1:100
F4/80-PE	Rat IgG2b, CI:A3-1	CL8940PE	1:100
Gr1-FITC	Rat IgG2b, κ, RB6-8C5	BD 553126	1:100
$H2D^d$-PE	Mouse IgG2a, κ, 34-2-12	BD 553580	1:100
IAd-PE	Mouse IgG2b, κ, AMS-32.1	BD 553548	1:100
Hamster IgG1-PE Isotype	IgG1, λ1, G235-2356	BD 554711	1:100
Mouse IgM+G+A-PE	Goat $F(ab')_2$	SouthernBiotech1012-09	1:100
Rat IgG-FITC	Goat $F(ab')_2$	R&D Systems F0104	1:100
Mouse IgG1	Rat IgG1, κ, A85-1	BD 550083	1:100
Mouse IgG2a	Rat IgG1, κ, R19-15	BD 553390	1:100
streptavidin-PE		BD554061	1:100
streptavidin-APC		BD554067	1:100

All staining was done in 50µL incubation volume.

3.4.5 Hemadsorption assay

The lymphocyte binding activity of HN proteins was determined by testing their ability to adsorb sheep erythrocytes. HN expressing BHK cell monolayers (48 h after transfection as described in 3.4.3) were incubated for 20 min with a 2% suspension of sheep red blood cells (purchased from Oxoid, Wesel, Germany) in PBS supplemented with 1% $CaCl_2$ and $MgCl_2$ (Gibco Life Technologies). Microscopic observations allowed the detection of bound erythrocytes at the surface of the cells. After extensive washings, adsorbed erythrocytes were lysed in 50 mM NH_4Cl, and the lysates were clarified by centrifugation. HAd activity was quantified by measuring the absorbance at 540 nm after subtracting the background absorbance obtained with BHK cells not expressing NDV proteins.

3.4.6 Immunohistochemistry

Freshly isolated tumor, ear and skin tissues were frozen in liquid nitrogen and then stored in -80^{o}C until use. Tissues were cut to frozen sections with 4μm thickness using a cryostat and stored in -80^{o}C until use. Frozen sections were stained by immunohistochemistry. For tumor infiltrated lymphocytes, CD4, CD8 T cells and NK cells were stained by anti-CD4 (h129.19), anti-CD8 (53-6.7) and anti-CD49b (Hal/29) antibodies (1:200). For DC in ear and flank skin, anti-CD11c and anti-CD207 antibodies (1:200) were used. Anti-Ig HRP Detection Kits (both anti-Hamster and Anti-Rat HRP Kits, BD Bioscience) were used for detection. Cytoseal 60 (Stephens Scientific), and visualized with Nomarski optics. Staining was followed the manufacturer's protocol (www.bdbioscience.com). All images were digitally captured on a Zeiss Axioplan 2 imaging microscope equipped with a AxioCam camera and imaged using AxisoVision 4.0 software.

3.4.7 Preparation of cell lysate

Cells were harvested, washed 3 times in PBS (250 g, 3 min.) and counted. Cells were resuspended in 200 μL PBS per 1×10^{7} cells. The cells were put directly to the liquid nitrogen till freeze and transferred immediately to 37^{o}C water bath. Shake the tube until the buffer by pipetting up and down and then they were incubated for 15 minutes

on a shaker at room temperature. After centrifugation in a table centrifuge (16000 g, 20 min, 4^{o}C), the supernatant was measured for protein concentration by Bradford protein assay, transferred to a chilled test tube and stored at -80°C.

3.5 *In vivo* experiments

3.5.1 Buffers and solutions

Tissue digestion buffer	Collagenase IV (Cell systems) 2.5 mg/mL DNase (Roche) 50U/mL FCS 1% (v/v) in PBS, freshly prepared
Skin digestion buffer	Trypsin 2.5% EDTA 2.5mM in PBS, freshly prepared

3.5.2 DNA immunization and electroporation

Mice were anesthetized by ip injection of Rompun (4.5mg/kg BW) (Bayer, Leverkusen, Germany) and Ketanest (45 mg/kg BW) (Bayer, Leverkusen, Germany). 25μg/50μL (for gene expression, immune responses and prophylactic tumor model) or 50μg/50μL (for therapeutic tumor model) of DNA, dissolved in PBS, were injected either ie or id or im into the ear or shaved flank or quadriceps by using BD Insulin syringe (29-gauge). To control the depth of needle penetration, the needle was covered with polyethylene tubing to expose only 2 mm of the bevel.

DNA electroporation (EP) was performed by ELGEN1000 electroporation-based DNA delivery system (Inovio) with optimal parameters (Table 3.1) suggested by this company. For DNA delivery to the ear pinna and flank skin, caliper electrode and pedal were used in the mouse program. After DNA injection with 50μL volume, Ultrasound gel was applied to the local injection site. Caliper electrode was placed at the injection site, with 1 mm distance between the two electrodes. EP was performed by pressing the pedal followed by a triple beep which indicated successful EP.

Table 3.1 Electroporation parameters

Time1	20 ms
Volt1	**80V/cm**
Number of sequence	5
Number of trains	1
Pulse Delay	100 ms
Train Delay	100 ms
Current Limit	1000 mA

3.5.3 Tumor inoculation

Tumor cells were collected, washed 3 times in PBS, and resuspended with desired concentration in PBS. 100μL tumor cells were inoculated sc or iv. Tumor growth was followed every 2 or 3 days.

3.5.4 Preparation of mouse serum

Blood samples were obtained from the retro-orbital plexus of mice, incubated at 37°C for 30 min or at 4°C for 4 h, centrifuged at 13,000 rpm, 4°C for 15 min. Aliquot the supernatant and store at -20 °C or -80 °C.

3.5.5 *In vivo* imaging of luciferase expression

The IVIS100 imaging system (Xenogen, Alameda, USA) was used for imaging mice. Bioluminescent color images were acquired by Living Image 2.50 software overlay (Xenogen, Alameda, USA) and analyzed by Igor Pro 4.09A software. D-luciferin potassium salt (SYNCHEM), the firefly luciferase substrate, was diluted to 30 mg/mL in PBS (filtered by 0.22μm filter). Imaging of mice was made 5 min after the intraperitoneal (ip) injection of 100 μL D-luciferin solution. Bioluminescence signals are expressed in units of photons per second per cubic centimeter per steradian (p/sec/cm^2/sr). Mice injected with DNA encoding firefly luciferase were imaged at 4 h, 8 h, and 1-7 days, then every week.

3.5.6 Preparation of single cell suspension from murine organs

Mice were sacrificed by CO_2 inhalation and the fur was sterilized with 70% ethanol. All the following steps were carried out under sterile conditions in a tissue culture hood. The mice were placed on a preparation pad and fastened with metal pins. They were then cut open on the ventral side through the skin and the peritoneum, and the organs were taken out.

Centrifugation in preparation of primary cells was taken at 4°C, 300g, 10 min.

3.5.6.1 Spleen

For preparation of splenocytes for ^{51}Cr release assay, spleen was taken out and placed into a 40µm cell strainer in a 60mm dish filled halfway with PBS. With a syringe plug the cells were carefully pushed out of the spleen by repeated strokes from the centre of the spleen towards its ends. This procedure was continued until all of the cells were in suspension in the PBS and only the outer skin of the spleen remained. The suspended cells were centrifuged and 1 mL ACK buffer was added the cell pellet. After 1min the cells were washed in complete medium twice and then they were counted and used in the subsequent experiments.

For FACS analysis, spleen was taken out and digested in Tissue digestion buffer at 37°C for 10 min. Then it was crushed as indicated in the protocol for preparation of splenocytes for ^{51}Cr release assay.

3.5.6.2 Lymph node

Lymph node was taken out, digested in Tissue digestion buffer at 37°C for 10 min, and crush in a cell strainer (40µm). Then the same protocol as for spleen cell preparation was followed.

3.5.6.3 Peripheral blood

For FACS analysis, 200µL fresh blood was mixed immediately with 1 mL 0.01% EDTA in PBS to prevent clotting and put on ice. Pellet was collected by centrifugation and 1 mL ACK buffer was added. After 10 min at RT, cells were washed twice in

complete medium and used in the subsequent experiments.

3.5.6.4 Bone marrow

Bone marrow cells were prepared as the protocol described in 3.3.4.

3.5.6.5 Tumor

A single cell suspension of DA3 tumor was obtained by tumor processing and enzymatic digestion. Briefly, the tumor was minced into small pieces (<5 mm), and washed with complete DMEM. The tumor digestion was carried out at 37°C for 20 min with shaking. The cell suspension was then filtered through 70 μm filter to remove cell clumps and undigested tissue fragments, and washed twice in complete DMEM. Cells were counted and used in the subsequent experiments.

3.5.6.6 Ear

Ear was cut and placed in a petri dish (6cm) until dry. Two ear halves were separated in skin digestion buffer (2.5% trypsin, 2.5mM EDTA in PBS). Ventral halves (thin) were incubated at 37^{o}C for 45 min, and dorsal halves (thick) were incubated at 37^{o}C for 90 min. Both epidermis and dermis (separated if necessary) were placed in a 40μm cell strainer and carefully dissociated in ice-cold PBS. Cells were then centrifuged and resuspended in 1mL ice-cold H_2O for exactly 30 s to lyse keratinocytes. Lysis was stopped by 10mL PBS. Cells were washed 3 times and used in the subsequent experiments.

3.5.7 Staining of metastases

Organs from the tumor bearing mice were stained in Boin's solution (Sigma) for metastases. Nodules were counted after 72 h.

3.6 Statistical methods

Experimental data are expressed as mean±SD if not illustrated. The statistical significance of differences in mean values was determined using Student's t test. Survival data are presented as a Kaplan-Meier survival curve and analyzed with log-rank test. Differences of at least $p < 0.05$ are considered to be significant.

4 Results

4.1 Superiority of ear pinna to flank skin for antigen expression and induction of immune responses by DNA immunization

Usually, intradermal DNA immunization is administered to the abdominal or flank skin in mouse experiments. Previous studies in our group showed, however, a superiority of DNA immunization into the ear pinna for induction of immune responses compared to abdominal skin and muscle (75).

4.1.1 Comparison of antigen expression in ear pinna and flank

To directly visualize and measure antigen (Ag) expression induced by DNA immunization *in vivo*, we used a plasmid CMV-luc construct encoding firefly luciferase as a reporter gene. The luciferase protein expression can be detected by an *in vivo* imaging system (IVIS 100) after applying the substrate D-luciferin.

To compare the Ag expression in the ear pinna and the flank skin by DNA immunization, we injected CMV-luc into both the ear pinna (ie) and the flank skin (id) with different amount of DNA (25μg to the left side and 10μg to the right side). *In vivo* imaging showed that luciferase expression was superior in the ear pinna compared to the flank skin by different amount of DNA injection. Quantitative analysis revealed 10 times higher luciferase expression in the ear pinna than in the flank skin (Figure 4.1). The Ag expression reached the plateau 24 h after of the DNA injection and maintained the high level for 1 week, before dropping a little after 2 weeks. 25μg and 10μg DNA induced similar Ag expression in the ear pinna, and induced also similar Ag expression for 3 days in the flank skin. From day 4 to day 14, 25μg DNA showed somewhat better Ag expression to 10μg DNA in the flank skin.

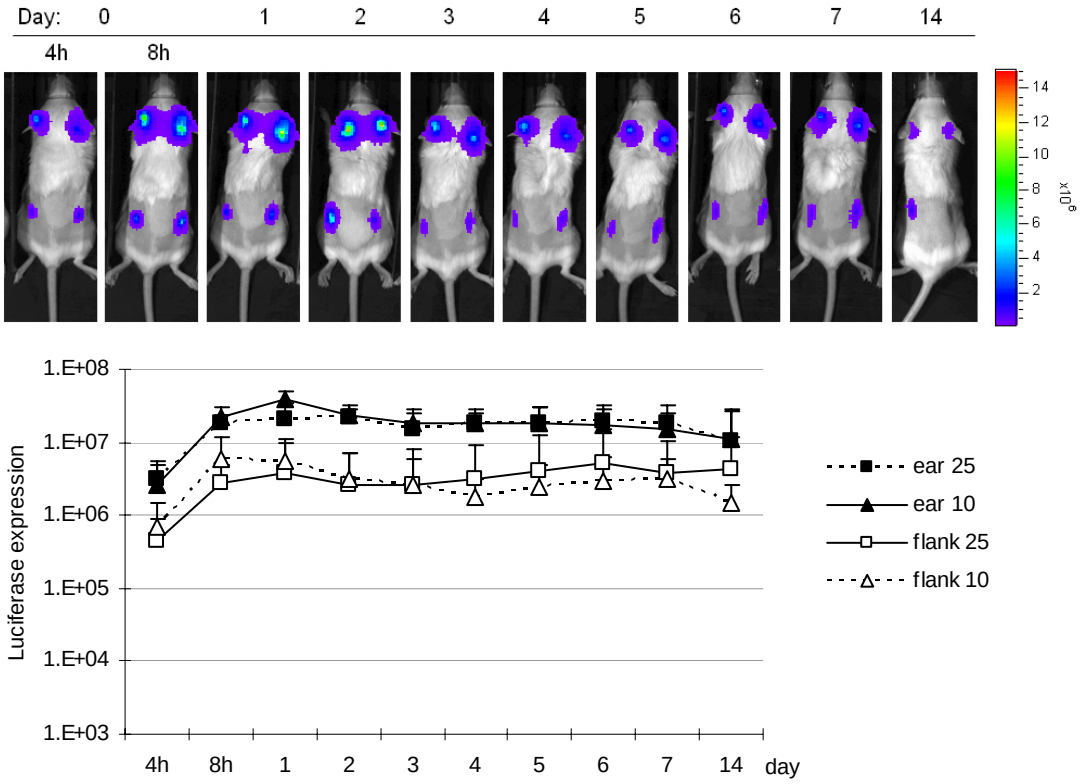

Figure 4.1 Ag expression in the ear pinna and flank skin by DNA immunization.

Balb/c mice (n=5) were immunized with a plasmid CMV-luc encoding firefly luciferase (left: 25μg; right: 10μg) ie and id. Luciferase (Ag) expression was monitored by *in vivo* imaging with the IVIS100 system at different time-points (exposure time: 60s). Bioluminescent signal was calculated for region of interest (ROI) (Unit: p/sec/cm^2/sr).

4.1.2 Humoral responses by ear pinna or flank skin DNA immunization

By DNA immunization with the plasmid CMV-lacZ (pCMV SPRORT-βgal, Invitrogen) encoding beta-galactosidase (β-gal) protein as a model Ag, specific anti-β-gal antibody and T cell cytotoxicity can be induced (75). To compare the humoral immune responses induced by DNA immunization to the ear pinna and to the flank skin, we applied CMV-lacZ (25μg/50μL) intradermally to mice at either site. Sera were taken at day 7 and day 14 of the immunization. Anti-β-gal antibodies were detected at day 7 in both groups. They were highly increased at day 14 (Figure 4.2). Antibody titer was higher by ie injection than by id injection at both time-points (about 1.7 times higher at day 7 and 15 times higher day 14). These results revealed that a better humoral immune response could be induced by injection of DNA to the ear pinna rather than flank skin which is used in most cases for DNA intradermal injection.

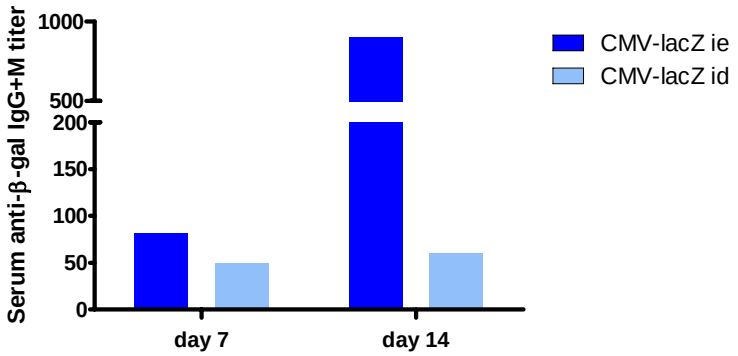

Figure 4.2 Titers of serum anti-β-gal antibodies in lacZ-immunized mice.

DBA/2 mice (n=3/group) were immunized with CMV-lacZ plasmid (25μg/50μL) ie or id. Serum anti-β-gal antibodies (IgG+M) at day 7 and day 14 were analyzed by β-gal ELISA. Experiments were repeated for 3 times with similar results.

4.1.3 Cellular responses by ear pinna or flank skin DNA immunization

4.1.3.1 Cytotoxicity

To evaluate T cell mediated immune responses induced by ie and id DNA immunization, splenocytes from mice immunized ie or id with CMV-lacZ (25μg/50μL) at day 14 were re-stimulated with an L^d-restricted β-gal peptide for 5 days *in vitro* and analyzed for β-gal peptide-specific CTL responses by a 4 h ^{51}Cr release assay as described before (75). Re-stimulated splenocytes were used as effector cells, $lacZ^+$ tumor cells P13.1 (P815 stably transfected with lacZ gene) were used as target cells, and P815 cells were used as the negative control. Spontaneous release was always below 10%. Results of one representative experiment from 3 are shown in Figure 4.3. Only by ie lacZ gene immunization (25μg), efficient cytotoxicity was induced with specific lysis around 60% at 100:1 effector to target cell ratio (E:T) and around 20% specific lysis at 12:1 E:T. By id lacZ gene immunization, no specific CTL responses were generated at day 14. These results showed ie DNA immunization could induce a stronger cytotoxicity than id DNA immunization.

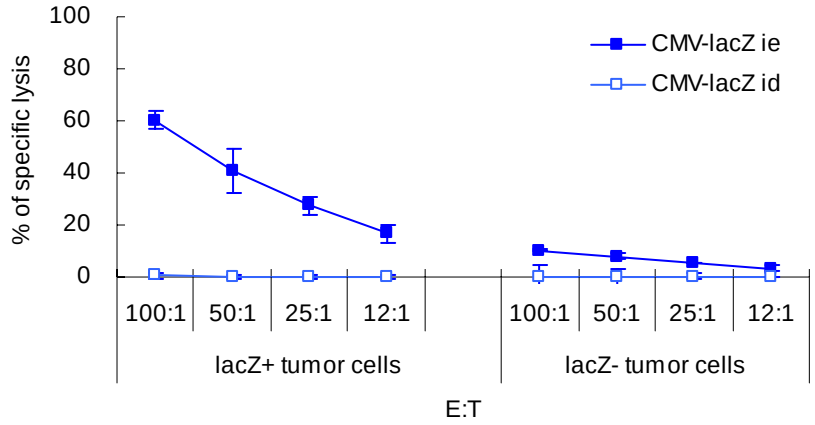

Figure 4.3 β-gal specific CTL responses in lacZ immunized mice.

Splenocytes were isolated from immunized DBA/2 mice (n=3/group) 14 days after a single injection with CMV-lacZ (25μg/50μL) ie or id. The splenocytes were re-stimulated for 5 days with 0.5μg/mL TPHPARIGL peptide and used as the effector cells in a 4 h ^{51}Cr release assay. lacZ^{+} tumor cells P13.1 were used as the target cells, and lacZ^{-} tumor cells P815 were used as the negative control. E:T, effector to target cell ratio. Experiments were repeated for 3 times with similar results.

4.1.3.2 IFN-γ and IL-4 secretion

To further prove the stronger cellular immune responses induced by ie DNA immunization than id DNA immunization, IFN-γ and IL-4 secretion to the supernatant from the re-stimulated splenocytes were analyzed by ELISA. Ie DNA immunization was better for IFN-γ secretion, which is a benefit for cellular immune response induction. In contrast, id DNA immunization was better for IL-4 production (Figure 4.4), which is a benefit to humoral immune response induction.

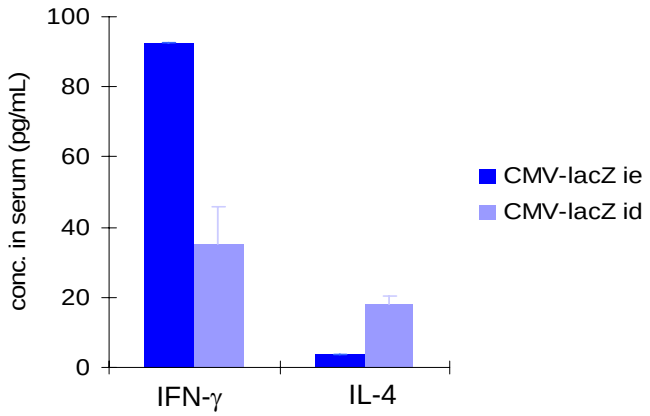

Figure 4.4 β-gal specific IFN-γ and IL-4 secretion in lacZ immunized mice.

Splenocytes were isolated from immunized DBA/2 mice (n=3/group) 14 days after a single injection with CMV-lacZ (25μg/50μL) ie or id. These splenocytes were re-stimulated for 5 days with 0.5μg/mL TPHPARIGL peptide and the supernatants from day 2 and day 5 were analyzed for IFN-γ and IL-4 ELISA respectively. Experiments were repeated for 3 times with similar results.

4.2 Adjuvant effect of Newcastle disease virus HN gene for ear pinna DNA vaccination with beta-galactosidase as a surrogate tumor antigen

Newcastle Disease Virus (NDV) is an avian paramyxovirus with replication competence in human tumor cells and interesting anti-neoplastic and immune stimulatory properties (84, 114). Viral hemagglutinin-neuraminidase (HN), a type II glycoprotein, is a receptor recognition site for binding sialic acid of host cell receptor glycoconjugates. It was shown in our previous studies that HN could stimulate a strong human natural interferon-α response (107-109) and could confer T cell co-stimulatory function (108, 115). Because of these immunostimulating activities of HN, we intended to evaluate the use of HN gene as an adjuvant in anti-cancer DNA vaccines.

4.2.1 *In vitro* activity of the HN molecule

4.2.1.1 Construction of a plasmid encoding the HN gene

The HN gene from NDV Ulster was copied by PCR and cloned into pTandem1 (Novagen) to construct the CMV-HN vector (Figure 4.5a). CMV-HN was transfected into BHK21 cells (BHK) which were then analyzed for cell surface HN expression by FACS. Figure 4.5b shows HN molecule expression by the transfected cells.

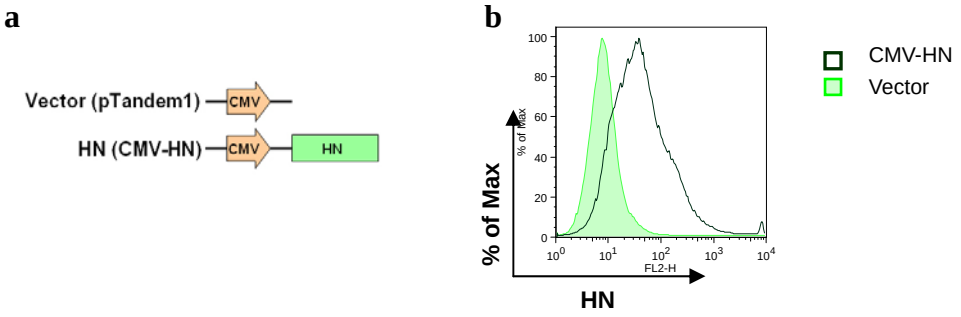

Figure 4.5 CMV-HN vector construction and HN expression analyzed by FACS.

The HN gene was cloned into the Vector to construct CMV-HN (a). CMV-HN was transfected into BHK cells. HN expression at the cell surface was analyzed by FACS with a monoclonal anti-HN antibody (HN.B) 24 h after transfection (b).

4.2.1.2 Cell binding activity of HN

The lymphocyte binding activity of HN proteins was determined by testing their ability to adsorb sheep erythrocytes (hemadsorption activity, HAd). BHK cells were transfected with CMV-HN or a control DNA CMV-lacZ. 24 h later, these transfected cells were coincubated with sheep erythrocytes for cell binding activity analysis. Transfection with a control DNA did not improve cell binding compared to non-transfected control cells. However, HN expression at the cell surface improved erythrocyte cell binding activity (Figure 4.6).

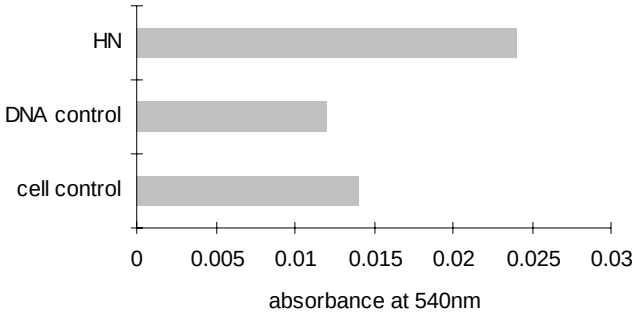

Figure 4.6 Cell binding activity of HN *in vitro*.

Cell binding activity of HN was analyzed by hemadsorption assay (HAd). Untransfecd BHK cells, CMV-HN or CMV-lacZ (pCMV SPORT-βgal, used as a DNA control) transfected BHK cells were coincubated with sheep erythrocytes. Bound erythrocytes were lysed in 50 mM NH_4Cl, and HAd activity was quantified by measuring the absorbance at 540 nm. Experiments were repeated 3 times with similar results.

4.2.1.3 IFN-α induction activity of HN

Human PBMCs were coincubated with BHK cells transected with CMV-HN to test for IFN-α induction. While transfected BHK cells themselves did not produce IFN-α (Figure 4.7 Cell control group), PBMC coincubated with CMV-HN transfected BHK cells produced 16 pg/ml IFN-α in the supernatant. This is 2.7 times higher than the IFN-α produced by coincubation with control DNA transfected BHK cells.

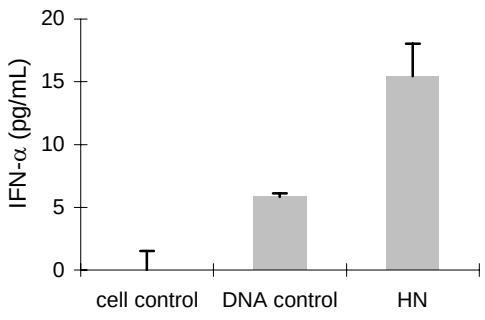

Figure 4.7 IFN-α induction activity of HN *in vitro*.

Human PBMCs were coincubated with BHK cells transfected with CMV-HN or a control DNA CMV-lacZ. Untransfected BHK cells were used as the negative control. Supernatants of the coculture were analyzed for IFN-α production by ELISA. Experiments were repeated 3 times with similar results.

4.2.2 *In vivo* activity by HN DNA injection

4.2.2.1 Serum IFN-α induction by NDV administration

To analyze the IFN-α induction activity by NDV *in vivo*, we injected NDV Ulster ip to the mice. Sera were taken at different time-points, and analyzed for IFN-α levels were by ELISA. Serum IFN-α was detected from 4 h after NDV injection, reached the peak at 8h, and then decreased. It is not detectable after 24 h with a low dose (500HU) and after 48 h with a high dose (2000HU) of NDV per injection. This shows that the IFN response is an early induced immune response.

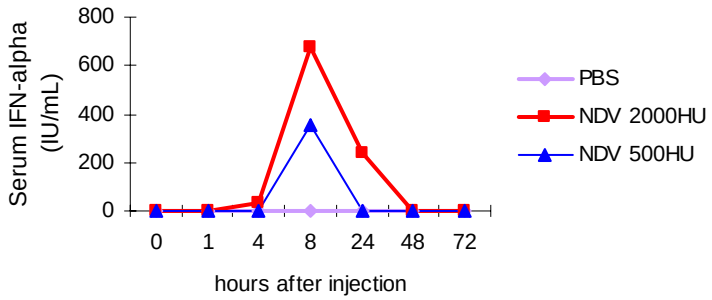

Figure 4.8 Serum IFN-α induction by NDV ip administration.

NDV Ulster (500HU or 2000HU) was injected ip to the Balb/c mice. Sera from different time-points were analyzed for IFN-α production by ELISA.

4.2.2.2 Serum IFN-α induction by HN DNA ie immunization

The peak serum IFN-α induction by NDV in mice was detected at 8 h (Figure 4.8). Since the gene expression level after DNA immunization reached its peak at 24 h, we analyzed serum IFN-α induction by HN DNA immunization at 32 h (24 h + 8 h). Mice immunized with HN DNA produced significantly more IFN-α than the control groups (Vector and PBS immunization).

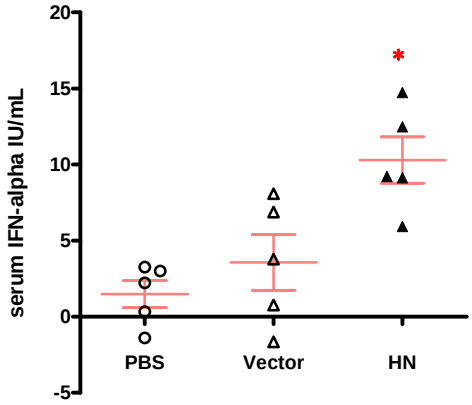

Figure 4.9 Serum IFN-α induction by HN DNA ie immunization

HN DNA (50μg/50μL) was applied ie to Balb/c mice (n=5/group), with Vector and PBS injection as controls. Sera at 32h were analyzed by IFN-α ELISA (shown are MEAN±SEM).
* Compared to the Vector and PBS groups, $p<0.05$

4.2.2.3 Prophylactic anti-tumor effect by HN DNA immunization

To further analyze the potential immunostimulating effect induced by HN DNA immunization, HN DNA was applied in a prophylactic immunization protocol of the mouse mastocytoma tumor model P815. In this non-aggressive tumor model, 40% of the mice with 3 prophylactic HN DNA vaccinations were protected from the tumor growth (Figure 4.10). We then applied the HN DNA to the metastatic mouse mammary carcinoma tumor model DA3. With 2 prophylactic HN DNA vaccinations (ie or sc), tumor growth was significantly inhibited compared to Vector and PBS groups as shown in Figure 4.11.

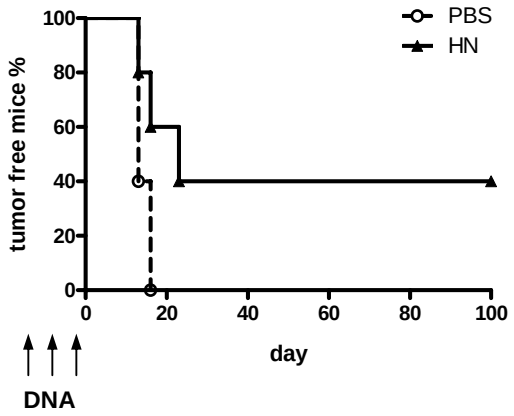

Figure 4.10 Prophylactic anti-tumor effect induced HN DNA ie immunization in P815 tumor model.

HN DNA (50μg/50μL) was immunized ie to the DBA/2 mice (n=5/group) 3 times with 2 weeks interval. 2 weeks after the 3rd DNA immunization, 2×10^6 P815 cells were inoculated sc to the mice. Compared to the PBS group, p=0.0528

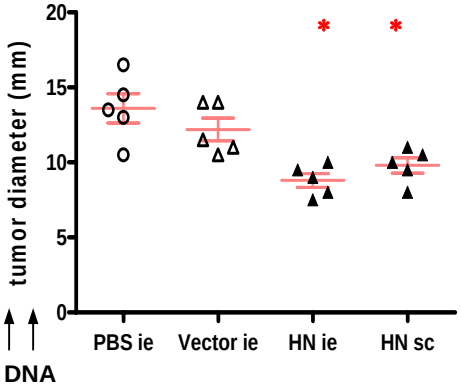

Figure 4.11 Prophylactic anti-tumor immunization effects by HN DNA in the DA3 tumor model.

HN DNA (50μg/50μL) was applied ie to Balb/c mice (n=5/group) twice with 2 weeks interval. 2 weeks after the 2nd DNA immunization, DA3 cells (1×10^7) were inoculated sc to the mice. Tumor diameters (MEAN±SEM) from day 48 are shown.

* Compared to the Vector and PBS groups, $p<0.05$

4.2.3 Adjuvant effect of HN in prophylactic mouse lymphoma models

The immunostimulating effect of the HN gene has thus far been shown *in vitro* and *in vivo*. Therefore, it was of interest to test the HN molecule as a potential adjuvant for an Ag specific DNA vaccine. We applied the HN gene as an adjuvant to lacZ DNA vaccine in a mouse lymphoma transfected with the lacZ gene so that the gene product beta-gal protein served as a surrogate tumor Ag.

4.2.3.1 Construction of vectors encoding HN and lacZ gene

The lacZ gene was cut with respective restriction enzymes from CMV-lacZ (CMV SPRORT-βgal, Invitrogen) and cloned into the CMV-HN vector either behind the HN gene as a fusion protein (expressed at the cell surface) as the HN-lacZ vector or in front of the HN gene separated by an IRES sequence (to be expressed separately inside the cells) as lacZ-HN vector (Figure 4.12). Those vectors were transfected to BHK cells, and analyzed for HN and lacZ expression *in vitro*. Figure 4.13a shows a strong HN expression at the cell surface by HN and lacZ-HN gene transfection, and a weak HN expression by HN-lacZ gene transfection. This indicated that by fusion with the lacZ gene, the expression of HN gene at the cell surface was decreased. lacZ gene expression was analyzed either by FDG staining with FACS assay or by a fluorometric assay (Figure 4.13b and c). lacZ and lacZ-HN transfection led to a high β-gal expression, while HN-lacZ transfection led only to a very low but detectable (about 30 times lower than lacZ and lacZ-HN) β-gal expression (Figure 4.13c). By X-gal staining, β-gal expression could also be detected in lacZ and lacZ-HN transfected cells (Figure 4.13d)

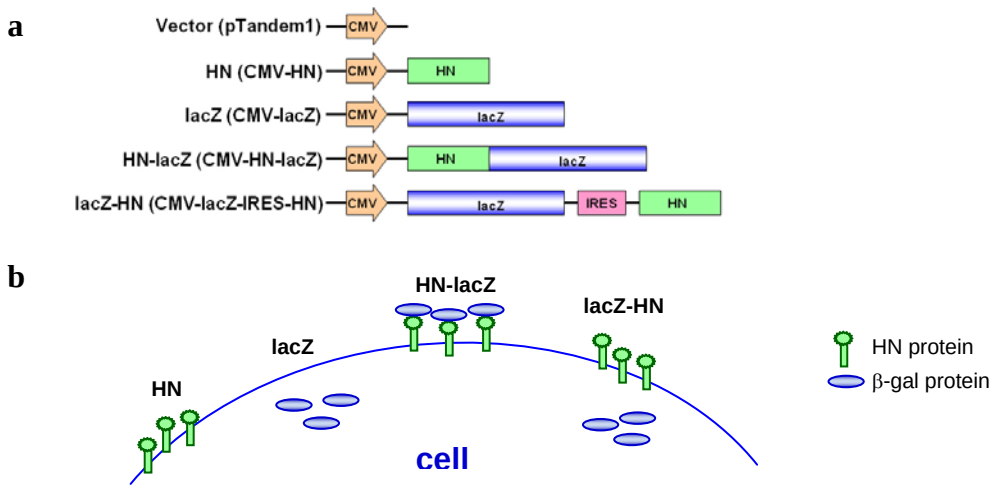

Figure 4.12 Construction of vectors encoding HN and lacZ genes.

CMV-lacZ (pCMV SPRORT-βgal, Invitrogen) was used as the CMV-lacZ vector. lacZ gene was cut out from CMV-lacZ and cloned into CMV-HN either behind the HN gene as a fusion protein or in front of the HN gene expressed separately. pTandem1 was used as the control vector (a). HN and lacZ expression patterns in cells are illustrated in b.

4.2.3.2 Adjuvant effect of HN in the Eb-lacZ tumor model

The above DNA vaccines were applied in a prophylactic immunization protocol in the mouse lymphoma model Eb-lacZ (Eb cell line with stable lacZ gene expression, Figure 4.14a). By 2 times prophylactic DNA vaccinations, mice vaccinated with lacZ and lacZ-HN were 100% protected from the tumor growth (Figure 4.14). 40% of the mice vaccinated with HN-lacZ were tumor-free. The anti-tumor effect was significant compared to the PBS group (Figure 4.14). Fusion of HN and lacZ genes impaired both the protein expression (Figure 4.13) as well as the anti-tumor activity.

4.2.3.3 Adjuvant effect of HN in ESb-lacZ tumor model

It was shown in the Eb-lacZ tumor model that lacZ gene immunization protected 100% mice from tumor growth no matter whether HN was used as an adjuvant or not. To analyze further the HN activity as an adjuvant for DNA ie immunization, these DNA vaccines were applied next to the ESb-lacZ tumor model (X-gal staining, Figure 4.15a). ESb is a highly aggressive subline of Eb lymphoma cells.

It was reported that type I IFN has an effect on DC maturation (116). Since HN is a strong IFN-α inducer, it is possible to induce IFN-α locally in the ear pinna. To avoid a possible interference with DC maturation at the local injection site, we also administered the HN plasmid separately subcutaneously to the flank.

In the prophylactic ESb-lacZ tumor model, a significant anti-tumor effect was achieved by lacZ gene vaccination (Figure 4.15b). With HN as an adjuvant, tumor inhibition was improved, especially by HN sc administration. HN sc immunization, rather than a vector sc immunization, induced a significant improvement to the anti-tumor activity compared to lacZ immunization alone. This suggested that the adjuvant effect resulted from the HN gene and was not just a vector effect. ESb-lacZ tumor weight at day 20 (c) corresponded the tumor diameters (b).

In another prophylactic experiment in this tumor model, mice were analyzed for survival (Figure 4.16). The median survival was 32 days by lacZ-HN immunization and 28 days by lacZ ie+HN sc, compared to 21 days by lacZ immunization and 25

days by Vector immunization (Table 4.1).

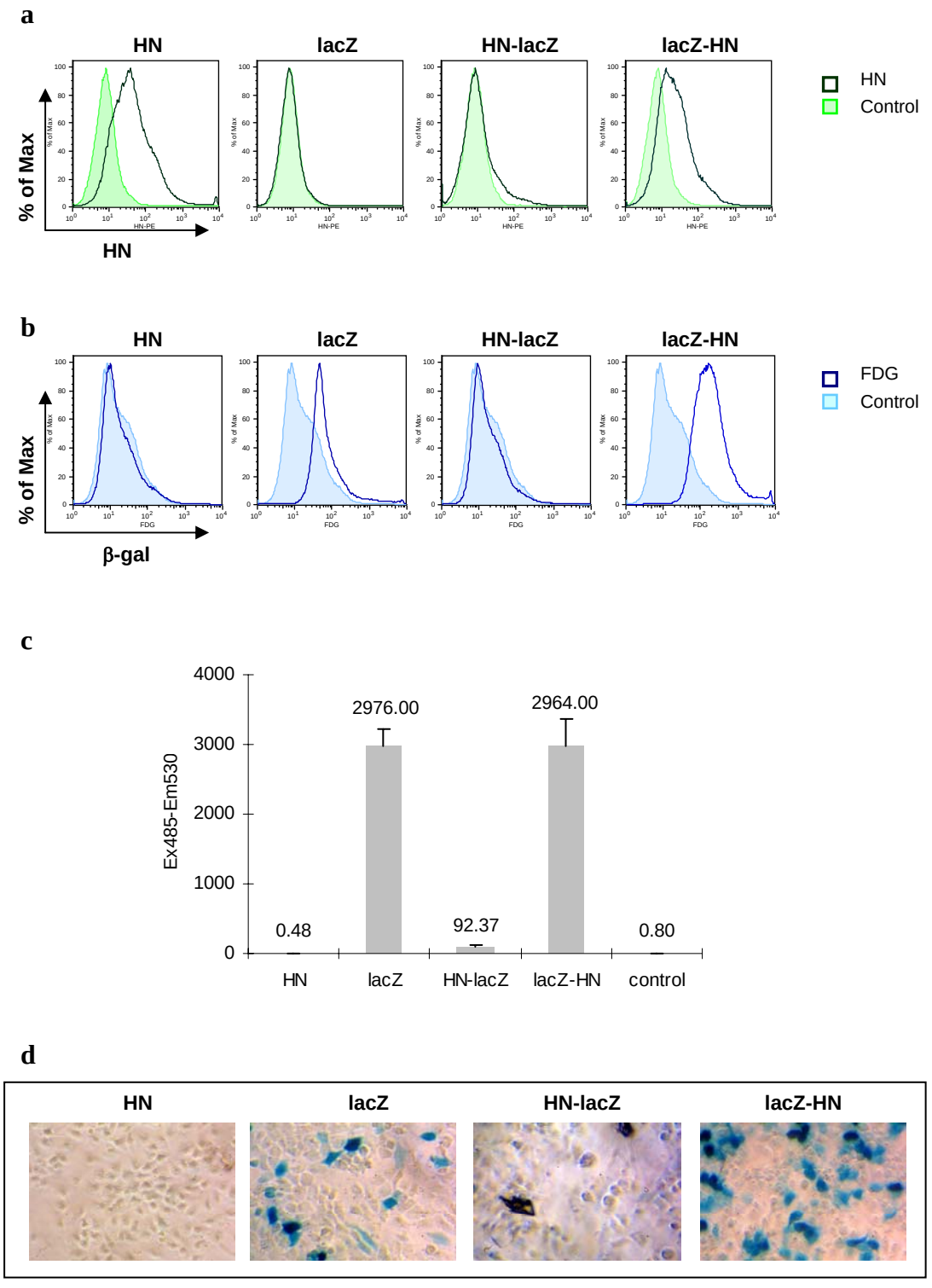

Figure 4.13 Verification of vectors encoding HN and lacZ gene.

Vectors encoding the HN and lacZ genes (Figure 4.12) were transfected to BHK cells. HN expression was analyzed by FACS with an anti-HN antibody (HN.B) (a). β-gal expression was analyzed by FDG staining with FACS assay (b) and fluorometric assay (c). β-gal expression was also analyzed by X-gal staining (d). Original magnification: ×400.

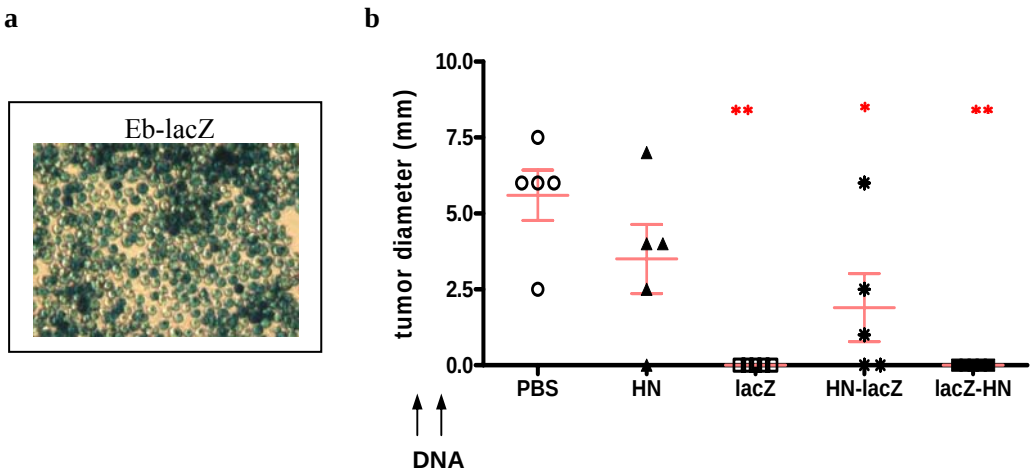

Figure 4.14 Prophylactic anti-tumor effect induced by lacZ gene immunization with HN as an adjuvant in Eb-lacZ tumor model.

a. X-gal staining of Eb-lacZ cells. Original magnification: ×400. **b.** Prophylactic anti-tumor effect of lacZ gene immunization with HN as an adjuvant in Eb-lacZ tumor model. DNA vaccines (50μg/50μL) were immunized ie to the DBA/2 mice (n=5/group) twice with 2 weeks interval. 2 weeks after the 2nd DNA immunization, 4×10^6 Eb-lacZ cells were inoculated sc to the mice. Tumor diameters (MEAN±SEM) from day 11 are shown.

* Compared to the Vector and PBS groups, $p<0.05$;

** Compared to the Vector and PBS groups, $p<0.01$

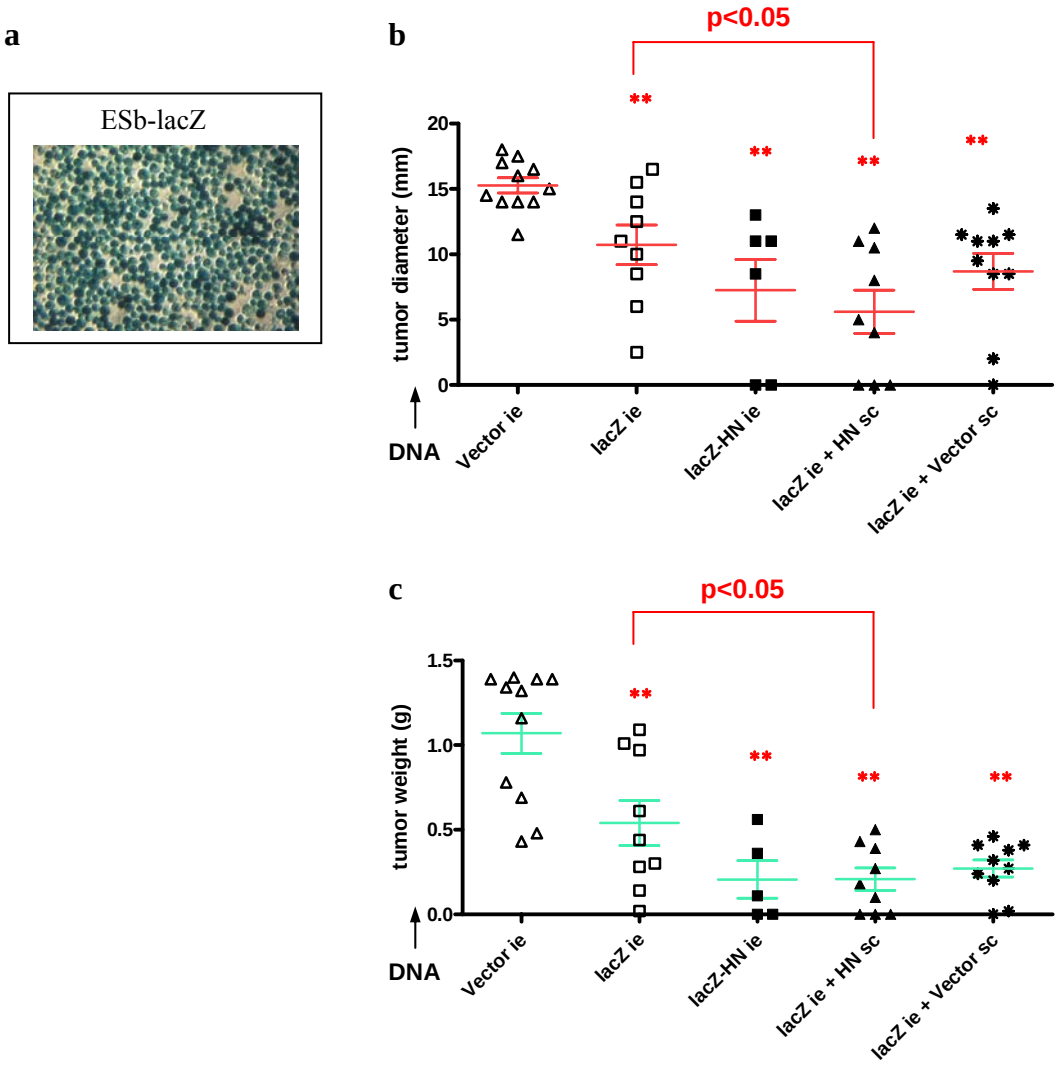

Figure 4.15 Improvement of anti-tumor immunity by HN in a prophylactic setting of the ESb-lacZ tumor model

a. X-gal staining of ESb-lacZ. Original magnification: ×400. **b.** ESb-lacZ tumor diameter at day 20. DNA vaccines (50μg/50μL) were immunized ie to the DBA/2 mice (n=5~11/group). 2 weeks after the DNA immunization, 2×10^5 ESb-lacZ cells were inoculated sc to the mice. Tumor diameters (MEAN±SEM) at day 20 are shown. **c.** ESb-lacZ tumor weight (MEAN±SEM) at day 20. Mice were sacrificed at day 20. Local ESb-lacZ tumors were taken out and weighed. ** Compared to the Vector group, $p<0.01$

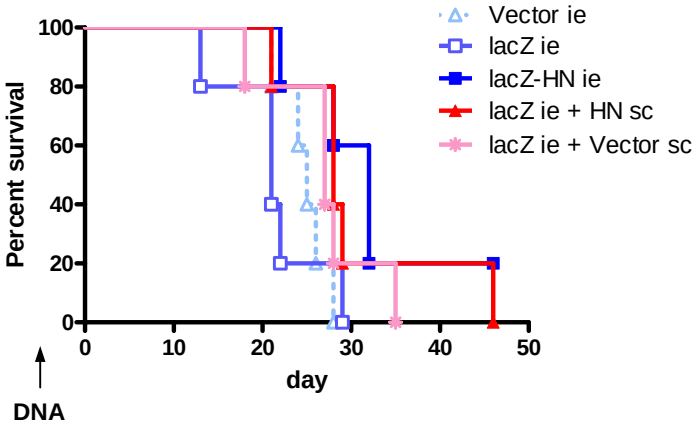

Figure 4.16 Survival of mice in the prophylactic ESb-lacZ tumor model.

DNA vaccines (50μg/50μL) were applied ie to the DBA/2 mice (n=5/group). 2 weeks after the DNA immunization, 2×10^5 ESb-lacZ cells were inoculated sc to the mice. Mice survival was followed.

Table 4.1 Median survival of tumor bearing mice

Group	Median survival (day)
Vector ie	25
lacZ ie	21
lacZ-HN ie	32
lacZ ie + HN sc	28
lacZ ie + Vector sc	27

4.3 Adjuvant effect of HN gene for ear pinna DNA vaccination with tumor associated antigen EpCAM

The adjuvant activity of HN was demonstrated when combining it with a surrogate tumor Ag, bacterial β-gal. A natural tumor Ag, epithelial cell adhesion molecule (EpCAM) was used for further study of the immunostimulating activity of HN.

EpCAM, also known as GA733-2, KSA, 17-1A Ag, is a cell surface glycoprotein expressed on some normal and over-expressed on many neoplastic epithelial cells. It is primarily expressed on colorectal carcinomas (CRCs), gastric, and pancreatic carcinoma and widely recognized as having an important role in tumor biology. Approximately 85% of the metastatic CRC lesions from various patients, and >80% of the cells within a lesion, are positive (117, 118). Thus, EpCAM is a suitable target for active immunotherapy of these cancers (119, 120). Although the Ag is also expressed on some normal tissues, such as gastrointestinal, lung, breast, and thyroid tissues, the density of the Ag is much higher on colonic tumor tissues than on normal colon tissues (121, 122).

4.3.1 Construction and verification of plasmids encoding HN and EpCAM genes

The human EpCAM gene was cut out from pSPORT6-EpCAM vector and cloned 1) into pTandem1 to construct the CMV-EpCAM vector and 2) into the CMV-HN vector in front of the HN gene separated by an IRES sequence as CMV-EpCAM-IRES-HN vector (Figure 4.17a). Those vectors were transfected to BHK cells, and analyzed for EpCAM and HN expression *in vitro*. Figure 4.17b shows a strong EpCAM expression (deep red) on the cell surface by EpCAM and EpCAM-HN gene transfection, and a strong HN expression (deep green) by HN and EpCAM-HN gene transfection.

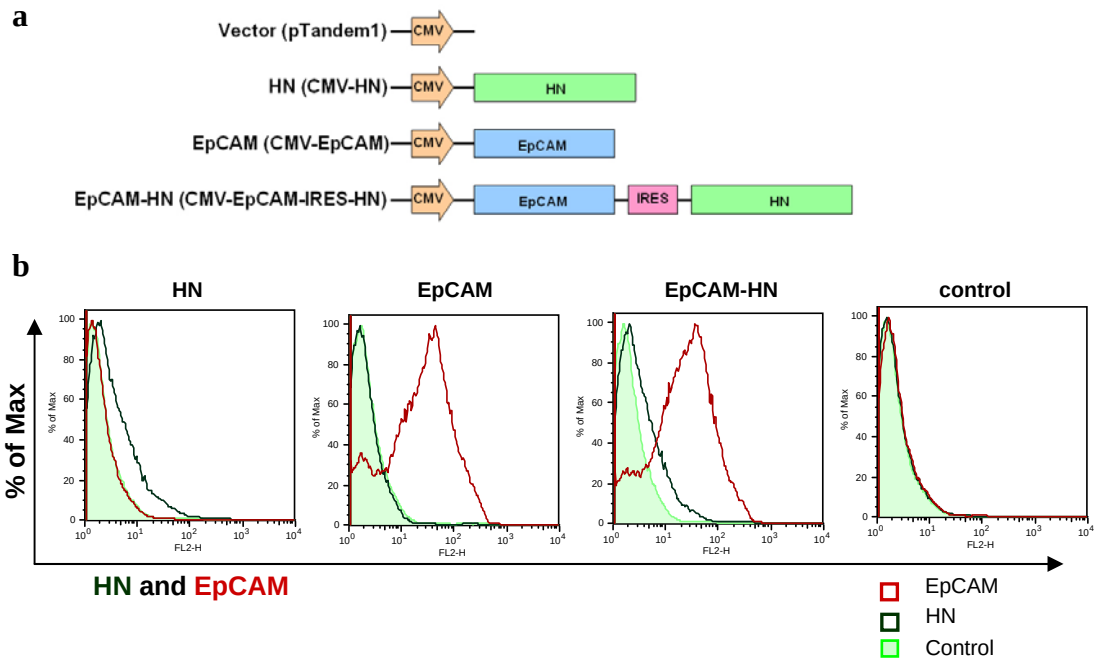

Figure 4.17 Construction of vectors encoding HN and human EpCAM genes.

Human EpCAM gene was cut out from pSPORT6-EpCAM and cloned into the pTandem1 vector as CMV-EpCAM vector or into CMV-HN in front of the HN gene separated by an IRES sequence as CMV-EpCAM-IRES-HN vector. pTandem1 was used as the control vector (a). Cell surface expression of HN and EpCAM was analyzed by FACS with anti-HN antibody (HN.B) and anti-human EpCAM antibody (HEA125) (b).

4.3.2 Adjuvant effect of HN in prophylactic mammary carcinoma models

A mouse mammary carcinoma cell line, DA3, transduced with the human EpCAM gene (DA3-EpCAM (DE)) (Figure 4.18a) was used for the prophylactic DNA vaccination. DNA vaccines (50μg/50μL) were applied ie to the mice twice with 2 weeks interval. 2 weeks after the 2nd DNA immunization (day 0), 5×10^6 DE cells were inoculated sc to the mice. Promisingly, EpCAM and EpCAM-HN gene immunization protected 100% of the mice from tumor growth (Figure 4.18b), which indicated that a strong anti-human EpCAM immunity was induced in these mice. These tumor-free mice (from EpCAM and EpCAM-HN groups) were then re-challenged with 1×10^7 DE cells at day 36 in the same flank. Re-challenged DE tumors first grew slowly (tumor diameters<2mm) and were then completely rejected in 4 weeks. These results indicated that memory immunity was induced by the prophylactic DNA vaccinations. Tumor diameters at day 50 (Figure 4.18c) and day 53 showed significant anti-tumor activity induced by HN gene vaccination ($p<0.05$ compared to PBS group). Anti-human EpCAM immunity was successfully induced in the mice by EpCAM

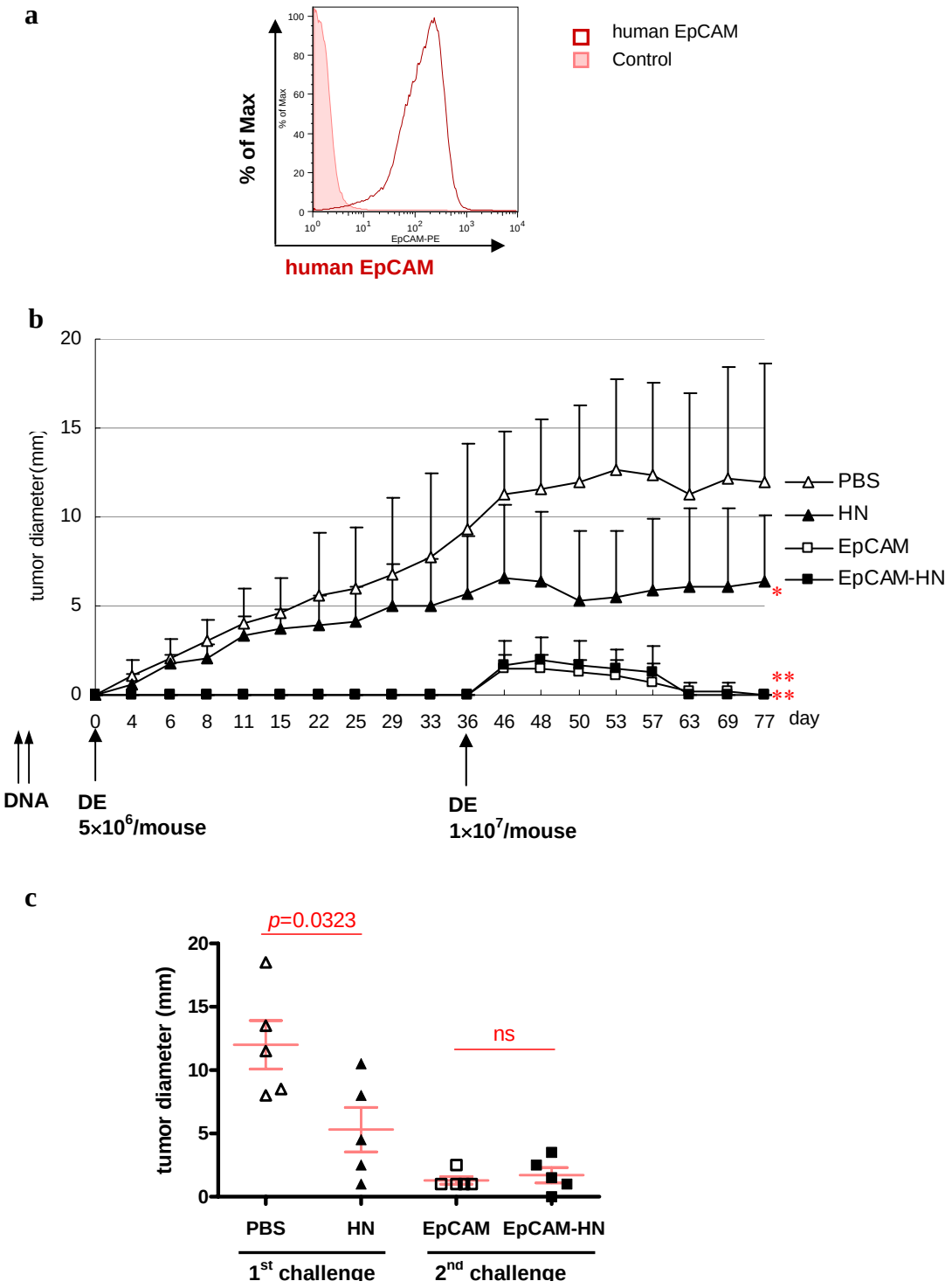

Figure 4.18 Prophylactic anti-tumor activity by HN and EpCAM DNA ie immunization in the DE tumor model.

a. Human EpCAM expression on the DE cells was analyzed by FACS with the anti-human EpCAM antibody (HEA125). **b.** DE tumor growth curve with 2 tumor challenges. DNA vaccines (50μg/50μL) were applied ie to the Balb/c mice (n=5/group) twice with 2 weeks interval. 2 weeks after the 2nd DNA immunization, 5×10^6 DE cells were inoculated sc to the mice. Tumor-free mice (all mice in EpCAM and EpCAM-HN groups) were re-challenged with 1×10^7 DE cells at day 36. * Compared to the PBS group, $p<0.05$; ** Compared to the PBS group, $p<0.01$. **c.** DE tumor diameter at day 50. DE tumor diameters by the 1st challenge for PBS/HN group and by the 2nd challenge for EpCAM/EpCAM-HN group at day 50 are shown.

DNA ie immunization. It was so strong that all immunized mice were completely protected and no adjuvant effect of HN could be detected. To further analyze the adjuvant activity of HN, all mice (with 2 prophylactic DNA vaccinations and DE tumor challenge at day 0) were re-challenged sc in the other flank with 1×10^7 parental DA3 cells (Figure 4.19a) which have mouse EpCAM expression (Figure 4.19b).The DA3 tumor growth curve showed significant improvement of anti-tumor immunity induced by HN compared to PBS and EpCAM-HN compared to EpCAM vaccination (Figure 4.19c). These results revealed the adjuvant effect by HN co-expression with a tumor Ag in a prophylactic mammary carcinoma tumor model. The xenogeneic human EpCAM DNA was apparently able to break tolerance against the mouse EpCAM.

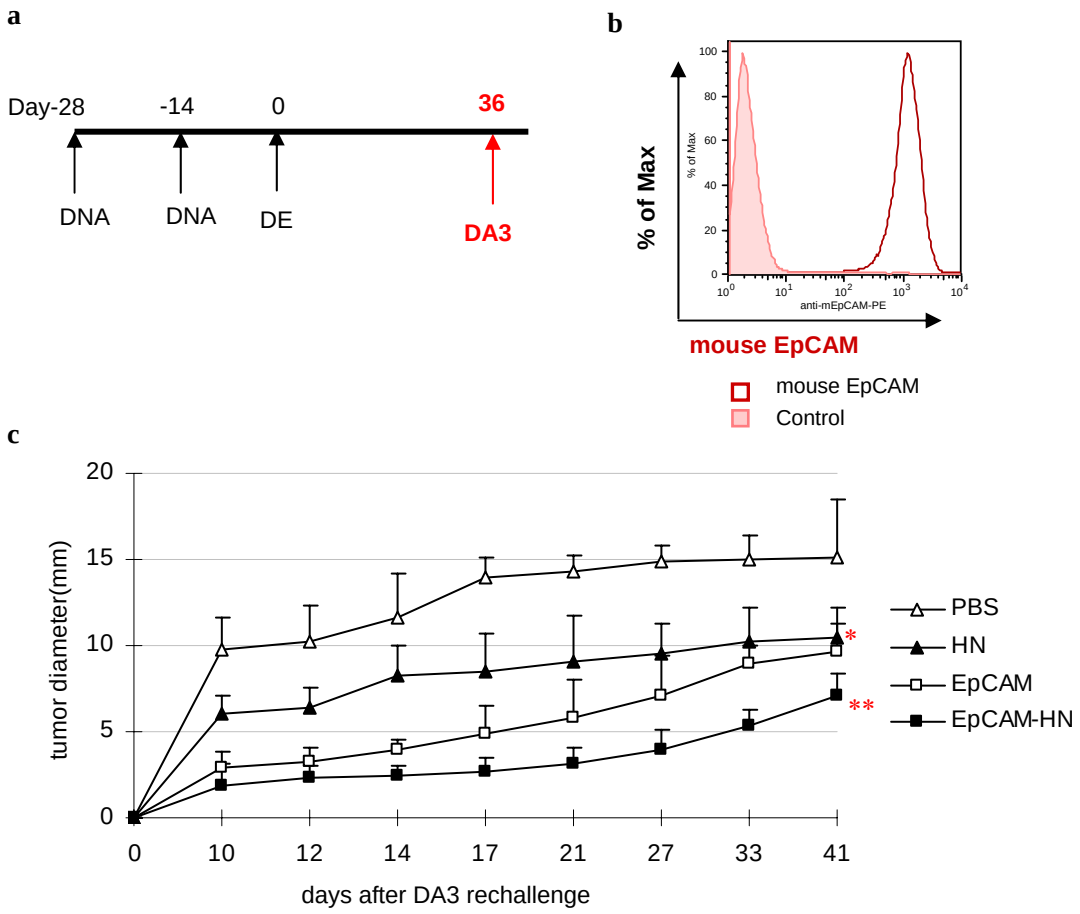

Figure 4.19 Improvement of anti-tumor activity by HN in DA3 rechallenge tumor model

Balb/c mice with 2 prophylactic DNA vaccinations and DE tumor challenge at day 0 were re-challenged at day 36 (**a**) by DA3 cells which have mouse EpCAM expression. (**b**) Mouse EpCAM expression on the DA3 cells was analyzed by FACS with the anti-mouse EpCAM antibody (G8.8). Mice were re-challenged with 1×10^7 DA3 cells to the other flank. The DA3 tumor growth curve is shown in (**c**). Statistical analysis (t-test) of tumor diameters at day 41 of the rechallenge: * Compared to the PBS group, $p<0.05$; ** Compared to the EpCAM group, $p<0.05$

4.3.3 Adjuvant effect of HN in a prophylactic colon carcinoma model

HN was successfully used as an adjuvant in the mouse mammary carcinoma tumor DE/DA3 which shows very low MHC I molecule expression. The anti-tumor activity might be dependent on innate immunity such as NK cells or on adaptive immunity induced by the vaccination because type I IFN induced by HN could up-regulate MHC I on the tumor cells. We further applied HN adjuvant to a mouse colon carcinoma tumor model, CT26 transfected with the human EpCAM gene. These cells showed relatively high expression of MHC I molecules and were possibly more affected by adaptive T cell immunity.

4.3.3.1 Generation of CT26EP with stable human EpCAM expression

The human EpCAM gene was cloned into the pcDNA3-hygro vector for pcDNA3-EpCAM-hygro (Figure 4.20a). The mouse colon carcinoma cell line CT26 was transfected with this vector. Stable transfection was achieved by using hygromycin selection. Human EpCAM expression on single clones was analyzed by FACS. Clone 22 with a good human EpCAM expression was used as CT26EP (Figure 4.20b).

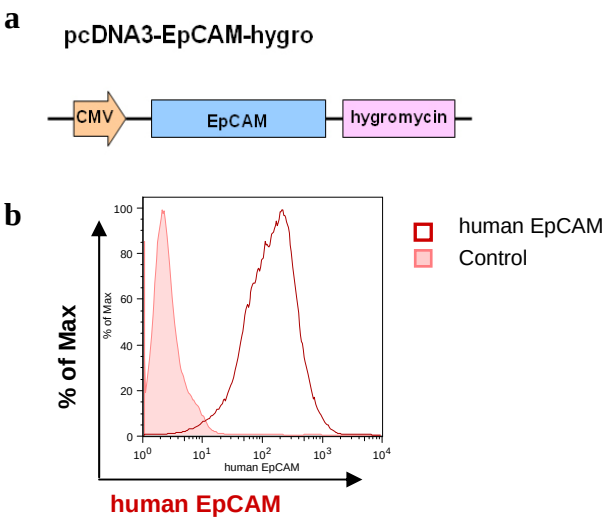

Figure 4.20 Generation of a mouse colon carcinoma cell line with human EpCAM expression.

a. Construction of pcDNA3-EpCAM-hygro vector. Human EpCAM gene was enzyme-cutted from pSPORT6-EpCAM and cloned into pcDNA3-hygro vector (Invitrogen) **b**. Human EpCAM expression on the surface of CT26EP. CT26 was transfected with pcDNA3-EpCAM-hygro vector. Single clone of the stable transfection was selected by hygromycin. Clone 22 with a good human EpCAM expression was used as CT26EP.

4.3.3.2 MHC I expression on the cell surface

Compared to DA3 and DE which express very low MHC I ($H2D^d$), CT26EP expresses a relatively high level of MHC I (Figure 4.21a). By IFN-α treatment, MHC I expression could be up-regulated on the cell surface of DA3 and DE (Figure 4.21b).

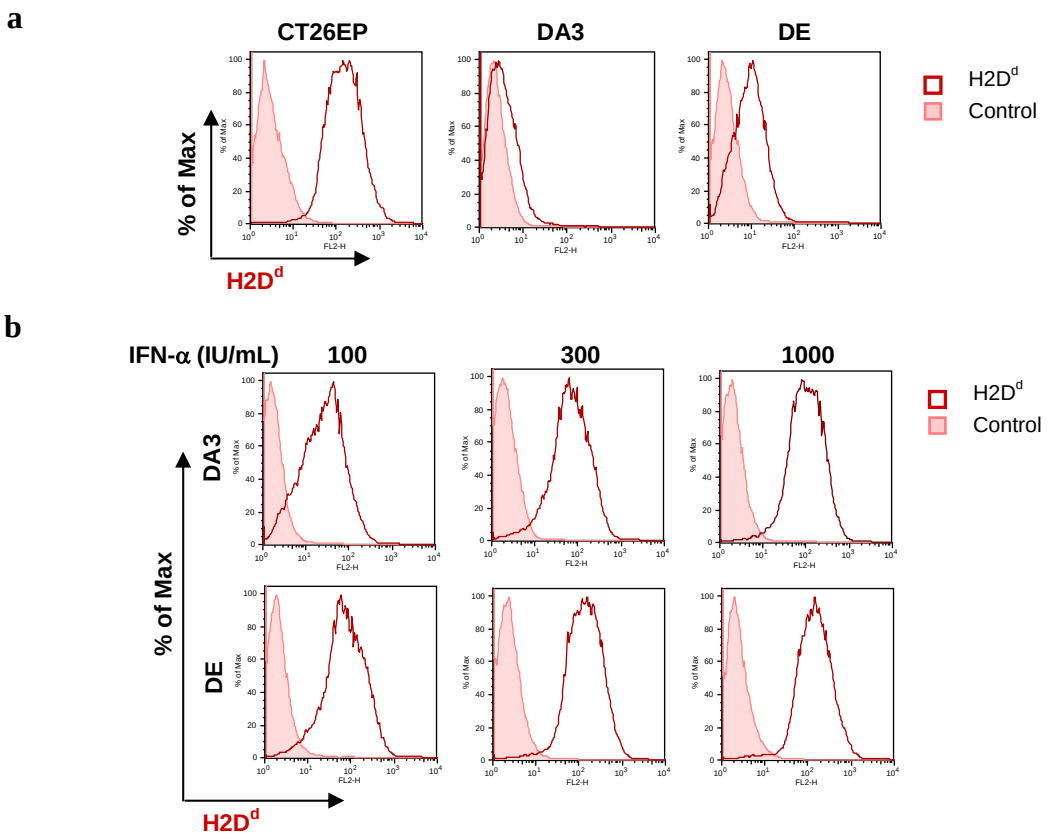

Figure 4.21 MHC I expression on the cell surface with IFN-α treatment

a. $H2D^d$ expression at the surface of CT26EP, DA3 and DE by FACS analysis. **b**. Up-regulation of $H2D^d$ expression at the cell surface of DA3 and DE by IFN-α treatment.

4.3.3.3 Improvement of prophylactic anti-tumor effect by HN

CT26EP cells are very aggressive. Tumor-bearing mice were dead in about 2 weeks (data not shown). In the ESb-lacZ tumor model, the best adjuvant effect for improvement of TAA DNA ie immunization by HN was achieved by sc inoculation (Figure 4.15b). In the CT26EP tumor model, EpCAM gene vaccination was combined with HN by separate application to get the best adjuvant effect. By 2 prophylactic vaccinations, 20% (1/5 mice) of the mice lived more than 50 days by HN sc injection as an adjuvant (Figure 4.22). In contrast, mice without adjuvant or with an empty vector as an adjuvant were all dead in about 20 days. These results revealed the adjuvant activity of HN in the tumor model CT26EP.

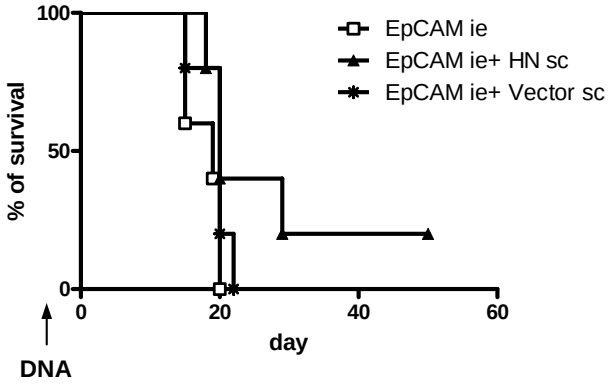

Figure 4.22 Adjuvant effect of HN in the CT26EP tumor model

Balb/c mice (n=5/group) were immunized with EpCAM DNA vaccines (50μg/50μL) ie or with HN/Vector sc injection twice with 2 weeks interval. 2 weeks after the 2nd DNA immunization, 5×10^5 CT26EP cells were inoculated sc to the mice.

4.3.4 Adjuvant effect of HN in therapeutic mouse tumor model

The adjuvant effect of HN has been demonstrated before in different prophylactic tumor models. For clinical application of cancer vaccines, therapeutic vaccination, however, is more important than prophylactic vaccination. For this reason, we applied the HN adjuvant into a therapeutic DE tumor model.

4.3.4.1 DNA treatment started from day 4 after tumor cell inoculation

Mice were inoculated sc with DE cells to the flank. After 4 days, tumor-bearing mice were treated with DNA (50μg/50μL) weekly for 4 treatments in total (Figure 4.23). Different treatment strategies were followed as shown in Table 4.2.

Table 4.2 Strategies of DNA treatment

Group	Strategy	Adjuvant
1	PBS ie	-
2	Vector ie	-
3	EpCAM ie	-
4	EpCAM-HN ie	HN
5	EpCAM ie + HN ie	HN
6	EpCAM ie + HN sc	HN

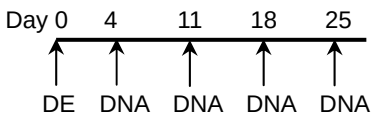

Figure 4.23 DNA therapeutic arrangements in DE tumor model

Balb/c mice were inoculated sc with 1×10^7 DE cells. DNA treatments (50μg/50μL/dose) were started 4 days later weekly for 4 times in total.

4.3.4.1.1 Therapeutic anti-tumor effect

Mice with established DE tumors benefited from EpCAM DNA treatment (anti-tumor effect is significant at day 14 compared to the Vector group). This effect was further improved by HN adjuvant co-expression and sc injection, but not by HN ie injection. HN sc application induced the best anti-tumor activity among the groups. Therapeutic anti-tumor activity was more significant in the early phase (from day 11 to day 21) of the tumor growth. Tumor growth was also inhibited to some extent in the Vector group after day 21. This might be due to the early interference by vaccination (day 4) and the strong immunogenicity of DE cells (high expression of a foreign Ag human EpCAM).

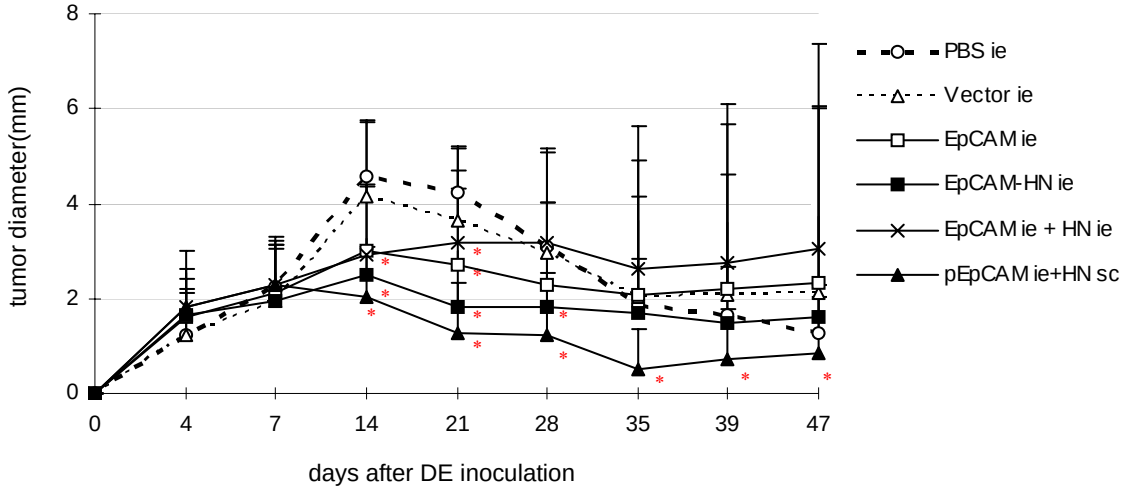

Figure 4.24 Adjuvant effect of HN in the therapeutic DE tumor model -early treatment

Balb/c mice (n=15/group) were inoculated with 1×10^7 DE cells and followed by DNA treatments as Figure 4.23. Tumor growth was followed. * Compared to the Vector group, $p<0.05$

The DE tumors grew very slowly in this therapeutic tumor model (an early DNA treatment from day 4). Although an HN effect was detected, tumor regression was also seen in the PBS and Vector groups after 3 weeks of the tumor inoculation. To further analyze the HN effect, these mice were re-challenged with the parental DA3 cells at day 47 (Figure 4.25a). EpCAM vaccinations did not affect DA3 tumor growth. With HN adjuvant (co-expression, ie and sc injection), significant tumor inhibition was seen (Figure 4.25b). These results demonstrate an adjuvant effect of HN in the therapeutic DE tumor model upon re-challenged with DA3cells.

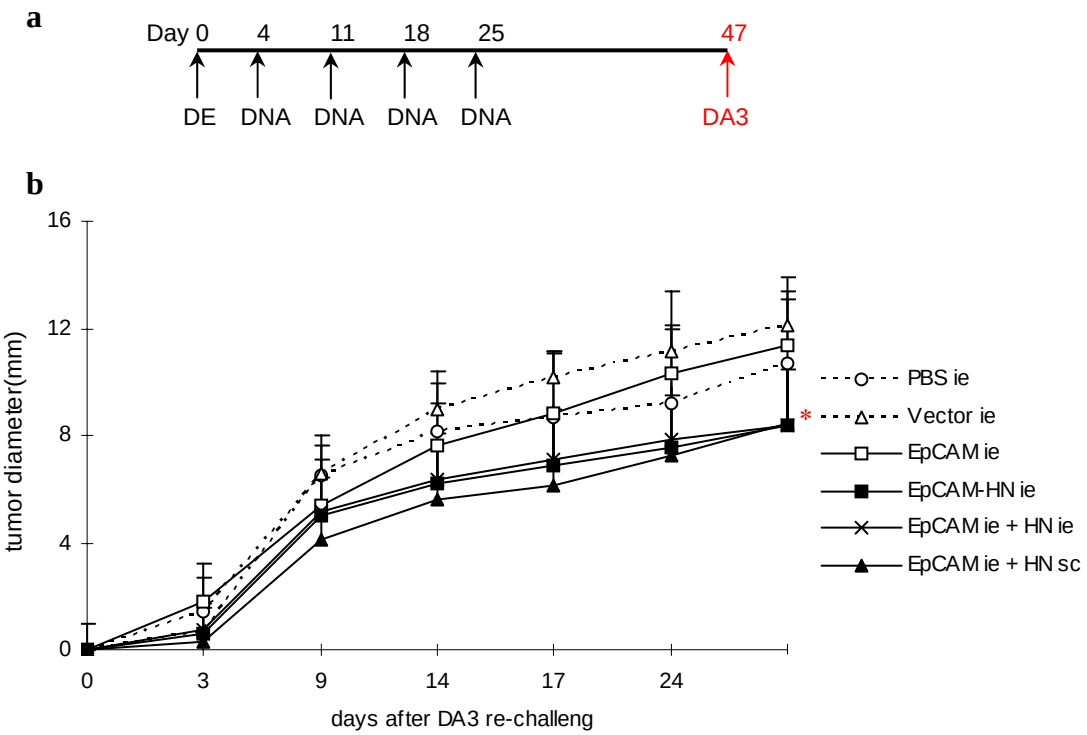

Figure 4.25 Adjuvant effect of HN in the DA3 re-challenge tumor model -early treatment

Balb/c mice (n=15/group) with established DE tumor and 4 DNA treatments were re-challenged with 1×10^7 DA3 cells (**a**) and tumor growth was followed (**b**). * For groups of EpCAM-HN ie, EpCAM ie+HN sc and EpCAM ie+Vector sc, compared to Vector and EpCAM groups, $p<0.05$.

4.3.4.1.2 Serum antibody level in tumor-bearing mice

Serum anti-human EpCAM and anti-mouse EpCAM antibodies were analyzed at day 80 by FACS with the human EpCAM positive cell line MCF-7 and the mouse EpCAM cell line DA3 (Figure 4.26a). Mice were grouped at day 80 as DE tumor-free mice "-" and DE tumor bearing mice "+". Mice with DE tumor had a high anti-human EpCAM antibody level, while mice without DE tumor had a low anti-human EpCAM antibody level. With EpCAM DNA immunization, the anti-human EpCAM antibody response was slightly improved in the large tumor-bearing mice compared to the PBS and Vector immunization groups (Figure 4.26b). Anti-mouse EpCAM antibody levels were similar in different groups (Figure 4.26c). These results indicated that the antibody response was induced mainly by the tumor cells themselves. Anti-tumor immunity apparently was not dependent on humoral immunity in this tumor model. High antibody levels in mice with large tumors indicated a bias towards a Th2 response in those mice.

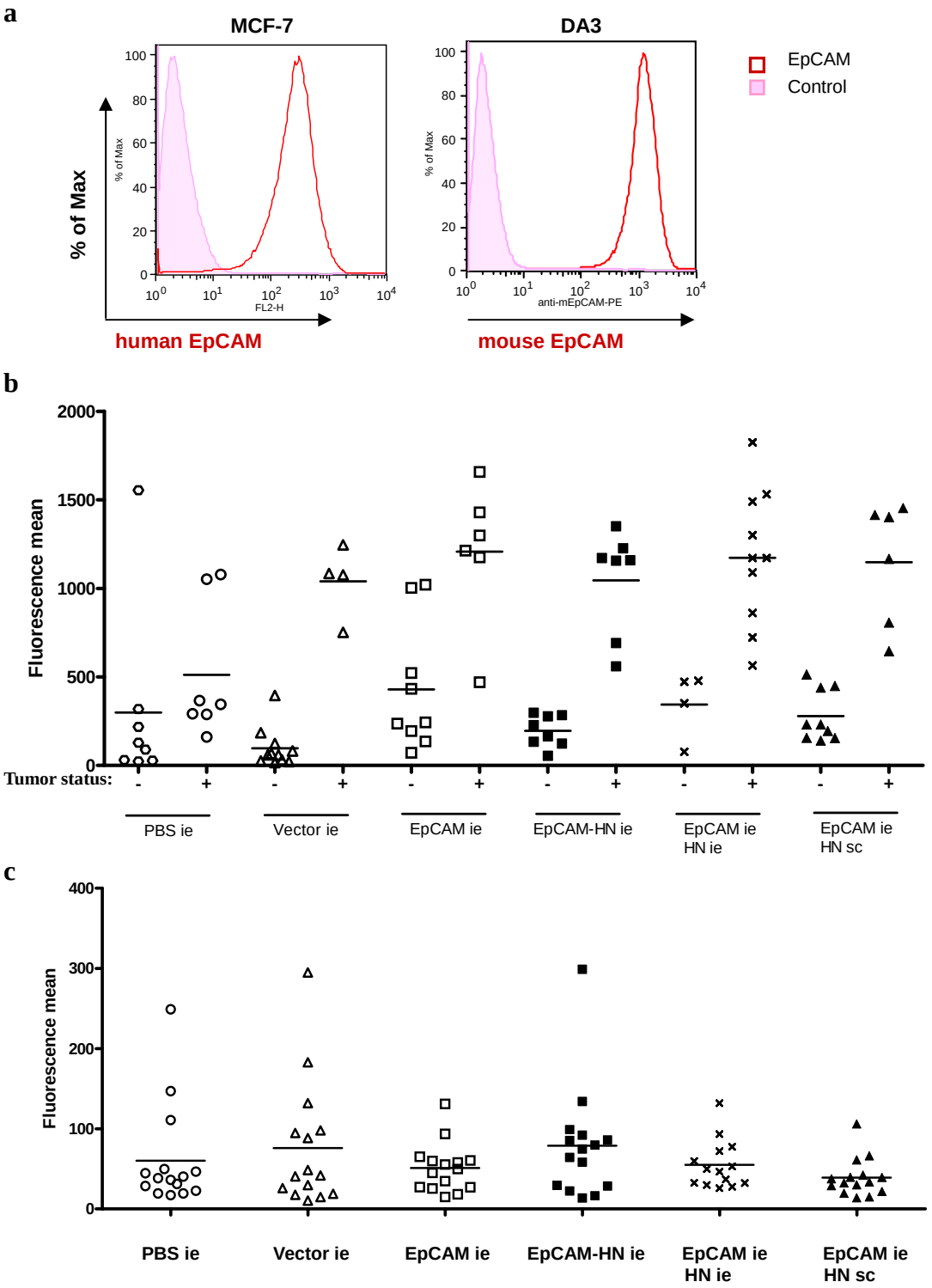

Figure 4.26 Antibody responses in DE and DA3 tumor-bearing mice.

DE and DA3 tumor-bearing mice were bled at day 80. Serum anti-human EpCAM antibody was analyzed (1:100 dilutions) by FACS with MCF-7 cells (with human EpCAM overexpression) and anti-mouse EpCAM antibody was analyzed by FACS with DA3 cells (with mouse EpCAM overexpression) (**a**). **b.** Anti-human EpCAM antibody level at day 80. Mice were grouped as DE tumor-free "-" and tumor bearing "+" mice at day 80. **c**. Anti-mouse EpCAM antibody level.

4.3.4.1.3 Lung metastases

Mice with DE and DA3 tumors were sacrificed during day 88 to day 101. Lung metastases were analyzed by counting the nodules. Figure 4.27 shows that EpCAM gene vaccination decreased lung metastases compared to the PBS and Vector group, and HN adjuvant improved this effect. By sc injection, the HN effect was the best.

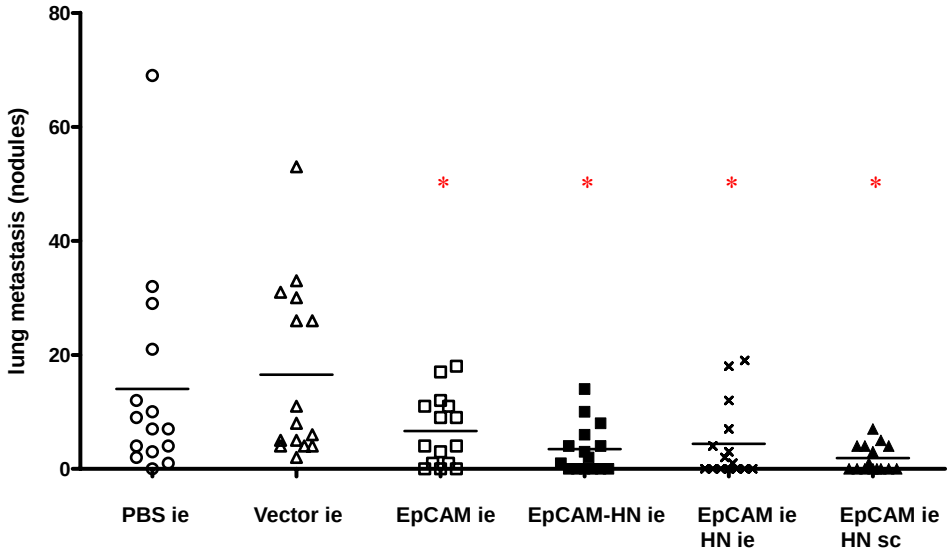

Figure 4.27 Effect on metastases of HN in DE and DA3 tumor models

DE and DA3 tumor-bearing mice were sacrificed during day 88 and day 101. Lungs were stained for metastases in Boin's solution. Nodules were counted after 3 days. *Compared to the Vector group, $p<0.05$.

4.3.4.2 DNA treatment started from day 7 after tumor cell inoculation

By DNA treatment from 4 days of DE tumor inoculation, therapeutic anti-tumor activity was significant in the early phase (from day 11 to day 21). Because of the early treatment and the strong immunogenicity of DE cells, tumor regression was also seen in the Vector and PBS groups after day 21 (Figure 4.24). To get a better tumor formation, we designed another therapeutic experiment in which we started DNA treatment from day 7 (Figure 4.28a). To further confirm the best adjuvant effect achieved by HN sc injection, we included a control group with a Vector sc injection. Significant anti-tumor activity was achieved by EpCAM DNA treatment with HN adjuvant (EpCAM-HN ie and EpCAM ie + HN sc) after 2 treatments (from day 21 to day 28). In correlation to the anti-tumor activity induced by the early DNA treatment (Figure 4.24), the best anti-tumor effects were achieved also by HN sc injection. Vector sc injection also improved the anti-tumor activity, suggesting that CpG motifs

also induced improvement for the DNA vaccination (Figure 4.28b). As shown in Figure 4.28c of tumor diameters at day 28, HN gene immunization induced significant improvement for anti-tumor immunity, especially by sc injection. Compared to Vector sc injection, HN sc injection significantly improved the therapeutic effect. In addition, HN as an adjuvant (both by co-expression and by sc injection) down regulated systemic TGF-β production (Figure 4.28d).

By DNA treatment starting at day 7 (late treatment), all mice had established DE tumors. Although DE tumor volumes were larger than at the time of early treatment (from day 4), they still grew slowly (average tumor diameter in Vector group was < 8mm without increase from day 14, Figure 4.28b). To further analyze the HN effect, parental DA3 cells were inoculated to these mice at day 59 (Figure 4.29a). EpCAM vaccinations did not inhibit DA3 tumor growth. With HN adjuvant (co-expression and sc injection), or even with Vector sc injection, significant tumor inhibition was induced (Figure 4.29b). Although CpG motifs in the plasmid backbone might help for the anti-tumor activity, HN expression further improved this effect (Figure 4.29c, compared to EpCAM ie + Vector, EpCAM ie + HN sc vaccination strategy induced significant improvement for anti-tumor immunity at day 14 of the rechallenge). These results further proved the existence of adjuvant effect of HN by late DNA treatment in the therapeutic DE tumor model and in the DA3 re-challenged tumor model.

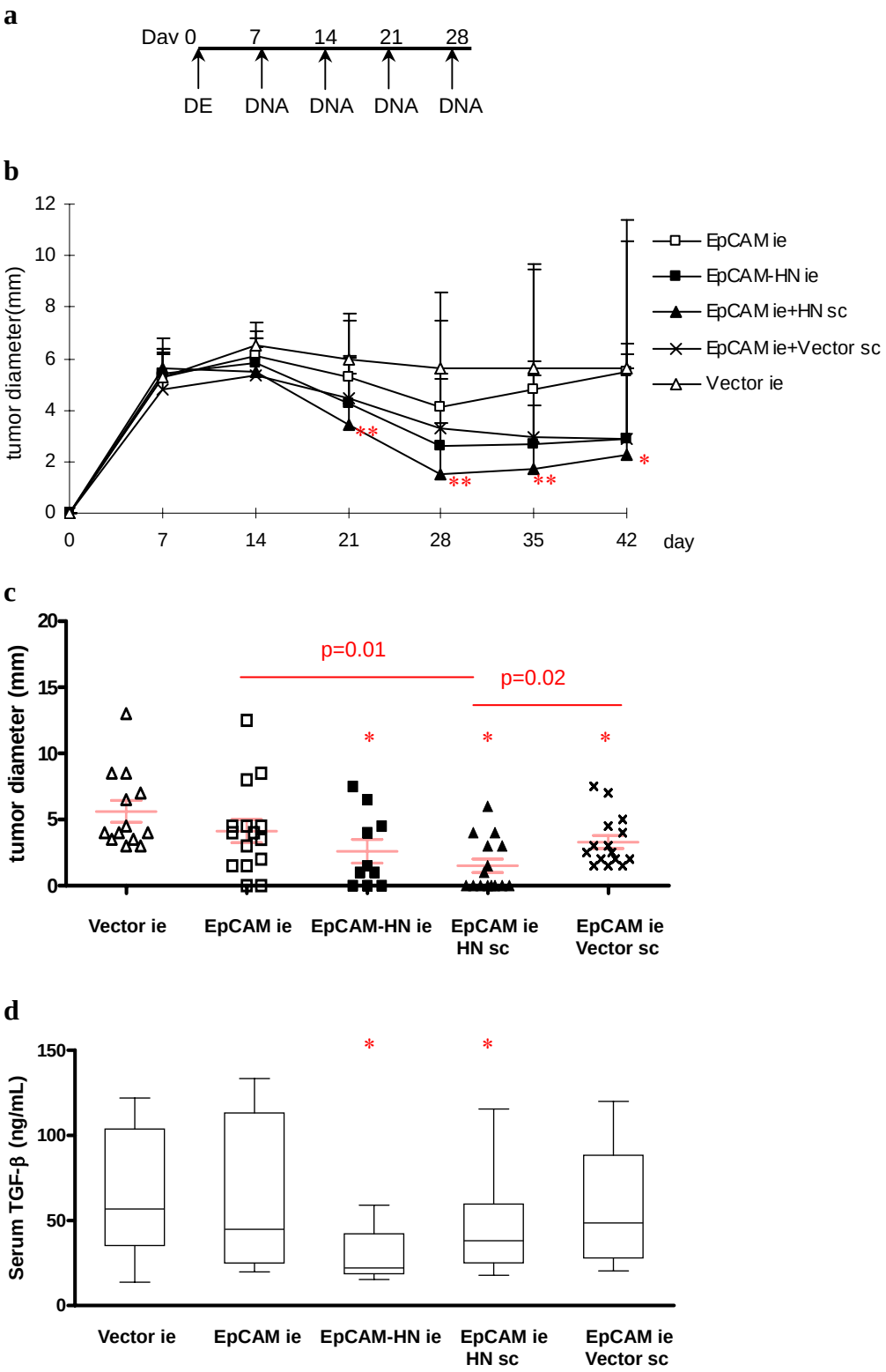

Figure 4.28 Adjuvant effect of HN in the therapeutic DE tumor model -late treatment

Balb/c mice (n=10~15/group) were inoculated with 1×10^7 DE cells and followed by DNA treatments (50μg/50μL DNA /immunization) (**a**). Tumor growth was followed (**b**). *from day 21 to day 28, DNA vaccines of EpCAM-HN ie, EpCAM ie + HN sc and EpCAM ie + Vector sc induced significant anti-tumor activity compared to Vector group, $p<0.05$; **compared to Vector and EpCAM ie groups, $p<0.05$. **c**. DE tumor diameters (MEAN±SEM) at day 28. *compared to Vector group, $p<0.05$. **d**. Serum TGF-β level at day 49. *compared to Vector group, $p<0.05$.

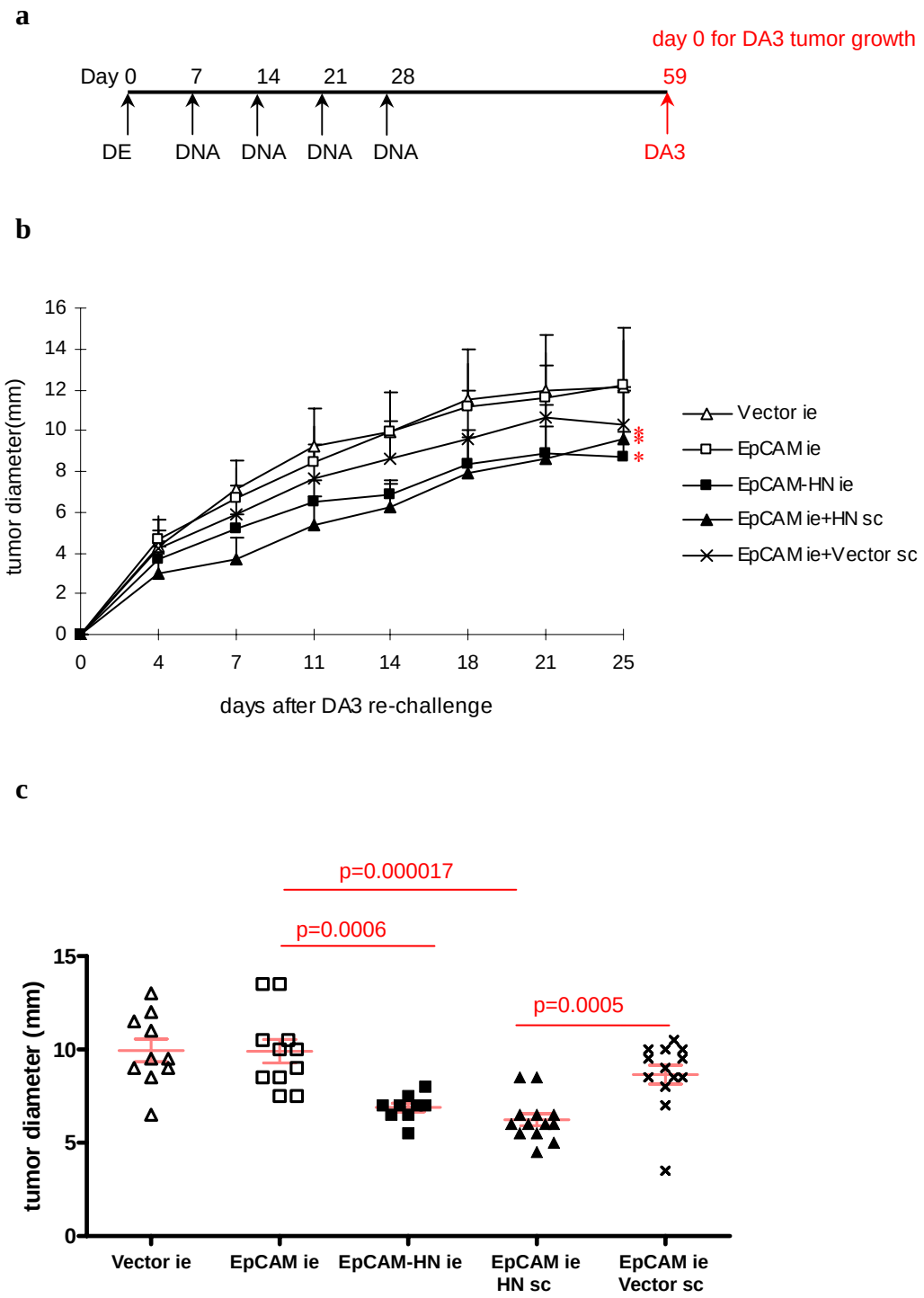

Figure 4.29 Adjuvant effect of HN in the DA3 rechallenge tumor model -late treatment

Balb/c mice (n=10~15/group) with established DE tumor and 4 DNA treatments were re-challenged with 1×10^7 DA3 cells at day 59 (**a**) and followed tumor growth (**b**). * For groups of EpCAM-HN ie, EpCAM ie+HN sc and EpCAM ie+Vector sc, from day 7 to day 25, compared to Vector and EpCAM groups, $p<0.05$. **c**. DA3 tumor diameters (MEAN±SEM) at day 14 of rechallenge.

4.3.5 Influence of humoral and cellular immune responses

The adjuvant effect of HN for DNA vaccination has thus been proven in prophylactic and therapeutic mouse tumor models. Although the immunostimulating effect of HN was detected in our studies, it is still not clear if there are improvements for adaptive immunity. Therefore, we analyzed the influence by HN adjuvant on humoral and cellular immune responses.

4.3.5.1 Influence of humoral immune responses

Mice were immunized with DNA by a prime-boost strategy (Figure 4.30a). Sera were taken after prime and boost, and analyzed for anti-β-gal antibody. Figure 4.30b showed that HN did not improve the antibody response, both for total antibody IgG+M as well as for subtypes IgG1 and IgG2a. However, the ratio of IgG2a/IgG1 was increased by HN sc application after prime but not after boost (Figure 4.30c). Although HN adjuvant did not improve the antibody level for the β-gal Ag, the increased ratio of IgG2a/IgG1 by lacZ ie + HN sc immunization indicated that HN sc injection might privilege Th1 responses.

4.3.5.2 Influence of cellular immune responses

Mice with 2 DNA immunizations for antibody analysis were also analyzed for CTL cell mediated cytotoxicity (Figure 4.31a) by a standard ^{51}Cr release assay. Co-expression of HN with the lacZ gene induced a significant improvement for CD8 epitope specific cytotoxicity. No improvement was seen, however, to the cytotoxicity by HN sc application. In contrast, Vector sc injection improved specific cytotoxicity, which indicated that CpG motifs might be involved. This could be an explanation for the improved anti-tumor activity seen after Vector sc injection in different mouse tumor models.

a

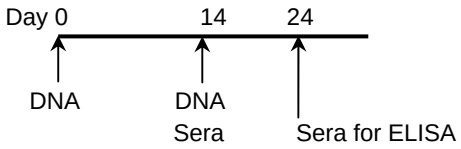

b

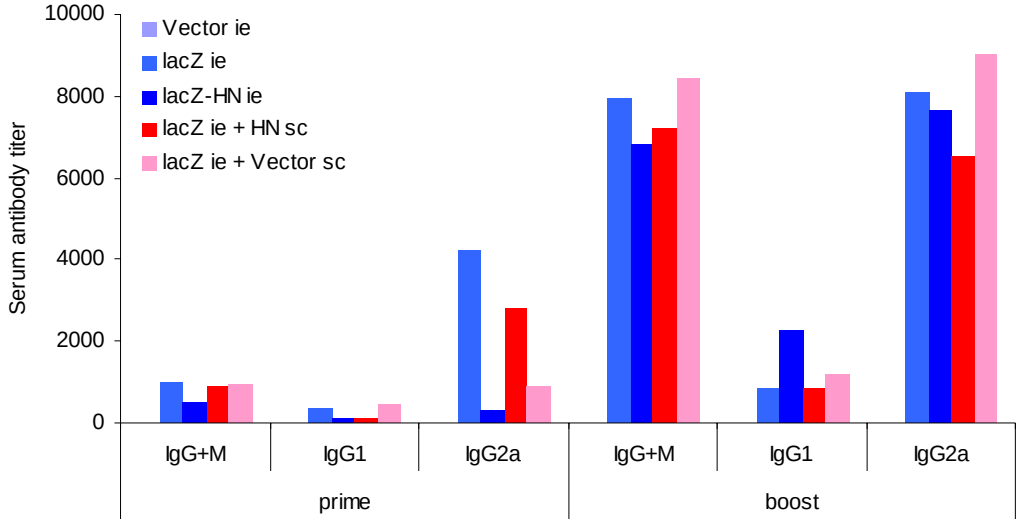

c

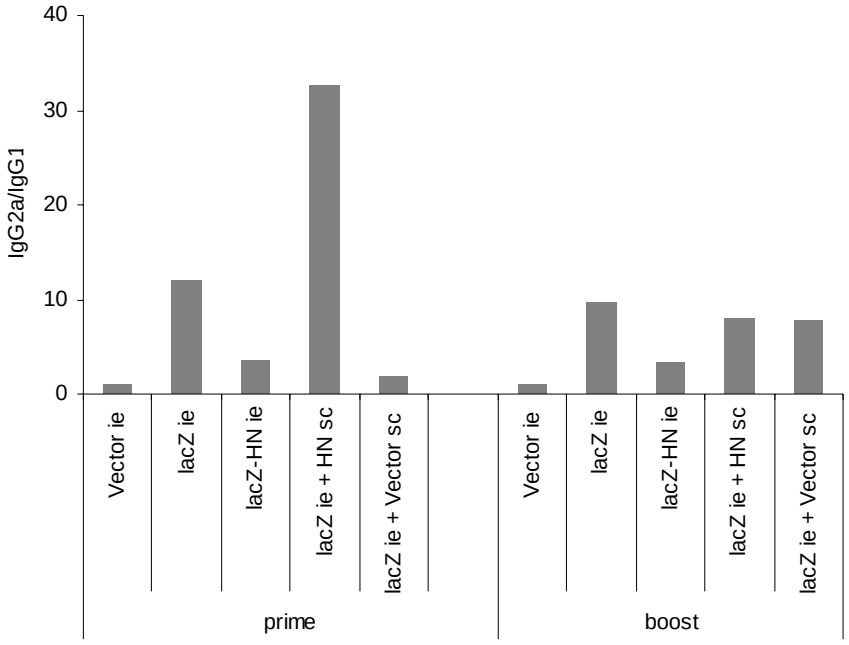

Figure 4.30 Influence of HN adjuvant on the humoral immune response.

DBA/2 mice (n=4/group) were immunized ie with lacZ gene with or without HN adjuvant by prime and boost strategy (the 2nd DNA vaccination was taken after 2 weeks of the 1st one, 50µg/50µL DNA /immunization). Sera from day 14 of the 1st DNA vaccination (prime) and day 10 of the 2nd DNA vaccination (boost) were analyzed for antibody responses (IgG+M, IgG1, IgG2a) by β-gal ELISA (a). b. IgG2a/IgG1 ratio. 1 of 3 independent experiments was shown.

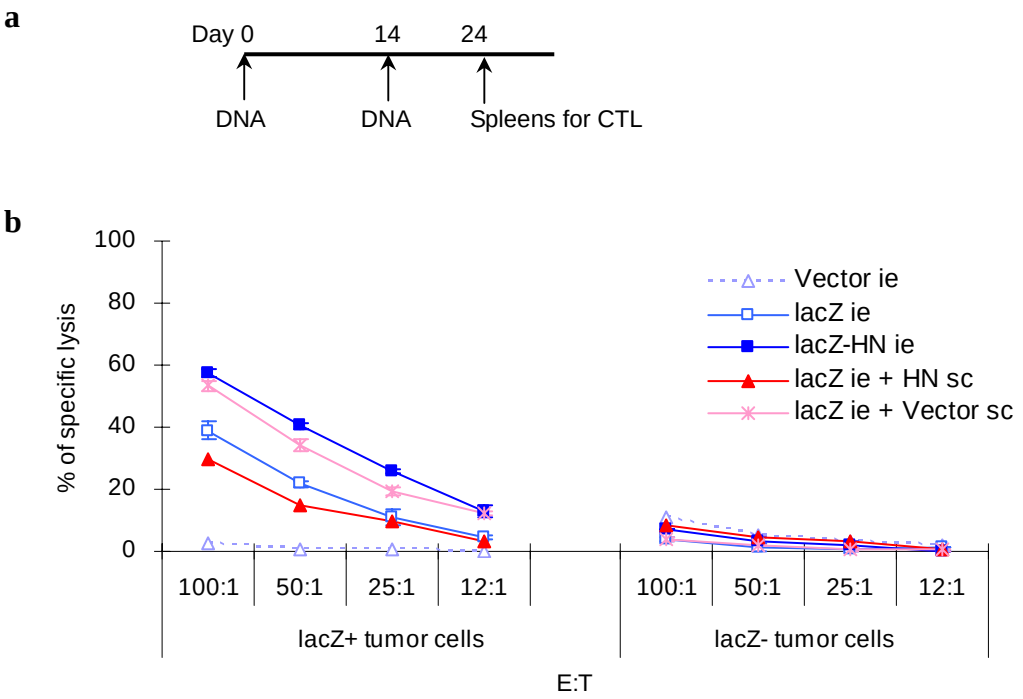

Figure 4.31 Influence of HN adjuvant on the cellular immune response
a. Immunization strategy. Mice with 2 DNA immunizations (from Figure 4.30) were sacrificed after 10 days of the 2nd immunization. Spleens were taken out and re-stimulated for 5 days *in vitro* and analyzed cytotoxicity to $lacZ^+$ tumor cells (P13.1) and $lacZ^-$ tumor cells (P815) by a standard 4 h ^{51}Cr release assay (b). 1 of 3 independent experiments was shown.

4.3.6 Adoptive transfer of Ag specific splenocytes

Although it is quite clear that HN sc application has the best adjuvant effect compared to HN co-expression and Vector sc immunization *in vivo*, no improvements of anti-β-gal antibody levels and cell mediated immune responses by HN sc injection were detectable in *in vitro* experiments.

Because DE is a tumor line with very low MHC I expression, it is not a good target for *ex vivo* killing assay. In addition, no T cell epitopes of human EpCAM were available for mouse experiments. Without *in vitro* peptide stimulation, it is difficult to achieve a good CTL response. We tried to use IFN-α treated DE cells as well as DE cell lysates and DCs for *in vitro* stimulation (data not shown). However, the specific cytotoxicity was not detectable.

Since *ex vivo* cytotoxic analysis might fail because some factors produced *in vivo* may be missing, we further tried to analyze cytotoxicity *in vivo*. T cell adoptive transfer is a promising method for clinical application. It is also a good way to analyze

functional activity of T cells. To analyze the HN effect *in vivo*, we designed an experiment with adoptive transfer of Ag specific splenocytes including Ag specific T cells, B cells as well as APCs. Adoptive transfer was applied to NOD/SCID mice which have no functional B and T cells, low natural killer (NK) cell function and absence of circulating complement.

4.3.6.1 Stable transfection of firefly luciferase in DA3/DE

The firefly luciferase gene was cloned into the pcDNA3-hygro vector to construct pcDNA3-luc-hygro (Figure 4.36a). The mouse mammary carcinoma cell line DA3 and DE were transfected with this vector. Stable transfection was achieved by using hygromycin selection. Firefly luciferase expression on single clone was analyzed by *in vitro* luciferase assay. 23 hygromycin resistant clones of DA3-luc (D1-D23, Figure 4.36b) and 32 single clones of DE-luc (DE1-DE32) were analyzed for firefly luciferase expression.

After 3 analyses of *in vitro* luciferase activity, clones D5, D8, D13, DE19, DE30, and DE31 were analyzed for luciferase expression by *in vitro* imaging. By this method, luciferase expression could be detected in all transfectants with cells. Only DE19 and D13 showed luciferase expression when cells were used at less than 1×10^3 cells (Figure 4.37a). Quantitative analysis confirmed the best luciferase expression by DE19 and D13 (Figure 4.37b). These 2 clones were applied to *in vivo* experiments as DE-luc and DA3-luc.

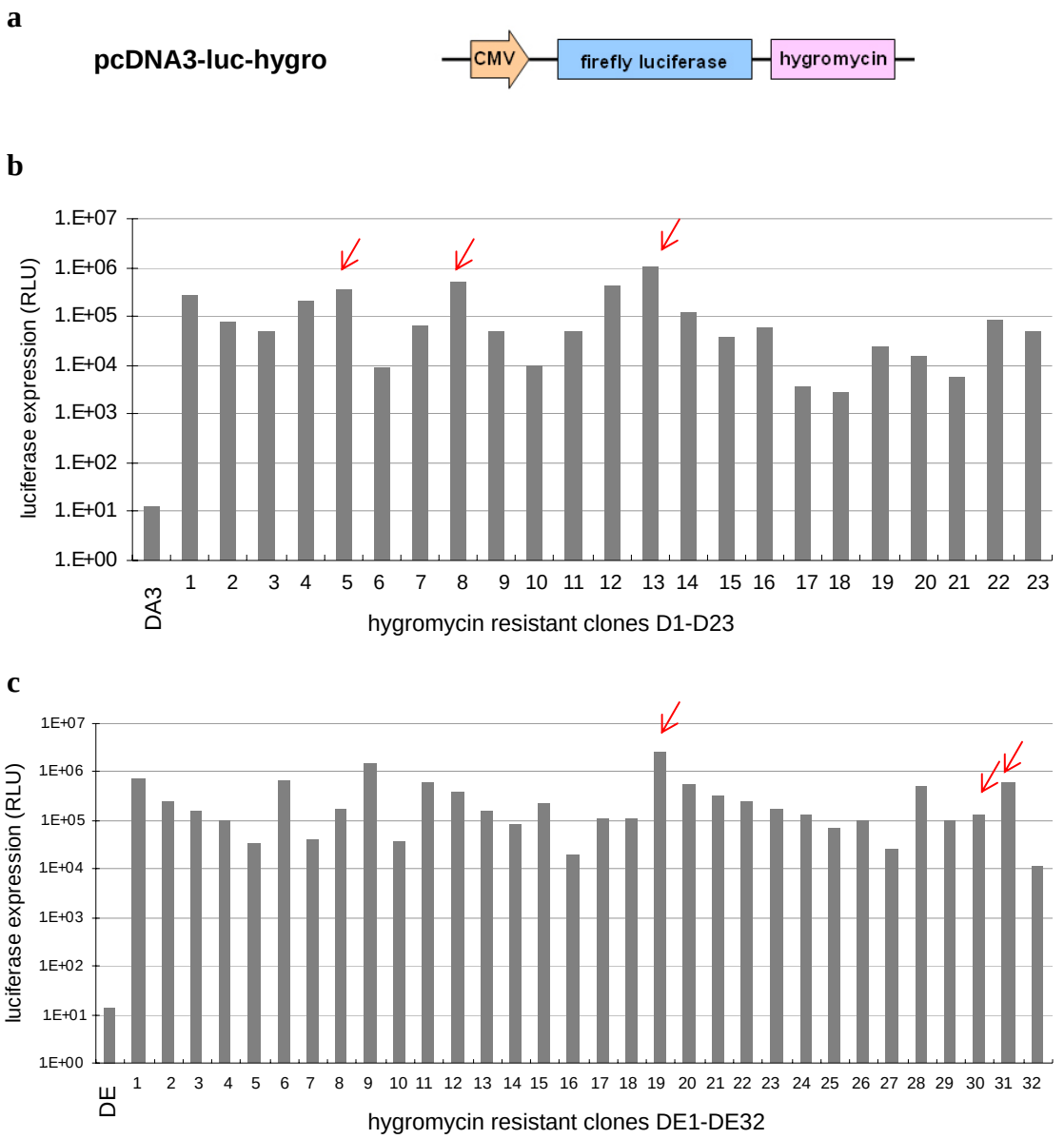

Figure 4.36 Generation of a mammary carcinoma cell line with firefly luciferase expression.

a. Construction of pcDNA3-luc-hygro vector. Firefly luciferase gene was enzyme-cutted from pGL3-Basic and cloned into pcDNA3-hygro vector (Invitrogen). **b**. *In vitro* luciferase activity of single clones of DA3-luc. DA3 was transfected with pcDNA3-luc-hygro vector. Single clones of the stable transfection were selected by hygromycin. 23 single clones were analyzed for *in vitro* luciferase expression calculated as Relative Light Units (RLU). c. *In vitro* luciferase activity of single clones of DE-luc. DE was transfected with pcDNA3-luc-hygro vector. Single clones of the stable transfection were selected by hygromycin. 32 single clones were analyzed for *in vitro* luciferase expression. Clones with the red arrows were further analyzed by *in vitro* imaging.

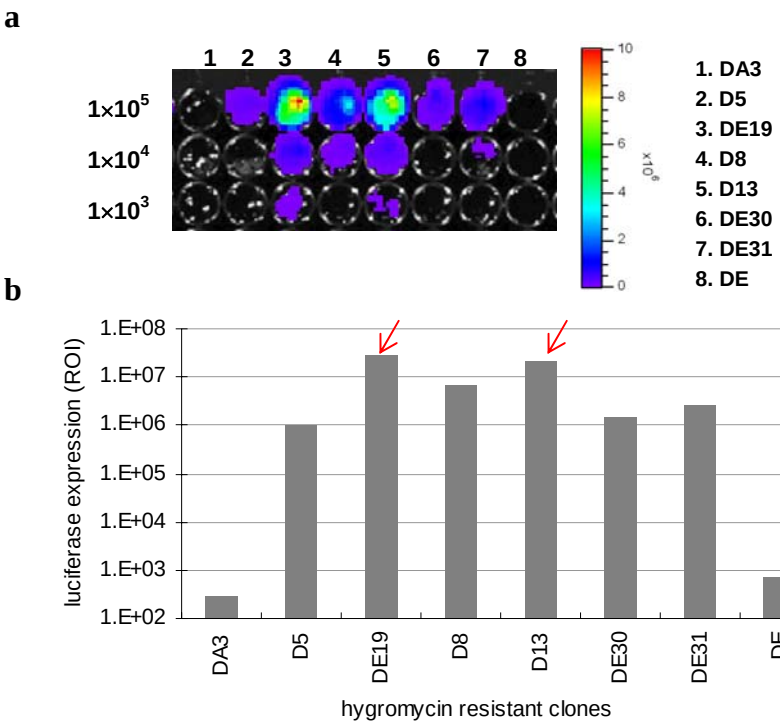

Figure 4.37 Verification of firefly luciferase expression in stably transfected single clones by *in vitro* imaging.

a. Firefly luciferase gene expression in stably transfected single clones with different amounts of cells. DA3/DE and their transfectants were imaged in IVIS100 imaging system for luciferase expression with the exposure time 30 s. **b**. Quantitative analysis of the luciferase expression. DE19 and D13 were used for further *in vivo* experiments as DE-luc and DA3-luc. Bioluminescent signal was calculated for region of interest (ROI) (Unit: p/sec/cm^2/sr).

To analyze local subcutaneous tumor formation by DE-luc and DA3-luc *in vivo*, NOD/SCID mice were inoculated sc with 2×10^6 cells. *In vivo* imaging showed successful local tumor formation with both transfectants (Figure 4.38a), with a stable luciferase expression for DE-luc (DE grows also but very slowly in Balb/c mice) and an increased luciferase expression for DA3-luc (DA3 grows faster in Balb/c mice). After 40 days, lung metastases were detected in both groups (Figure 4.38b). DA3-luc produced a higher metastatic load (stronger luciferase signal in the lungs) which was also detected by *in vivo* imaging if the mice (Figure 4.38a, day 40).

To analyze systemic tumor formation of DE-luc and DA3-luc *in vivo*, NOD/SCID mice were inoculated iv with 5×10^5 cells. *In vivo* imaging showed tumor located only to the lungs with both transfectants (Figure 4.38c), with a decreased luciferase expression for DE-luc and an increased luciferase expression for DA3-luc. Following iv inoculation, DA3-luc grew very aggressively. One mouse (of 3 mice) was dead

after 4 days. DA3-luc induced a much stronger luciferase signal in the lung than did DE-luc cells (proven by *in vivo* imaging of the mice as well as by *ex vivo* imaging of the lungs, Figure 4.38d). These results showed that DA3-luc is suitable for a systemic tumor formation, while DE-luc is not.

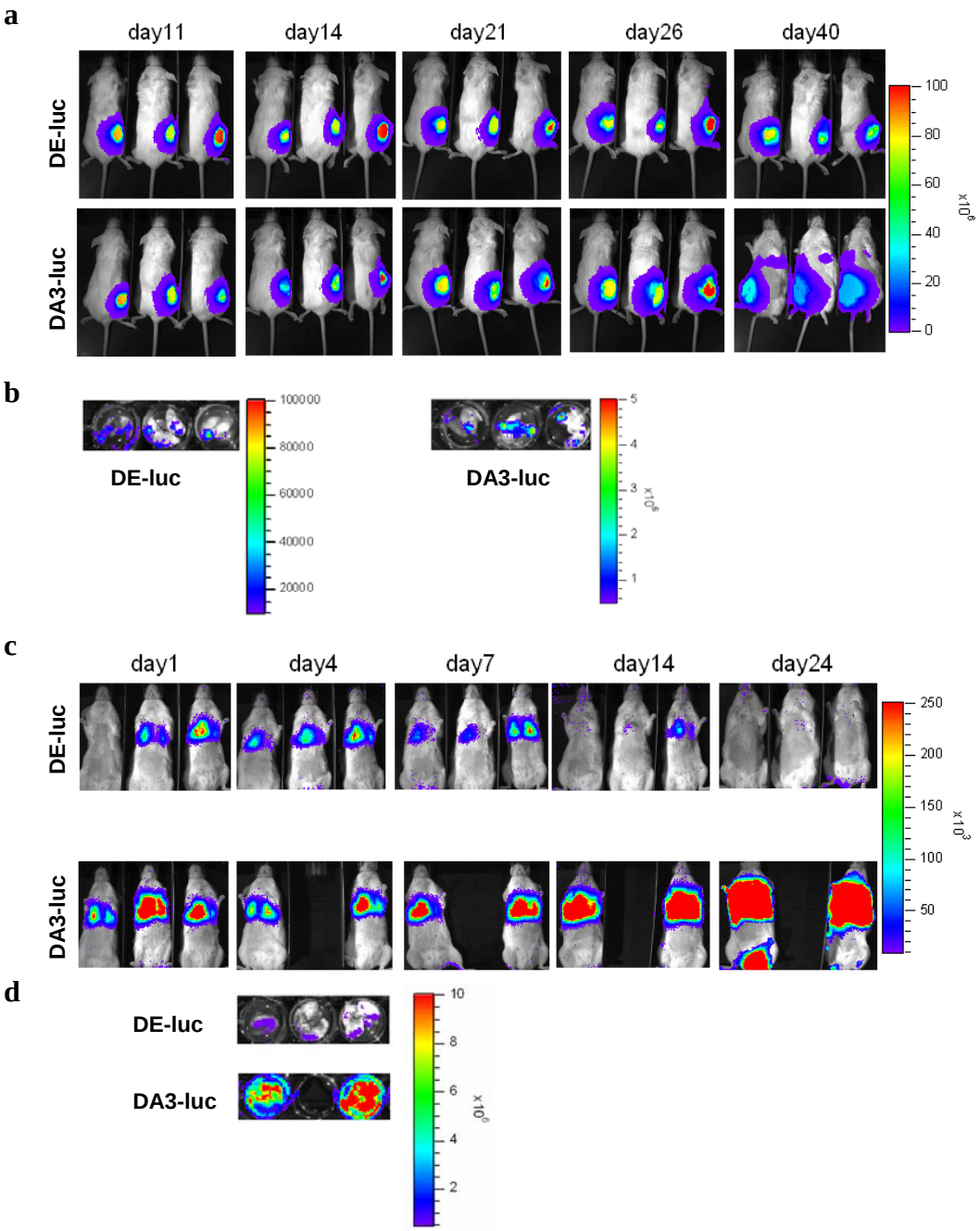

Figure 4.38 *In vivo* imaging of tumor formation of DE-luc and DA3-luc.

a. Local subcutaneous tumor formation. Stable transfectants DE-luc (DE19) and DA3-luc (D13) (2×10^6) were inoculated sc to NOD/SCID mice (n=3/group). Tumor growth was followed by *in vivo* imaging (10 s exposure time). Lungs from tumor-bearing mice at day 40 were imaged for metastases (**b**) (exposure time: 120 s for DE-luc, 10 s for DA3-luc). **c**. Systemic tumor formation. DE-luc and DA3-luc (5×10^5) were inoculated iv to NOD/SCID mice (n=3/group). Tumor formation was followed by *in vivo* imaging (60 s exposure time). Mice were sacrificed at day 24. Lungs were imaged *ex vivo* for metastases (**d**) (exposure time: 30 s for DE-luc, 1 s for DA3-luc). Bioluminescent signal was shown in pseudophoton unit: p/sec/cm^2/sr. Experiments were repeated for 3 times with similar results.

4.3.6.2 Adoptive transfer of Ag specific splenocytes

To get the best Ag specific splenocytes, we first tried the vaccination protocol with EpCAM ie + HN sc. Immuno-competent Balb/c mice were immunized twice with 2 weeks interval. 2 weeks after the 2nd vaccination, mice were challenged with 1×10^7 DE cells. 1 week later, tumor-free mice were sacrificed to obtain Ag specific splenocytes (Figure 4.39a). 1×10^7 splenocytes from immunized mice or control splenocytes from naïve mice were transferred iv to NOD/SCID mice with established DE-luc tumor (day 7 after tumor inoculation). The luciferase signal decreased in both groups from day 7 to day 45 (immune and non-immune transfer, Figure 4.39b), although tumor diameters increased (Figure 4.39c). Thus, no specific anti-tumor activity could be seen by adoptive transfer of immune splenocytes. No anti-metastatic activity was detectable either (Figure 4.39d).

These results showed that splenocytes from immunized mice upon adoptive transfer could not affect tumor cells *in vivo* in NOD/SCID mice. One possible reason might be the low MHC I expression which might facilitate tumor escape. When HN was applied to immuno-competent mice, type I IFN production might have up-regulated MHC I expression on the tumor cells, thereby improving their sensitivity to anti-tumor immunity. In addition, it was reported that NK cell could be activated by hemagglutinin neuraminidase of influenza virus. Therefore, it is possible that HN of NDV induced NK cell activation. However, NOD/SCID mice have no functional B and T cells, low NK cell function and absence of circulating complement. Therefore, the failure of adoptive transfer might be due to the various immuno-defects of NOD/SCID mice.

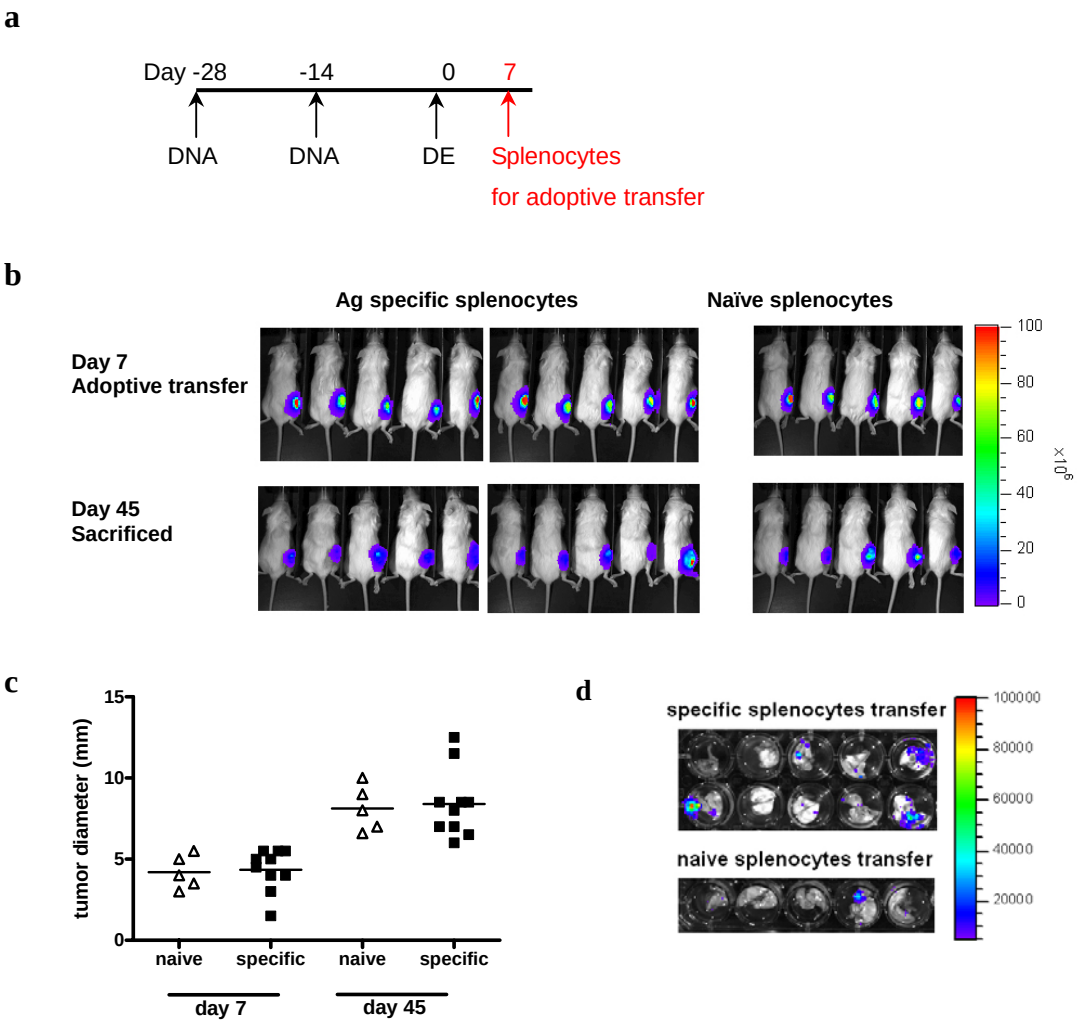

Figure 4.39 Adoptive transfer of splenocytes from pre-immunized mice

a. Immunization protocol. Balb/c mice (n=5) were immunized twice with EpCAM ie + HN sc with 2 weeks interval. 2 weeks after the 2nd vaccination, mice were challenged with 1×10^7 DE cells. 1 week later, tumor-free mice were sacrificed to get Ag specific splenocytes. **b**. *In vivo* imaging of tumor bearing mice before and after adoptive transfer. 1×10^7 immune splenocytes or control splenocytes from naïve mice were transferred iv to NOD/SCID mice (n=10/group for specific transfer, n=5/group for naïve transfer) with established DE-luc tumor (day 7 of the inoculation). Tumor growth was followed by imaging until day 45 (data between day 7 to day 45 were not shown, 10s exposure time). **c**. Tumor diameters at day 7 (before adoptive transfer) and day 45 (38 days after adoptive transfer). **d**. *Ex vivo* imaging of lungs at day 45. Lungs from tumor bearing mice at day 45 were imaged *ex vivo* for metastases (120 s exposure time). Bioluminescent signal was shown in pseudophoton unit: p/sec/cm^2/sr.

4.3.7 Adjuvant effect of HN in immuno-deficient mice

The fact that adoptive transfer of splenocytes from immunized mice did not inhibit DE-luc tumor growth in NOD/SCID mice indicated that adaptive immunity is not enough to kill tumor cells with low MHC I expression. In the DA3/DE tumor model, innate immunity might be very important for the anti-tumor activity induced by the vaccination, especially for HN induced improvement because HN is an important molecule to stimulate innate immunity.

To analyze the adjuvant effect of HN for innate immunity, RMA-S tumor cells were used which express very low levels of MHC I molecules and can be influenced by NK cells for their tumor growth. We applied HN DNA or Vector DNA at day -1, 3, 6 relative to RMA-S tumor application (Figure 4.40a). We used the following strains of mice: 1) wild-type (WT) C57BL/6, 2) $RAG2^{-/-}$ (lack of functional T and B cells, to test the efficiency of innate immunity in anti-tumor responses), 3) $RAG2^{-/-}IFNAR^{-/-}$ (lack of functional T and B cells as well as of type I IFN effects, because of absence of type I interferon receptor, to analyze the importance of type I IFN response in innate immunity) mice. Tumor growth was not inhibited by HN in WT mice (Figure 4.40b), but it was inhibited by HN in $RAG2^{-/-}$ mice (Figure 4.40c). In $RAG2^{-/-}$ $IFNAR^{-/-}$ mice, tumor inhibition was diminished but not completely impaired (Figure 4.40d). This indicated that type I IFN is crucial but not an absolute factor for HN induced RMA-S tumor inhibition. Moreover, peripheral myeloid derived suppressor cells (MDSC, $CD11b^{+}Gr1^{+}F4/80^{+}$) showed a trend towards down-regulation in HN immunized $RAG2^{-/-}$ mice. This is correlated with the down-regulation of serum TGF-β level in DE therapeutic tumor model (Figure 4.28d). These results demonstrated a crucial role for innate immunity mechanisms in HN induced anti-tumor activity.

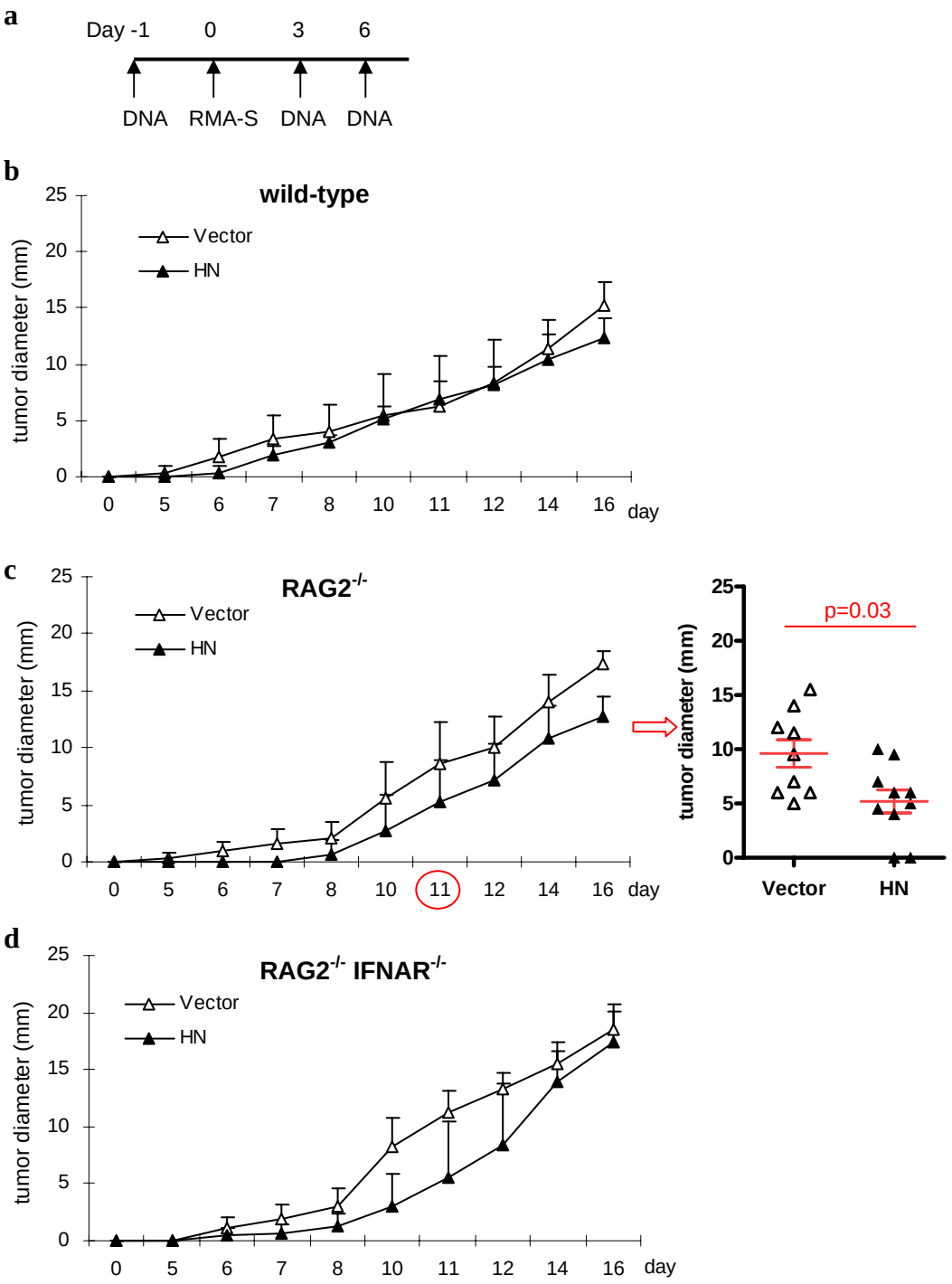

Figure 4.40 Adjuvant effect of HN in immuno-difficient mice.

C57BL/6 wild-type (10mice/group), RAG2$^{-/-}$ (5mice/group, 2 independent experiments were performed), and RAG2$^{-/-}$IFNAR$^{-/-}$ mice (10mice/group) were inoculated with 1×10^6 RMA-S T cell lymphoma cells after 1 DNA pre-treatment either with HN or with Vector. DNA treatments were applied also at day 3 and day 6 (**a**). Tumor growth was followed in different groups (**b-d**). RMA-S tumor diameters in RAG2$^{-/-}$ mice at day 11 (outline from 2 experiments, MEAN±SEM) was shown (**c**). **e**. Percentage of peripheral MDSC (CD11b^{+}Gr1^{+}F4/80^{+}) in PBMC at day 7 from RAG2$^{-/-}$ mice.

4.3.8 Adjuvant effect of HN in tumor infiltrating lymphocytes

HN activated innate immunity might affect tumor infiltration by lymphocytes. Tumor infiltrating lymphocytes (TILs) are essential for the anti-tumor activity. To analyze if there is an improvement of TILs by HN vaccination, mice with established DA3 tumor (tumor diameter is about 8~9 mm) were immunized ie with HN or Vector. 4 days later, TILs were analyzed by FACS (Figure 4.41a). The lymphocyte population of single cell suspension from the tumor was gated with the same gate as defined for lymph node cells (Figure 4.41b). TIL (defined as Figure 4.41c-d) were then analyzed for $CD3^+CD4^+$, $CD3^+CD8^+$, $CD3^+CD49b^+$ and $CD11b^+Gr1^+F4/80^+$ cells (CD4, CD8 T cells, NK cells and MDSC) respectively. Figure 4.41e showed that the percentage of CD4 and CD8 T cells in TIL was not significantly improved by HN vaccination, while NK cells were significantly increased. Suppressive MDSC were down-regulated in the tumor by HN vaccination. Immunohistochemistry results (Figure 4.41f) corroborated the FACS analysis. These results demonstrated significant effects on TILs induced by HN vaccination.

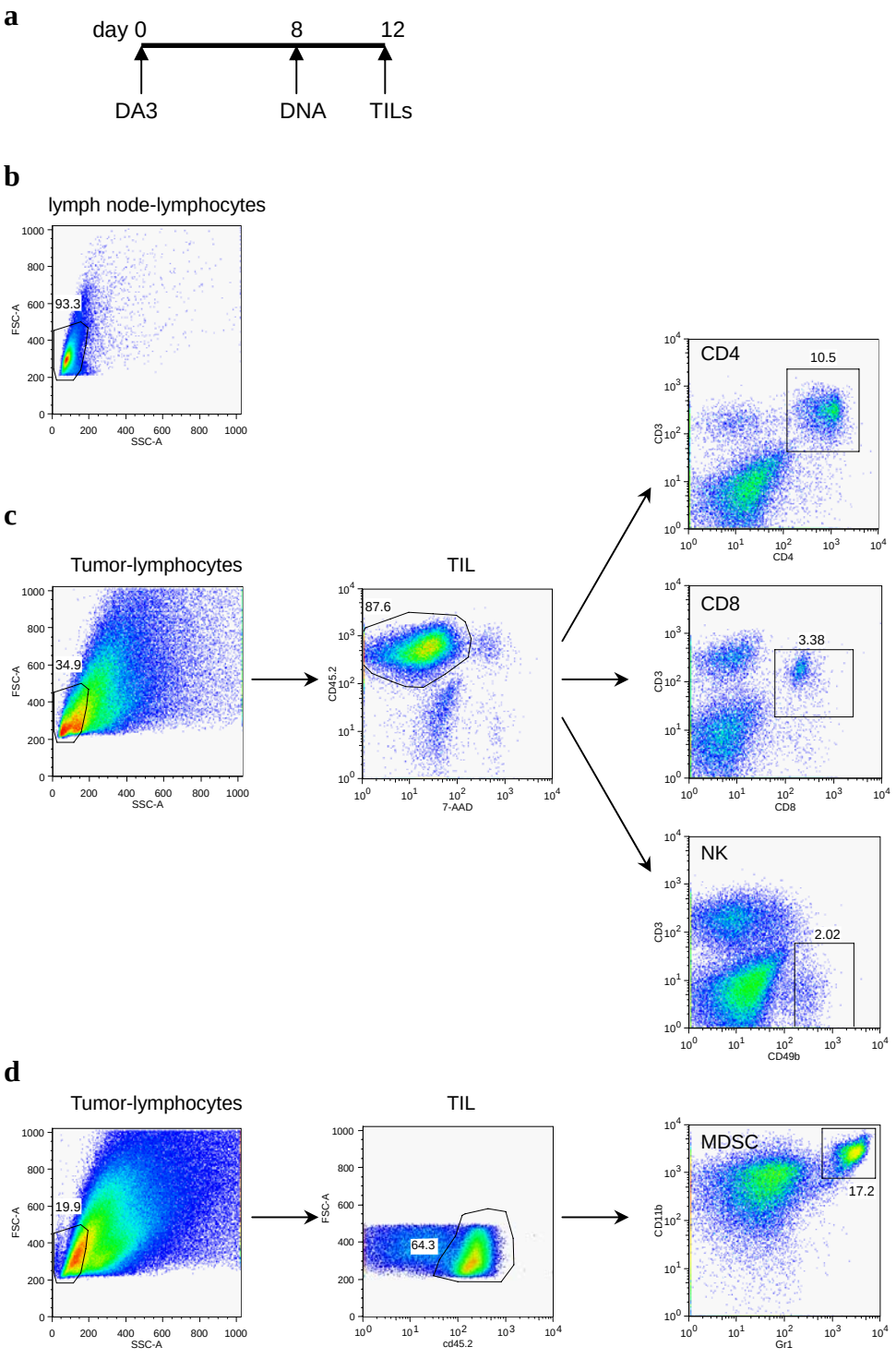
a
day 0
8
12
DA3
DNA
TILs
b
lymph node-lymphocytes
93.3
FSC-A
SSC-A
c
Tumor-lymphocytes
34.9
TIL
87.6
CD45.2
7-AAD
CD4
10.5
CD3
CD4
CD8
3.38
CD8
NK
2.02
CD49b
d
Tumor-lymphocytes
19.9
TIL
64.3
cd45.2
MDSC
17.2
CD11b
Gr1

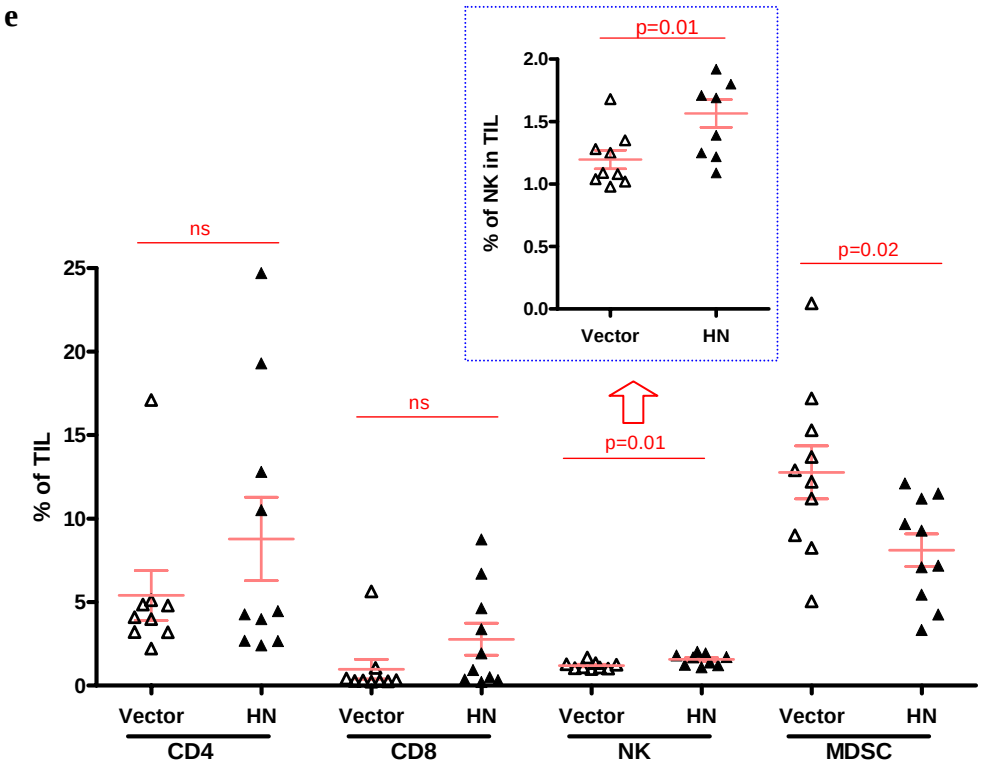

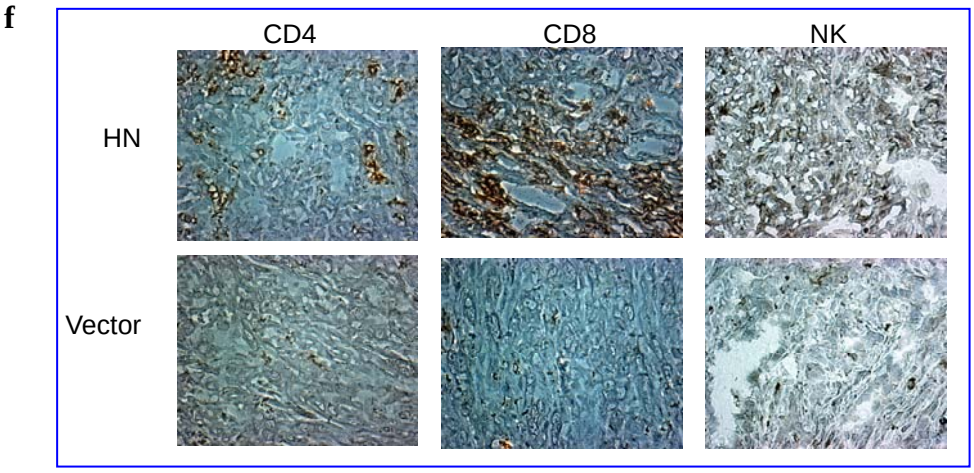

Figure 4.41 Adjuvant effect of HN on tumor infiltrating lymphocytes

a. Strategy of TIL analysis. Balb/c mice (n=10/group) were inoculated sc with 1×10^7 DA3 cells at day 0 and immunized ie with 50µg/50µL HN or Vector DNA at day 8. 4 days after DNA treatment, TILs were analyzed by FACS and immunohistochemistry. **b**. Definition of lymphocyte population by cell size. Lymph nodes were taken from vaccinated mice. Cells were analyzed by FACS. The lymphocyte gate was used for definition of lymphocyte population by size in tumor. **c**. Definition of CD4, CD8, NK cells in TIL. Single cell suspension of tumor was analyzed by FACS. For CD4, CD8 T cells and NK cells, living cells in lymphocyte gate with CD45.2 expression were defined as TIL. Then $CD3^+CD4^+$, $CD3^+CD8^+$ and $CD3^+CD49b^+$ cells were defined as CD4, CD8 and NK cells respectively. **d**. Definition of MDSC in TIL. For MDSC, $CD45.2^+$ cells in the lymphocyte gate were defined as TIL, and then $CD11b^+Gr1^+F4/80^+$ cells were defined as MDSC. **e**. Percentage of CD4, CD8, NK and MDSC in TIL (shown are MEAN±SEM). f. Immunohistochemistry of lymphocyte infiltration in tumor. Frozen sections of DA3 tumor after DNA treatment (as indicated in a) were stained by anti-CD4 (h129.19), anti-CD8 (53-6.7) and anti-CD49b (Hal/29) (1:200), and Anti-Ig HRP Detection Kits (all from BD Bioscience). Original magnification: ×250.

4.4 Improvement of ear pinna DNA vaccination by electroporation

One of the most substantial improvements in the efficiency of plasmid based gene transfer *in vivo* has been achieved by DNA electroporation. This approach can be considered as a strategy with low cost, safety, and ease of use. Other beneficial qualities are a decreased interindividual variability and an increased cellular infiltration at the vaccination site.

4.4.1 Parameters and strategy for electroporation

In this study, we used the ELGEN1000 DNA delivery system (Inovio, San Diego, USA) which is applied in many clinical trials. For small animals such as rat and mouse, a pedal and an electrode are provided (Figure 4.42a). By application of the electrode locally to the DNA injection site, electroporation (EP) can be started by clicking the pedal. To compare Ag expression without and with EP, mice were immunized with CMV-luc (25µg/50µL) ie and id without (left side) or with (right side) EP. Luciferase expression was monitored by *in vivo* imaging. *In vivo* DNA electroporation was performed with the parameters suggested by the Inovio Company (Table 4.3).

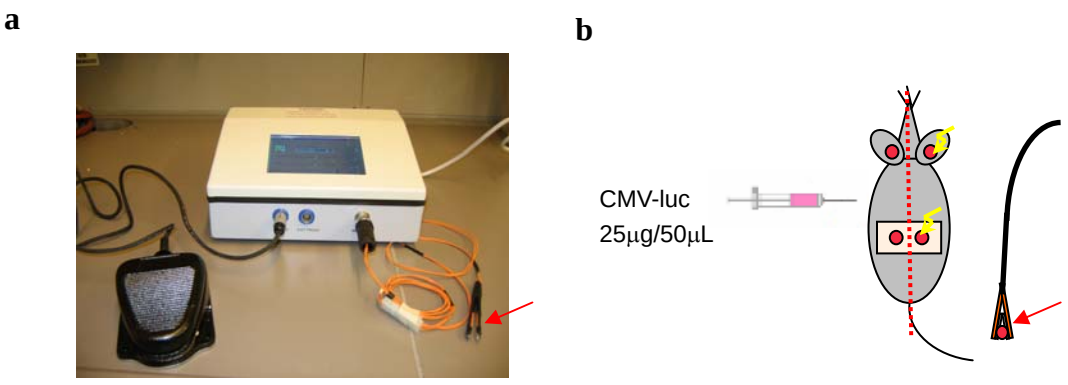

Figure 4.42 ELGEN1000 electroporation based DNA delivery system.

a. ELGEN1000 DNA delivery system supplemented with a pedal and an electrode. **b**. DNA immunization strategy in order to compare Ag expression in the ear pinna and flank skin without and with electroporation (EP). CMV-luc DNA (25µg/50µL) were injected intradermally to the ear pinna and flank skin without (left side) or with (right side) EP. Ag expression was monitored by *in vivo* imaging.

Table 4.3 Electroporation parameters

Time1	20
Voltage1	120
Nsequence	5
Ntrains	1
Pulse Delay	250
TrainDel	250
CurrLimit	1000

4.4.2 Optimization of DNA injection volume to ear pinna and flank skin

To optimize the DNA injection volume for Ag expression by the help of electroporation, 25μg CMV-luc DNA was injected either in 25μL or in 50μL (the largest volume which can be applied to the ear pinna) to the ear pinna or flank skin without (left side) and with (right side) EP. Luciferase expression was monitored by *in vivo* imaging (Luciferase expression at 1 d of DNA injection is shown in Figure 4.43a). Kinetics of luciferase expression (from 8 h to 28 d) showed that 50μL injection volume induced a slightly superior Ag expression than 25μL injection volume both in the ear pinna (Figure 4.43b) and in the flank skin (Figure 4.43c). With the help of EP, Ag expression was improved 2~3 times in the ear pinna and ~10 times in the flank skin.

4.4.3 Optimization of DNA electroporation voltage

Promising improvement of Ag expression in both ear pinna and flank skin induced by EP is shown in Figure 4.43. However, tissue damage induced by EP was serious. The ear pinna became punctured (Figure 4.44a) after a few days (4-7 d) of EP. Serious inflammation was also found in the local flank skin (data not shown). To avoid serious tissue damage, lower voltages (40, 60, 80, 100V) were compared to 120V for the efficiency of improving Ag expression and tissue inflammation. Inflammation index was defined as in Table 4.4. Short-term tissue inflammation induced by different voltages is shown in Figure 4.44b. With 120V of EP, the injected ear pinnas had locally concentrated red spots for the first 3 days, and then the tissue got punctured in 100% mice from day 4 to day 7. 100V of EP induced tissue damage which was not as serious as with 120V. 30% of the mice had a hole in the treated ear pinna. Voltages lower than 80V induced slight inflammation, which recovered in 1 week. Long term

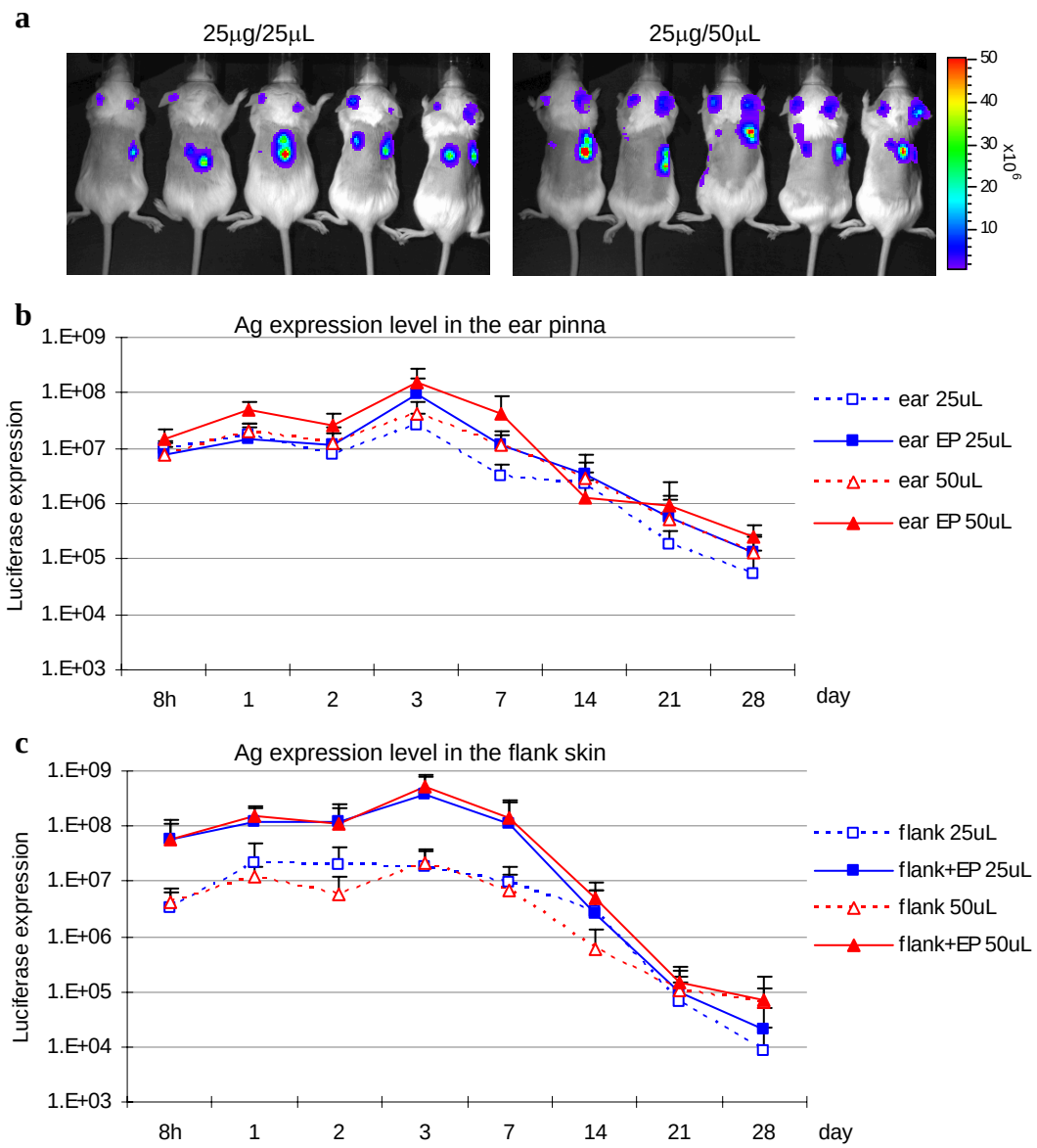

Figure 4.43 Optimization of DNA injection volume to ear pinna and flank skin.

To optimize DNA injection volume, 25µg CMV-luc DNA was injected either in 25µL or in 50µL volume to the ear pinna or flank skin without (left side) and with (right side) EP (Balb/c mice, n=5). Luciferase expression was monitored by *in vivo* imaging. **a**. Luciferase expression at 1 d of DNA injection. Kinetics of quantitative luciferase expression from 8 h to 28 d with 25µg CMV-luc in 25µL or in 50µL volume to the ear pinna (**b**) or flank skin (**c**). Bioluminescent signal was shown and calculated in pseudophoton unit: p/sec/cm^2/sr. Exposure time: 10 s.

Table 4.4
Definition of tissue inflammation

Inflammation index	inflammation description
0	none
1	red
2	deep red
3	concentrated red spot + burns
4	concentrated red spot + hole*

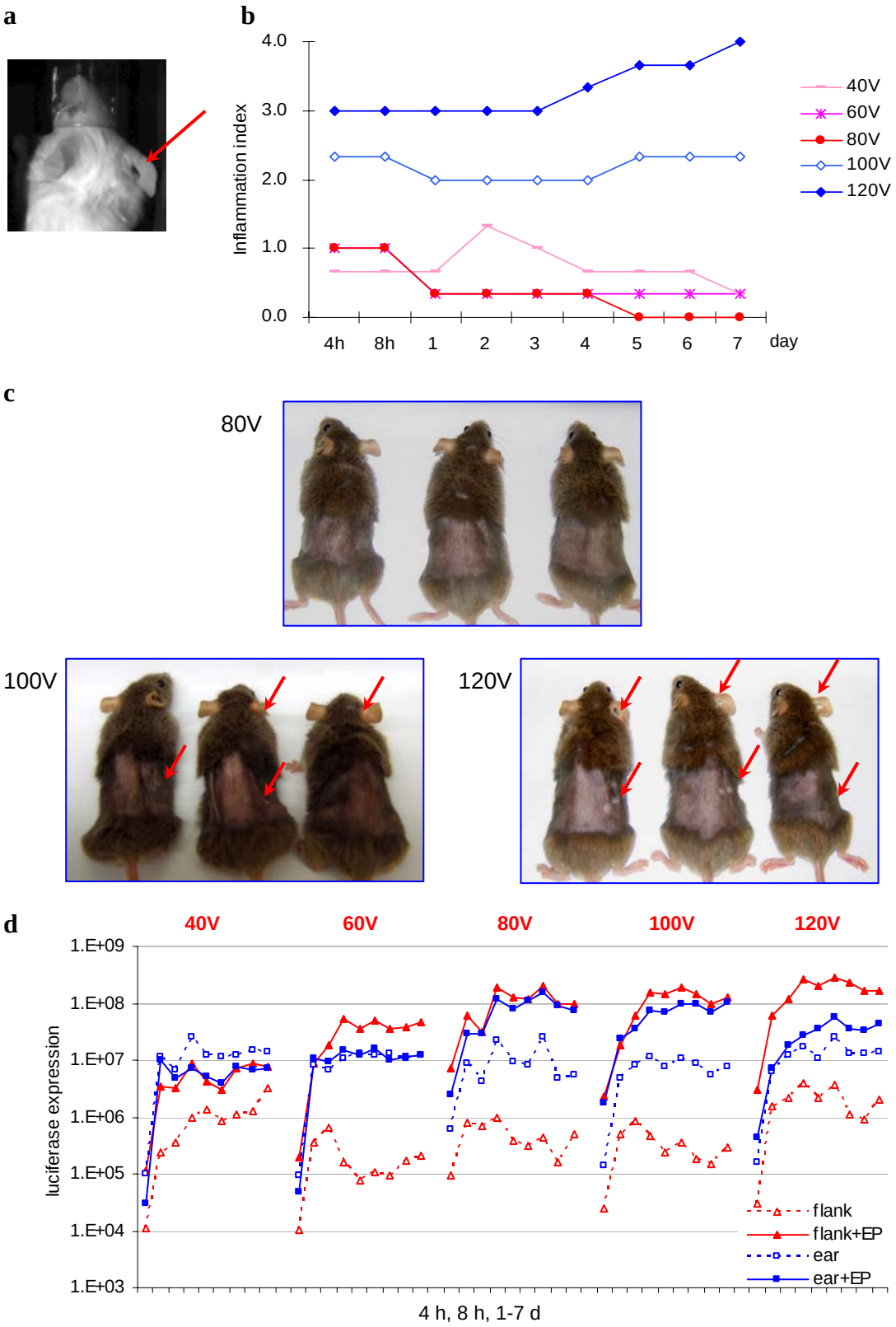

Figure 4.44 Optimization of DNA electroporation voltage

a. Local tissue damage in the ear after 7 d of EP with 120V. **b**. Kinetics of short-term (1-7 d) tissue inflammation index in the ear of EP with different voltages (40-120V). DBA/2 mice, n=3. **c**. Long-term (day 319) tissue damage in the ear and flank skin. **d**. Kinetics of short-term (1-7 d) Ag expression in the ear and flank skin without and with EP. Bioluminescent signal was calculated in pseudophoton unit: p/sec/cm^2/sr. Exposure time: 10 s.

tissue damage was checked after 319 days (Figure 4.44c). It revealed no visible tissue damage with 80V, slight scars in the flank skin and little holes in the ear with 100V, and obvious scars in the flank skin and big holes in the ear pinna with 120V. Ag expression (Figure 4.44d) revealed similar improvements (~100 times higher) in the flank skin by EP with 80V, 100V and 120V (maximum plateau is 1-7 d), and a slight improvement in the ear pinna by EP with 80V (~10 times higher). 100V and 120V resulted in too much tissue damage. With 40V and 60V, Ag expression was not significantly improved. These results showed that EP could be applied intradermally to mouse skin with an optimal voltage 80V.

4.4.4 Improvement of long-term Ag expression

To analyze long-term effects on Ag expression by DNA electroporation, mice were immunized ie and id with CMV-luc (25μg/50μL) with 80V of EP. Luciferase expression was monitored by *in vivo* imaging from 4 h to 350 d. Ag expression induced by DNA electroporation was similar in the ear pinna and flank. However, Ag expression induced by naked DNA injection was 10-100 times higher in the ear pinna than in the flank. With EP, plateau Ag expression was found during the first week in both ear pinna and flank, and went down from day 7 in the flank and from day 14 in the ear pinna. After 4 weeks, Ag expression decreased about 10-100 times. It maintained a stable low expression for almost 1 year. In fact, Ag expression was still relatively high after 4 weeks by DNA electroporation (similar level as Ag expression in the first week of naked DNA injection). These results revealed that electroporation could significantly improve the level and duration of Ag expression.

4.4.5 Improvement of humoral immune responses

Since DNA electroporation led to increased Ag expression, it might improve immune responses to the Ag. Serum antibodies (day 14 after CMV-lac immunization) were analyzed by β-gal ELISA. Stronger humoral immunity (IgG+M, IgG1, IgG2a) was induced by naked DNA immunization upon ie as compared to id immunization (Figure 4.46). Electroporation dramatically improved IgG+M and IgG1 levels and improved IgG2a levels upon id DNA immunization because of no detectable IgG2a by naked DNA id injection. These results further confirmed the superiority by ie DNA

immunization than id DNA immunization and showed the influence of EP could improve immune response at both sites.

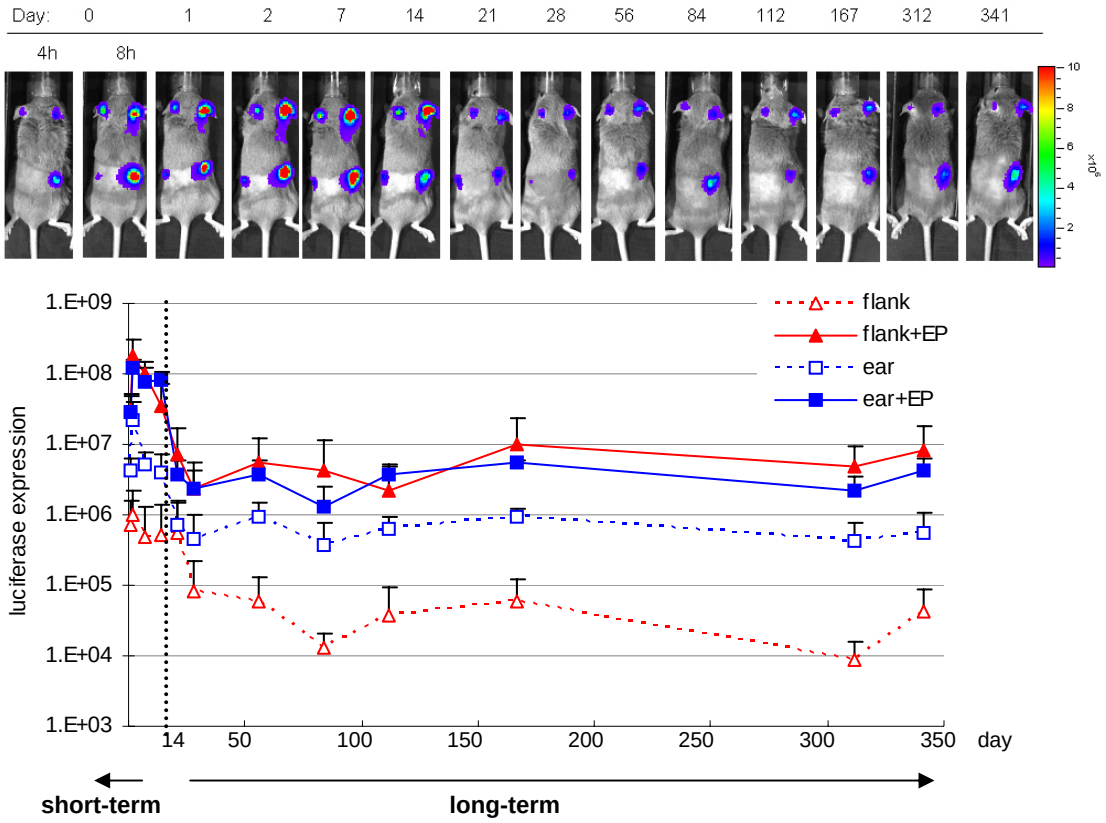

Figure 4.45 Improvement of long-term Ag expression by DNA electroporation.

DBA/2 mice (n=3) were immunized ie and id with CMV-luc (25µg/50µL) without (left) and with (right) 80V of EP. Luciferase expression was monitored by *in vivo* imaging from 4 h to 350 d. Bioluminescent signal was shown and calculated in pseudophoton unit: p/sec/cm^2/sr. Exposure time: 20 s. 1 representative experiment of 3 was shown.

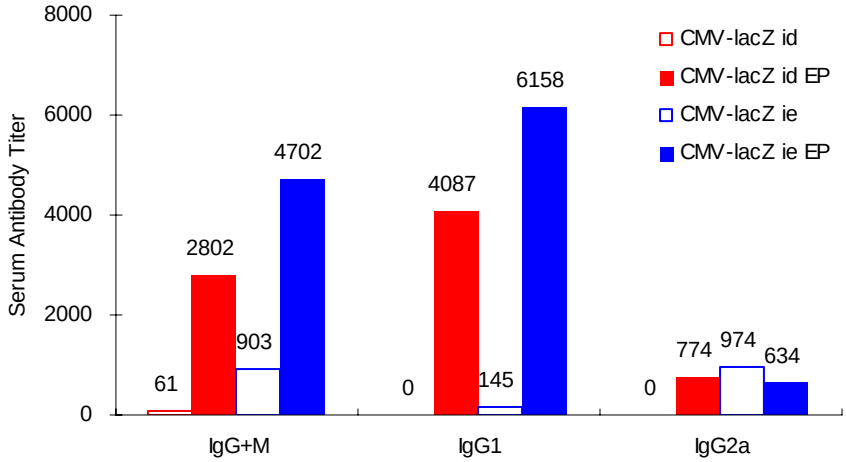

Figure 4.46 Improvement of antibody responses by DNA electroporation.

DBA/2 mice (n=3/group) were immunized ie or id with CMV-lacZ (25µg/50µL) without or with EP. Sera from day 14 of the DNA vaccination were analyzed for antibody responses (IgG+M, IgG1, IgG2a) by β-gal ELISA. 1 of 3 independent experiments was shown.

4.4.6 Improvement of cellular immune responses

Although improvements of humoral immunity were induced by DNA electroporation, it is more important to induce strong cellular immunity for anti-tumor activity. For this purpose, we further analyzed the influence of EP on CTL mediated cytotoxicity and on IFN-γ and IL-4 production from *in vitro* re-stimulated splenocytes.

4.4.6.1 Cytotoxicity

Mice with 1 DNA immunization without or with EP were analyzed for specific lysis to CTL activity against $lacZ^+$ tumor cells (Figure 4.47) by a standard ^{51}Cr release assay. Detectable specific cytotoxicity was induced by naked DNA injection only to the ear pinna but not to the flank skin. By help of EP, specific lysis was strongly improved both for ie and id DNA+EP (71% for ie and 56% for id when E:T is 100:1). EP applied to the flank skin affected more unspecific lysis of $lacZ^-$ tumor cells. These results revealed that improvements of specific CTL activity could be achieved by EP at the ear pinna but less so at the flank skin.

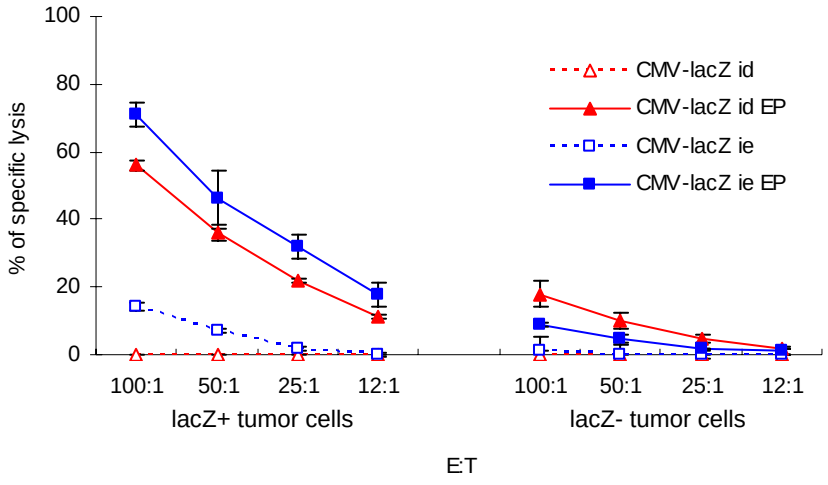

Figure 4.47 Improvement of specific cytotoxicity by DNA electroporation.

Mice for antibody analysis were sacrificed at day 14 of the DNA immunization. Spleens were taken out and re-stimulated for 5 days *in vitro* with 0.5µg/mL TPHPARIGL peptide and analyzed cytotoxicity by a standard 4 h ^{51}Cr release assay to $lacZ^+$ tumor cells (P13.1) and $lacZ^-$ tumor cells (P815).

4.4.6.2 IFN-γ and IL-4 secretion

To further substantiate the improvement of cellular immune responses induced by DNA+EP, IFN-γ and IL-4 secretions into the supernatants from the re-stimulated splenocytes were analyzed by ELISA. Ie DNA immunization induced higher IFN-γ secretion activity compared to id DNA immunization. EP dramatically improved IFN-γ secretion upon ie but not upon id DNA immunization (Figure 4.48). Conversely, id DNA immunization induced higher IL-4 production and EP improved it (Figure 4.48). This would support humoral immune responses. No IL-4 was detectable from splenocytes after ie DNA immunization. These results further support the benefit to cellular immune responses from ie DNA immunization that was reported before (75) and its further improvement by EP.

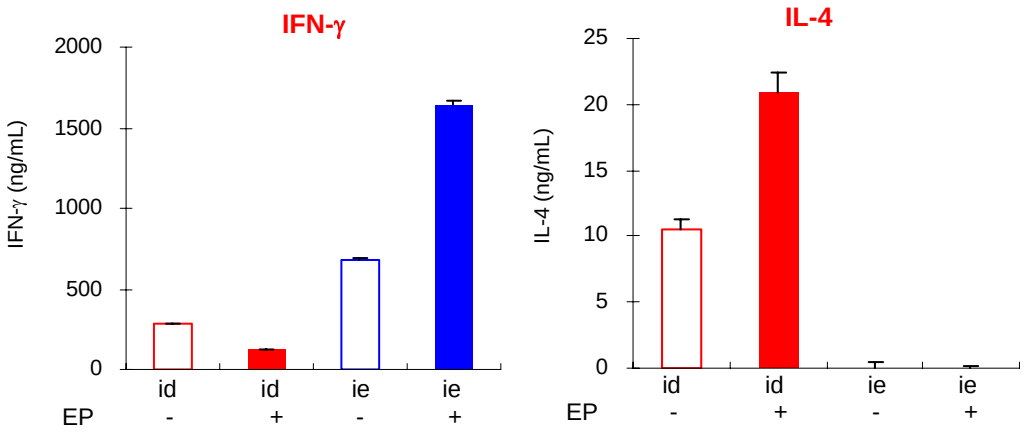

Figure 4.48 Improvement of cytokine production by DNA electroporation.

Supernatants from re-stimulated splenocytes (Figure 4.47) were collected and analyzed for IFN-γ (day 2 supernatant) and IL-4 (day 5 supernatant) by ELISA.

4.4.7 Improvement of prophylactic anti-tumor effect

Thus, DNA electroporation could improve both humoral and cellular immune responses. To analyze if it was possible to improve the anti-tumor effect by DNA+EP, vaccination was applied to the prophylactic ESb-lacZ tumor model in which naked CMV-lacZ DNA immunization was not sufficient to protect mice completely from tumor growth. Vaccinated mice died after about 3 weeks.

2 weeks after DNA immunization without or with EP, mice were challenged with ESb-lacZ cells (Figure 4.49a). Tumor growth was followed until day 18 (some of the

mice died after day 18). Figure 4.49b shows tumor diameters at day 18. Naked CMV-lacZ DNA immunization ie or id did not induce significant anti-tumor activity compared to Vector immunization. Significant anti-tumor effects were achieved by EP to the ear pinna as well as to the flank skin. Tumor inhibition was better by ie then id DNA immunization (compared to Vector EP, $p<0.01$ for CMV-lacZ ie EP, $p<0.05$ for CMV-lacZ ie EP).

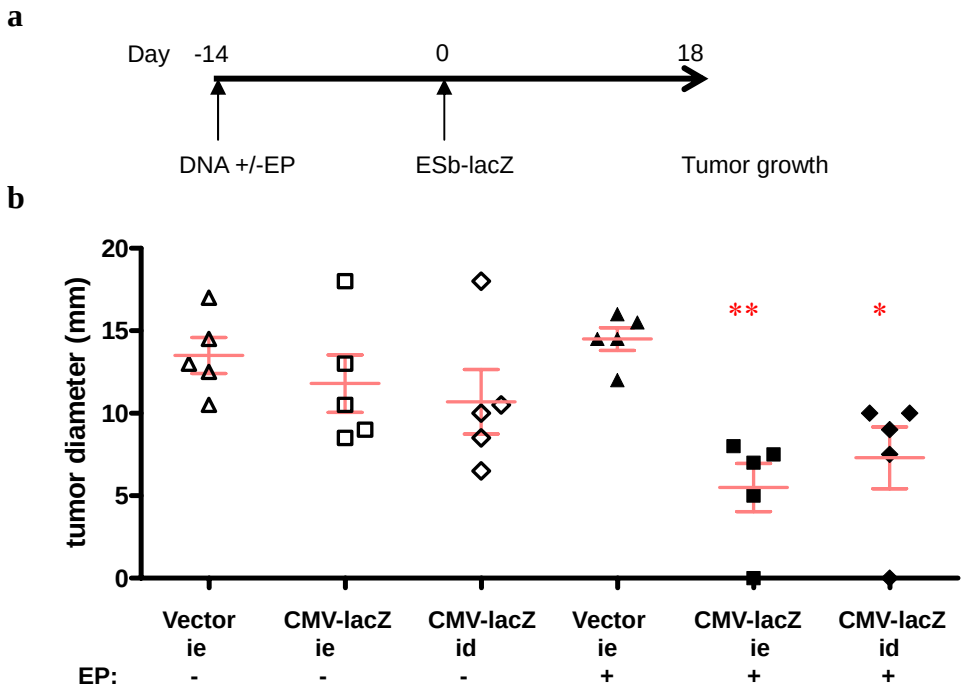

Figure 4.49 Improvement of anti-tumor effect in the prophylactic ESb-lacZ tumor model by DNA electroporation.

a. Vaccination strategy. DNA vaccines (25μg/50μL) were immunized ie or id to the DBA/2 mice (n=5/group) without or with EP. 2 weeks after the DNA immunization, 2×10^5 ESb-lacZ cells were inoculated sc to the mice (day 0). Tumor growth was followed until some of the mice died (since day 18). b. Tumor diameters (MEAN±SEM) at day 18.
* Compared to the Vector ie EP group, $p<0.05$, ** Compared to the Vector ie EP group, $p<0.01$

4.4.8 Improvement of therapeutic anti-tumor effect

Results from Figure 4.49 show that prophylactic anti-tumor activity was significantly improved by DNA combined with EP at the ear pinna as well as at the flank skin. The effects from ear pinna were superior to those from flank skin (Figure 4.49b). We then combined ie DNA vaccination with EP in the therapeutic DE tumor model. 1 week after DE tumor inoculation, tumor bearing mice were treated by DNA vaccines without or with EP weekly with 4 treatments in total (Figure 4.50a). EpCAM ie DNA immunization did not induce significant tumor inhibition compared to Vector ie

injection. DE tumor growth was, however, significantly inhibited by EpCAM ie+EP immunization compared to Vector ie or EpCAM ie immunization (Figure 4.50b). After day 42, the DE tumors did not grow further and maintained a stable volume (the average tumor diameters in the Vector group was less than 8 mm) due to the strong immunogenicity of human EpCAM. To further demonstrate the anti-tumor activity induced with the help of EP, the DE tumor bearing mice were re-challenged with parental DA3 cells at day 59. DA3 tumor growth was significantly slowed down in the EpCAM ie+EP immunized group. These results provided evidence for the efficiency of therapeutic DNA vaccination by ie DNA application and its improvement by EP.

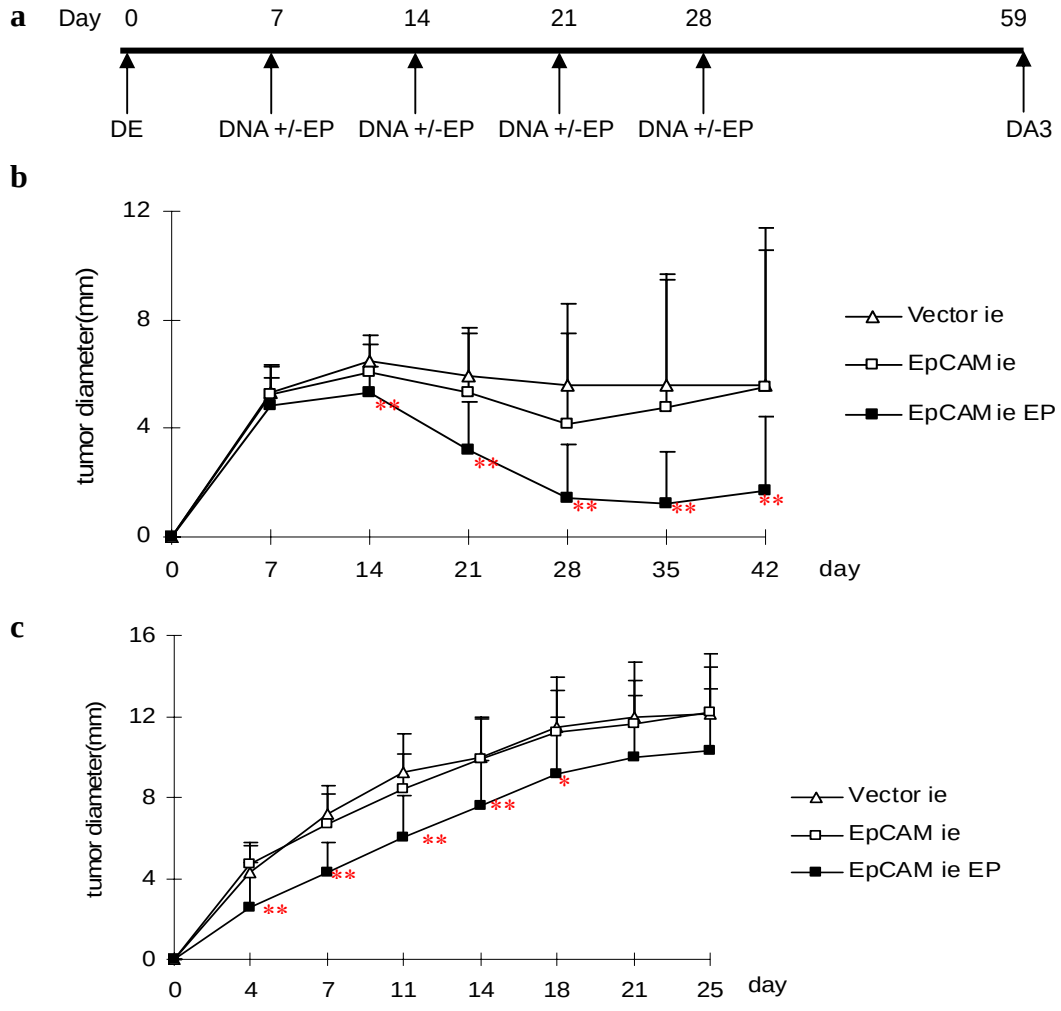

Figure 4.50 Improvement of anti-tumor effect in the therapeutic DE/DA3 tumor model by DNA ie electroporation.

a. Therapeutic DNA vaccination strategy. Balb/c mice (n=13~15/group) were inoculated with 1×10^7 DE cells and followed by DNA treatments 1 week later (50μg/50μL DNA /immunization) for 4 treatments in total. DE tumor growth was followed (**b**). DE tumor bearing mice were re-challenged with 1×10^7 DA3 cells at day 59 and followed tumor growth (**c**). **Compared to the Vector and EpCAM ie groups, $p<0.01$.

4.4.9 Down-regulation of suppressive factors

Therapeutic anti-tumor effects were improved by DNA ie EP. This suggested that suppressive factors might be down-regulated because established tumors usually produce factors to suppress host anti-tumor immunity (123-125). DE/DA3 cells constitutively secrete TGF-β to the supernatant when cultured *in vitro* (data not shown). To analyze the potential influence of EP on TGF-β levels *in vivo*, sera from day 49 in the DE therapeutic tumor model (Figure 4.50a) were analyzed for peripheral TGF-β level. DNA ie EP significantly down-regulated the serum TGF-β level in the DE tumor bearing mice (Figure 4.51). Myeloid derived suppressor cells (MDSCs) in spleen were analyzed during day 88~101. A lower percentage of MDSCs in spleen was found in DNA ie EP vaccinated mice (Figure 4.52), but this was not significant. This result might be influenced by the time of the analysis (very late tumor phase (day 88~101)) when a suppressive situation was already formed.

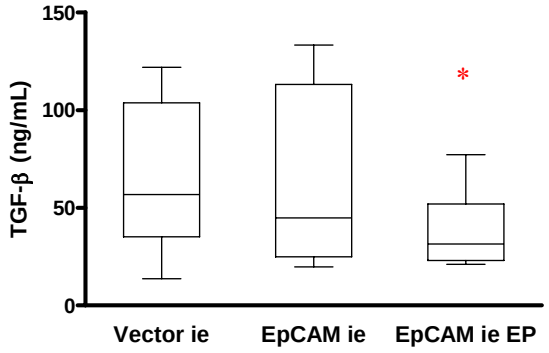

Figure 4.51 Serum TGF-β at day 49.

Sera from DE tumor bearing mice (Figure 4.50a DE therapeutic tumor model) at day 49 were analyzed for TGF-β level by ELISA.

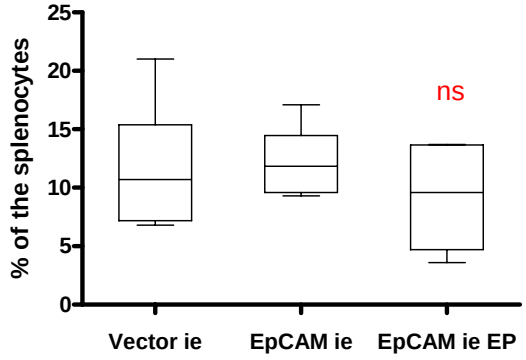

Figure 4.52 Splenic MDSC at day 88~101.

Spleens from DE/DA3 tumor bearing mice (Figure 4.50a DE therapeutic tumor model) at day 88~101 were analyzed for percentage of MDSC by FACS analysis of $CD11b^{+}Gr1^{+}F4/80^{+}$ cells.

4.5 Crucial function of dendritic cells in ear pinna DNA immunization

Dendritic cells (DCs) are the most potent professional Ag presenting cells (APC) capable of priming naïve T cells. In DNA vaccination, they are efficient to present Ags by direct and cross-presentation. It is reported that *in vitro* genetically transfected DCs with a plasmid DNA elicited immune responses and anti-tumor effects *in vivo*. Ear pinna is a special site and form of skin, where there are two layers of epidermis and dermis separated by a cartilage. APCs, especially DCs are concentrated in the epidermis and dermis, which suggests that high amounts of APCs are concentrated in the ear pinna compared to normal skin. That could be one of the explanations that ear pinna is superior to the flank skin for DNA vaccination.

4.5.1 Distribution of dendritic cells in ear pinna and flank skin

DC distribution in ear pinna, flank skin and muscle was analyzed by immuno-histochemistry staining for $CD11c^+$ dermis DC and $Langerin^+$ epidermis Langerhans cells. $Langerin^+$ and $CD11c^+$ cells are abundant in epidermis and dermis (red arrow), with higher numbers in the ear pinna because of the special structure of double layers of epidermis and dermis. No DCs or LCs were detected in muscle tissue.

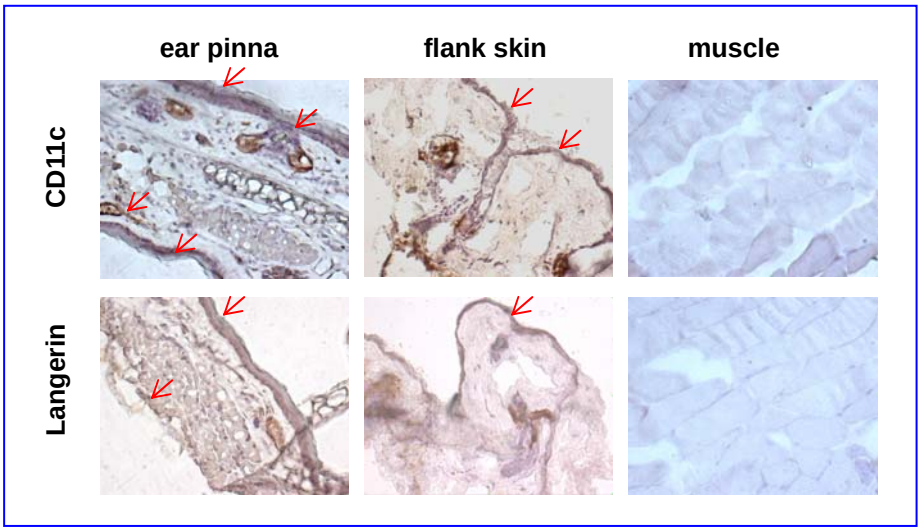

Figure 4.53 Distribution of dendritic cells in ear pinna and flank skin compared to muscle.

Frozen sections were stained for $CD11c^+$ and $Langerin^+$ cells with CD11c and CD207 antibodies (1:200), as well as Anti-Ig HRP Detection Kits (BD Pharmingen). Original magnification: ×250.

4.5.2 Generation of a short murine CD11c promoter

A 5.5-kb CD11c promoter is widely used by many groups for DC specific gene expression (126-128). This promoter was employed for targeting gene expression directly to DC *in vivo* (126, 128). Previous studies showed restricted gene expression in DC by this promoter, but failed to show efficient humoral and cellular immune responses following gene gun DNA immunization (127). This might be due to the low level of Ag expression. Since *in vitro* transfection is hard to achieve with high efficiency due to the long DNA sequence, we hypothesized that a short version of CD11c promoter might be easier for the application both *in vitro* and *in vivo*.

4.5.2.1 Verification of the functional region of murine CD11c promoter

To test if a short fragment of the murine CD11c promoter could achieve specific promoter activity in DC, we generated CD11c promoters by PCR with different length (700-bp, 1105-bp, 2448-bp, 3383-bp, 5534-bp) from the BAC vector containing the mouse CD11c gene (Figure 4.54). These were cloned into the pGL3-Basic vector containing a firefly luciferase as a reporter gene (Table 4.5). These vectors were transfected to bone marrow derived DCs (BMDCs) to verify promoter activity and compared to the CMV promoter. Luciferase expression revealed a much stronger (~100 times) promoter activity for CMV than for all the CD11c promoters. Among the

Figure 4.54 Schematic representations of CD11c promoters in the CD11c genome.

Mouse CD11c promoters with different lengths were generated by PCR from the BAC vector containing mouse CD11c genome based on the sequence in the promoter region.

Table 4.5
Construction of CD11c promoters with different lengths

name	Promoter length	sequence in CD11c genome	Encoding gene
pCD11c700	700-bp	0~-700	Firefly luciferase
pCD11c1105	1105-bp	0~-1105	
pCD11c2448	2448-bp	0~-2448	
pCD11c3383	3383-bp	0~-3383	
pCD11c5534	5534-bp	0~-5534	

CD11c promoters, the 3 shorter versions (700, 1105, and 2448) were better than the 2 long ones (3383, 5534) (Figure 4.55a). These 3 short ones were then tested for their promoter activity in a CD11c positive cell line (RMA264) and compared to the long one (5534-bp) which is normally used DC specific gene expression. Figure 4.55b shows similar promoter activity of the 3 short CD11c promoters. These were all better than the long one. Therefore, the shortest one, pCD11c700, and the longest one pCD11c5534 were used for further study as CD11cS (short CD11c promoter) and CD11cL (long CD11c promoter). DNA sequencing results revealed mutations at 2 bases in the CD11cS promoter (Figure 4.56) (99.7% identity) and 100% identity with the CD11cL promoter compared to the genomic sequence.

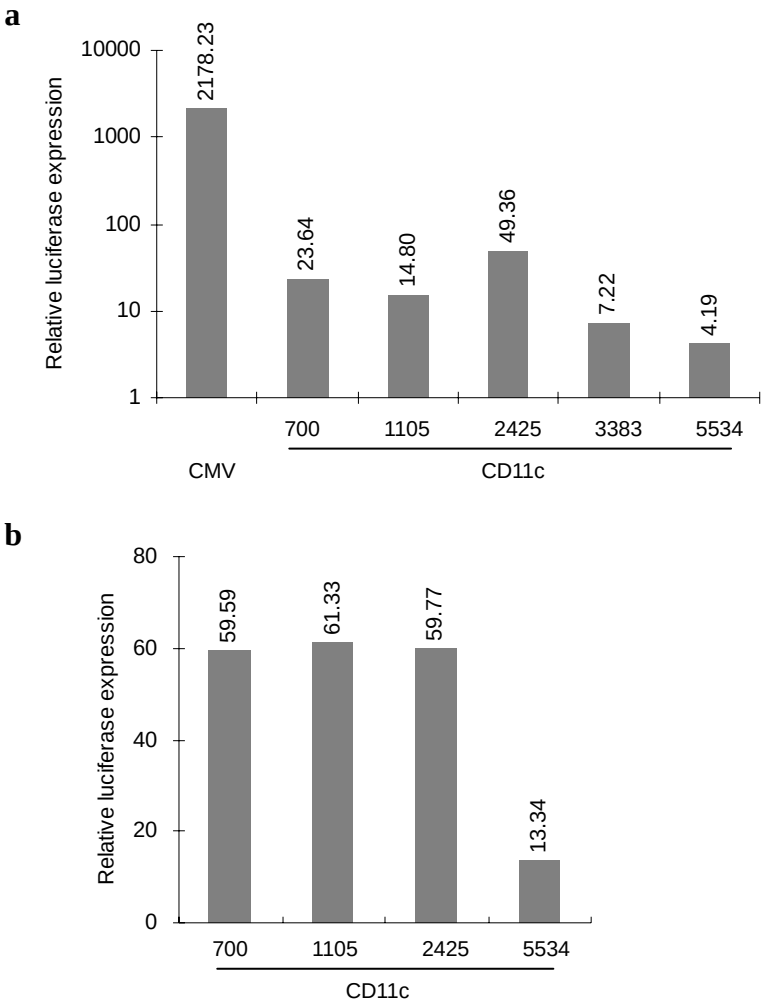

Figure 4.55 Verification of *in vitro* promoter activity of CD11c promoters.

BMDC (**a**) and RAW264 (**b**) were transfected with DNA vectors encoding firefly luciferase regulated by CD11c promoters, as well as pGL3-Basic (negative control) and CMV-luc (positive control). A vector CMV-Ruc encoding renilla luciferase was used for co-transfection (1:25) to control the transfection efficiency. Promoter activity is expressed relative to the luciferase activity produced by the promoterless plasmid, pGL3-Basic, after correction for transfection efficiency by Renilla luciferase. Transfections were made by triplicate, and repeated for 3 times.

Figure 4.56 Two bases of mutations revealed by DNA sequencing in CD11cS promoter.

4.5.2.2 *in vitro* specific activity of the CD11cS and CD11cL promoters

To test the specific promoter activity of CD11cS and CD11cL *in vitro*, $CD11c^+$ and $CD11c^-$ mouse cell lines as well as mouse bone marrow derived DC (BMDC) were transfected with CD11cS-luc or CD11cL-luc. Luciferase expression revealed a stronger promoter activity of CD11cS than CD11cL in $CD11c^+$ cells (BMDC, DC2.4, RAW264), and a very low activity of both promoters in $CD11c^-$ cells (Figure 4.57). Both CD11c promoters induced restricted Ag expression in $CD11c^+$ cells. The short CD11cS sequence showed a stronger activity. This might be due to the higher copy number of plasmid based on the same amount of DNA and the better transcription efficiency achieved by the small vector.

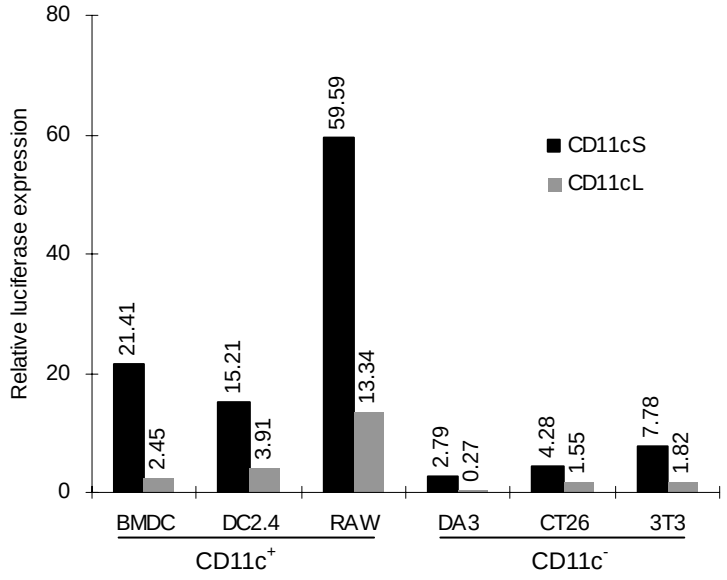

Figure 4.57 *In vitro* specific activity of the CD11cS and CD11cL promoters.

Cells were transfected with CD11cS-luc and CD11cL-luc vectors (encoding firefly luciferase), as well as pGL3-Basic (negative control) and CMV-luc (positive control). A vector CMV-Ruc encoding renilla luciferase was used for co-transfection (1:25) to control the transfection efficiency. Promoter activity is expressed relative to the luciferase activity produced by the promoterless plasmid, pGL3-Basic, after correction for transfection efficiency by Renilla luciferase. Transfections were made by triplicate, and repeated for 3 times. CD11c positive cells: BMDC, DC2.4, RAW; CD11c negative cells: DA3, CT26, 3T3.

4.5.2.3 *in vivo* activity of the CD11cS and CD11cL promoters

To prove the stronger promoter activity of CD11cS *in vivo*, the two DNA constructs CD11cS-luc and CD11cL-luc were applied ie and id to mice. Via bioluminescence imaging, luciferase expression induced by CD11cS was visible 4 hours after DNA injection in both ear pinna and flank, while the expression induced by CD11cL was seen only later (at 8 h) and only in the ear pinna (Figure 4.58). Quantitative bioluminescence analysis revealed that CD11cS induced a stronger gene expression than CD11cL in both ear pinna (~10 times higher) and flank (~1.5 times higher) at all time points (from 4 h to 7 d) (Figure 4.58). Both promoters induced a stronger luciferase expression than the luciferase containing pGL3-Basic vector with no promoter (data not shown). These results demonstrated the stronger promoter activity of CD11cS compared to CD11cL *in vivo*. Therefore, we applied the CD11cS promoter to further study gene targeting to DC.

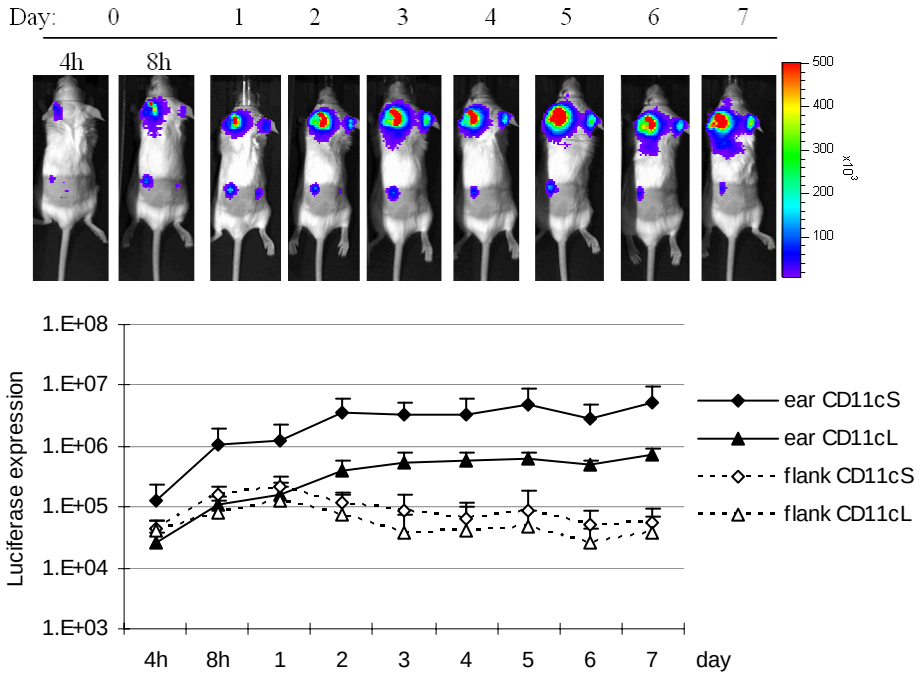

Figure 4.58 *In vivo* activity of the CD11cS and CD11cL promoters.

In vivo activity of CD11c promoters was tested by bioluminescence imaging after ie and id DNA injection. 25µg/50µL CD11cS-luc (left) or CD11cL-luc (right) DNA was injected ie or id to the ear or shaved flank skin (Balb/c mice, n=5). Mice were imaged for firefly luciferase expression at different time points using the IVIS100 system with 2 min exposure time. Experiments were repeated 3 times with similar results. Below: quantitative analysis of firefly luciferase expression was calculated in the Igor Pro 4.09A software for ROI (region of interest, Unit: p/sec/cm^2/sr).

4.5.3 Verification of the specific activity of the CD11cS promoter *in vivo*

4.5.3.1 *In vivo* activity of CD11cS in mouse muscle tissue

To further analyze the specific activity of CD11cS in different tissues, we injected the CD11cS-luc plasmid into both the ear skin and the muscle (right side), with CMV-luc immunization as an unspecific control in the same mice (left side). DNA was applied by electroporation (EP) to favor strong gene expression. No luciferase expression was detected in muscle tissue (no resident DC) with CD11cS-luc injection, while luciferase expression was found in the ear pinna which is a DC rich tissue. CMV-luc injection led to luciferase expression in both ear pinna and muscle (Figure 4.59).

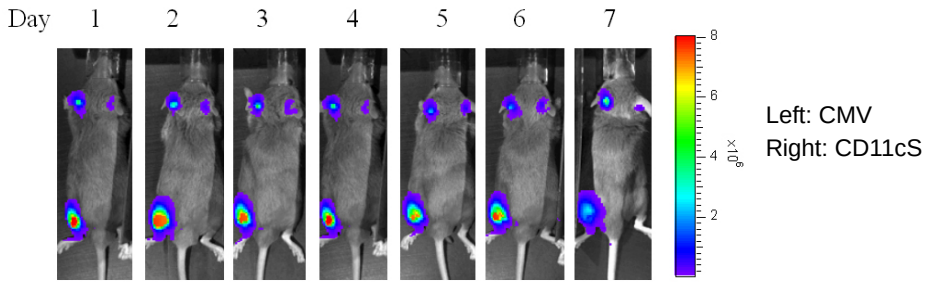

Figure 4.59 CD11cS-luc expression in skin compared to muscle.

25µg/50µL CMV-luc (left) or CD11cS-luc (right) DNA was injected ie or im with electroporation to the ear or muscle (DBA/2 mice, n=5). Mice were imaged for firefly luciferase expression at different time points with 2 min exposure time. Experiments were repeated 3 times with similar results.

4.5.3.2 *In vivo* activity of CD11cS in dendritic cell-depleted mice

To further corroborate the DC specific activity of CD11cS, we used CD11c-DTR-tg mice in which DC could be depleted by DT injection. CD11c-DTR-tg and C57BL/6 mice were injected ie with CD11cS-luc 24 h after DT ie injection, with CMV-luc as a control. No luciferase expression was found by CD11cS-luc injection after DC depletion (ROI less than 5×10^3-1×10^4 is the background) in CD11c-DTR-tg mice, while luciferase was expressed to a similar level in CD11c-DTR-tg mice without DC depletion and in C57BL/6 mice (Figure 4.60a). Decreased luciferase expression was also found in the ear pinna of C57BL/6 mice after DT ie injection, which indicated that DT injection could interfere with Ag expression induced by DNA immunization. However, the down-regulation of Ag expression derived from interference of DT injection (5-10 times) could not compare to the effect achieved by depletion of DC (completely blocked). CMV-luc expression also was decreased in DC depleted mice

(5.1 times less at 24 h and 7.8 times less at 48 h compared with the mice without DC depletion), but by far not as strong as CD11cS-luc expression (33.5 times less at 24 h and 82.5 times less at 48 h, visible bioluminescence not detected) (Figure 4.60b). These results strongly support the conclusion that the CD11cS promoter regulates gene expression specifically in DC.

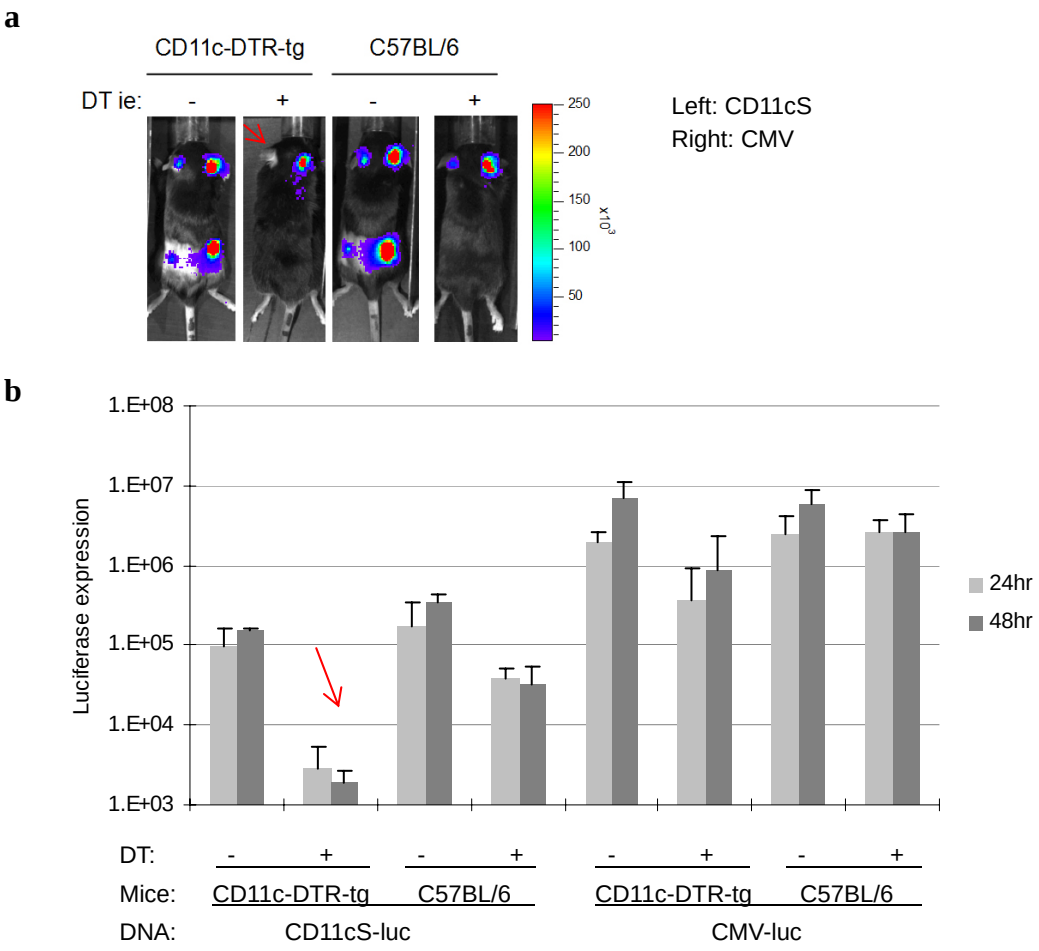

Figure 4.60 Selective expression of CD11cS-luc in DCs.

CD11c-DTR transgenic mice (CD11c-DTR-Tg, n=3) and C57BL/6 (n=5) were injected DT (100ng/50µL) to both ears. 24 h later, 25 µg/50 µL CD11cS-luc (left) or CMV-luc (right) was injected i.e. to the DC depleted mice. Mice were imaged for firefly luciferase expression at different time points with 2 min exposure time. Pictures shown are 24 h after DNA injection. Experiments were repeated 3 times with similar results. Below: quantitative analysis of luciferase expression.

4.5.4 Comparison of CMV and CD11cS promoter activity *in vivo*

To compare the *in vivo* promoter activity of CD11cS to CMV, mice were injected with CD11cS-luc and CMV-luc ie and id. Bioluminescence signals revealed that luciferase expression regulated by CD11cS was much lower in comparison to CMV in both ear pinna and flank skin (Figure 4.61). According to the quantitative analysis, it took 24 hours for CD11cS-luc to achieve plateau expression levels in comparison to 8 hours

for CMV-luc. High level of Ag expression was maintained for about 2 weeks, and then started to decrease. After 28 days, there was 10 times lower expression for CMV-luc (ie and id), and only 2 times lower expression for CD11cS-luc (ear pinna). CD11cS-luc expression was ~30-40 times lower than CMV-luc in the ear pinna, and ~100-200 times lower in the flank dermis. Furthermore, CD11cS-luc expression was 10-20 times lower in the flank dermis than in the ear pinna.

CD11cS promoter induced much lower Ag expression than the CMV promoter *in vivo*. In order to induce an efficient immune response by DNA vaccine with this promoter, EP was applied to improve Ag expression. Ag expression regulated by CMV and CD11cS was improved by EP both in the ear pinna (~1-5 times) and the flank skin (~10-100 times) (Figure 4.62). These results corroborated the improvement of Ag expression by DNA+EP as indicated before (Figure 4.45), but still the CD11cS promoter induced much lower Ag expression than the CMV promoter even after EP. In addition, although EP improved CMV-luc expression in the flank dermis to a level similar in the ear pinna (Figure 4.62a), it improved CD11cS-luc expression only to a level comparable to naked DNA ie injection (Figure 4.62b). These results indicated that ear pinna is a superior site, especially for CD11cS controlled Ag expression.

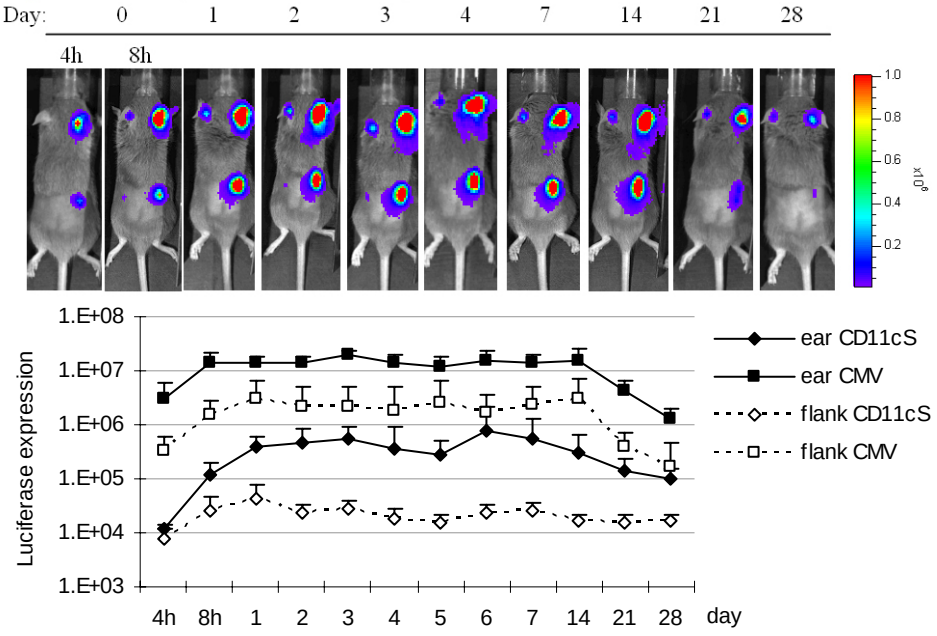

Figure 4.61 Comparison of the CMV and CD11c promoter activity *in vivo*.

In vivo activity of the CD11cS and CMV promoters were analyzed by *in vivo* imaging. 25µg/50µL CD11cS-luc (left) or CMV-luc (right) was injected ie and id (DBA/2 mice, n=5). Mice were imaged for firefly luciferase expression at different time points with 2 min exposure time. Experiments were repeated 3 times with similar results. Below: quantitative analysis of luciferase expression with CD11cS and CMV promoters.

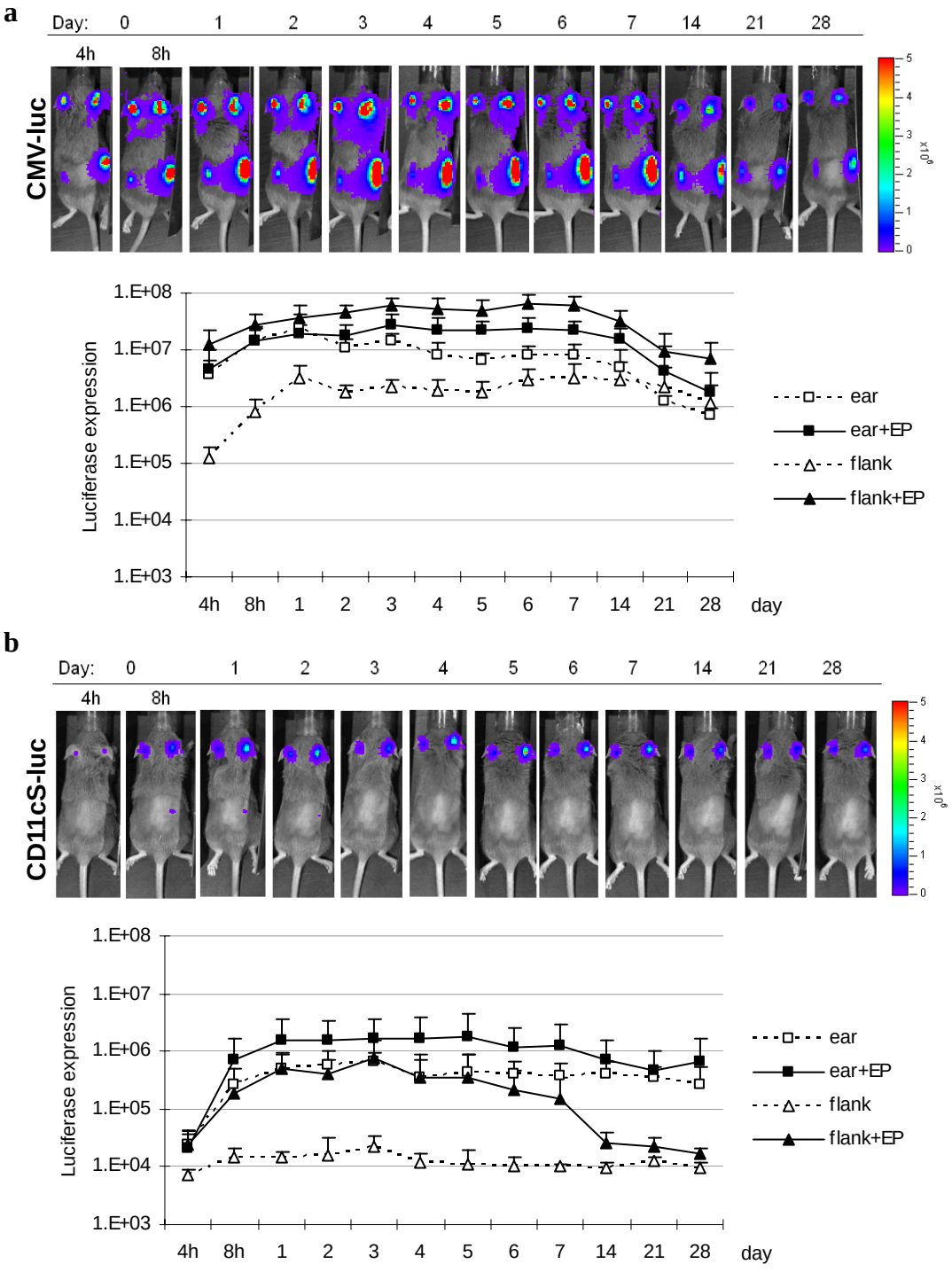

Figure 4.62 Improvement of Ag expression by DNA electroporation.

Improvement of Ag expression regulated by CMV and CD11cS by DNA EP was analyzed by *in vivo* imaging. 25µg/50µL CD11cS-luc (a) or CMV-luc (b) was injected ie and id (DBA/2 mice, n=5) without (left) and with EP (right). Mice were imaged for firefly luciferase expression at different time points with 1 min exposure time. Experiments were repeated 3 times with similar results. Below: quantitative analysis of luciferase expression with CMV and CD11cS promoters.

No improvements of early Ag expression were detected in the ear pinna before 1 d for CMV-luc and 8 h for CD11cS-luc (Figure 4.62). This indicated that EP-dependent improvements might take a few hours to result in increased Ag expression. We then analyzed Ag expression in the very early time point (Figure 4.63) after DNA injection. Ag expression by naked DNA injection was detected in the ear pinna as early as 1 h after injection, increased with time and benefited from EP (right side) after 8-24 h. Ear pinna was again superior to flank skin with regard to very early Ag expression. This might be of great advantage for early and strong immune responses.

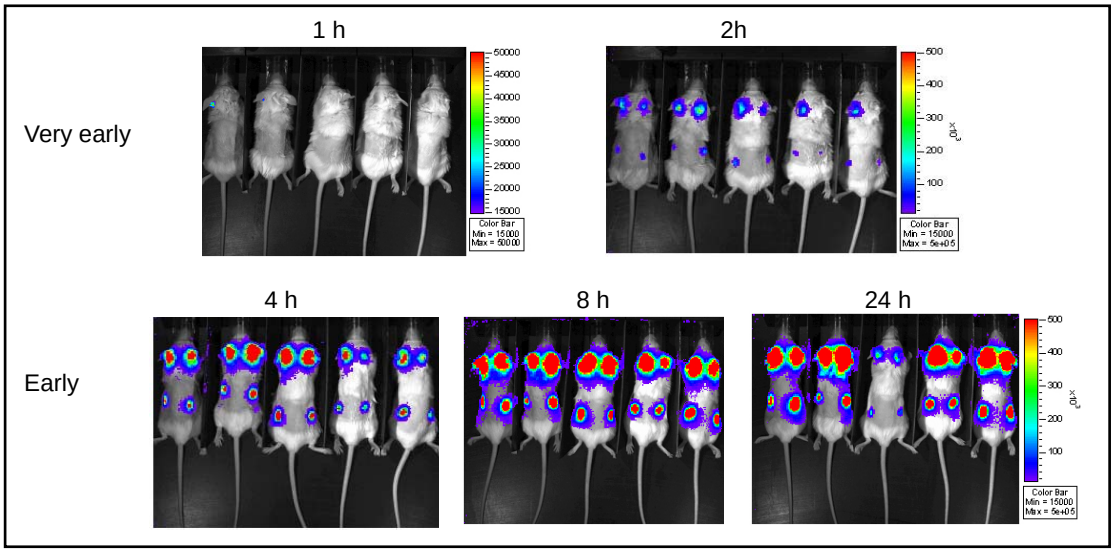

Figure 4.63 Improvement of early Ag expression by DNA EP.

25µg/50µL CMV-luc was injected ie and id (DBA/2 mice, n=5) without (left) and with EP (right). Mice were imaged for firefly luciferase expression at different time points (from 1 h, 2 h till 24 h) with 5 min exposure time for 1 h and 1 min for the other time points.

4.5.5 Humoral immunity by DNA vaccination with the CD11cS promoter

Although the CD11cS promoter leads to a specific and stable gene expression in DC, the promoter activity is much weaker compared to CMV. To analyze if it is enough to induce immune responses *in vivo*, we applied CD11cS in a DNA vaccine encoding the lacZ gene as a model tumor antigen. Plasmid DNA (CMV-lacZ, CD11cS-lacZ or Vector) was applied ie or id, and EP was given additionally to improve DNA uptake. Two weeks after a single immunization, serum anti-β-gal antibodies could be detected in mice immunized ie and id with CMV-lacZ. In contrast, CD11cS-lacZ induced antibody production only by ie injection, and the antibody titer was much lower than after CMV-lacZ immunization (Figure 4.64). These results showed that humoral immune responses could be induced by ie injection of DNA vaccine with the CD11cS

promoter.

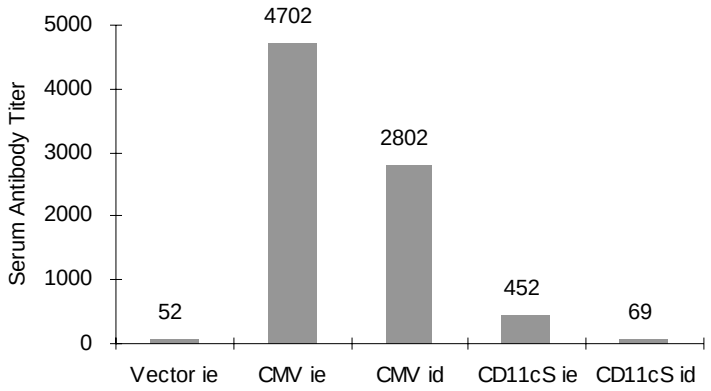

Figure 4.64 Antibody response induced by DNA with the CD11cS promoter.

DBA/2 mice (n=3/group) were immunized ie with 25μg/50μL CMV-lacZ, CD11cS-lacZ or Vector (pSPORT) with or without electroporation. Serum anti-β-gal antibodies were measured 2 weeks after DNA injection. Titers were calculated by the formula from the antibody curves when the OD at 450nm is equal to 0.5. Experiments were repeated 3 times with similar results.

4.5.6 Cellular immunity by DNA vaccination with the CD11cS promoter

We then analyzed the cellular immune responses by a 4 h chromium (^{51}Cr) release assay as well as by IFN-γ and IL-4 production by *in vitro* re-stimulated splenocytes (from the immunized mice in Figure 4.64). After 2 weeks of DNA immunization, splenocytes isolated from CD11cS-lacZ ie electroporated mice showed a β-gal specific CTL lysis (55%, E:T 100:1) compared with CMV-lacZ ie EP (71%, E:T 100:1) and CMV-lacZ id EP (56%, E:T 100:1) (Figure 4.65). DNA id immunization induced very high unspecific lysis to $lacZ^-$ tumor cells (18% for CMV-lacZ and 16% for CD11cS-lacZ at E:T 100:1).

Following *in vitro* re-stimulation with the CD8 CTL specific β-gal peptide, splenocytes from CD11cS-lacZ immunized mice secreted IFN-γ to a lower extent compared to CMV-lacZ ie immunized mice, but to a higher extent compared to CMV-lacZ id immunized mice. Detectable IL-4 secretion was only found in the vector control group as well as in DNA id immunized groups (Figure 4.66). These results (together with Figure 4.64) demonstrate induction of specific immune response by the DNA plasmid with the CD11cS promoter, especially for Th1 T cell medicated (CTL) immune responses.

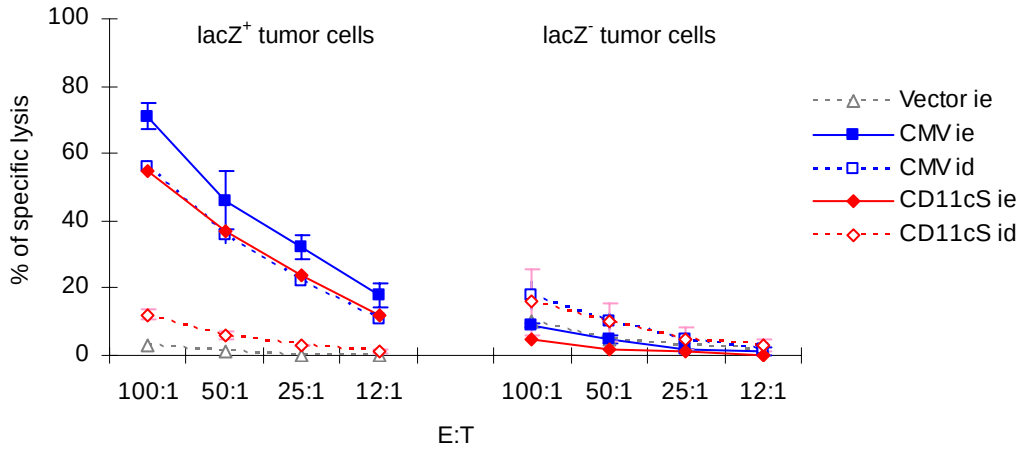

Figure 4.65 Specific cytotoxicity induced by DNA vaccines with the CD11cS promoter.

In vitro re-stimulated splenocytes (by 0.5μg/mL TPHPARIGL peptide for 5 days) from the DNA EP immunized mice (CMV-lacZ, CD11cS-luc or Vector, 25μg/μL) were taken a traditional 4 h ^{51}Cr cytotoxicity assay targeted to lacZ^{+} tumor cells (P13.1) and lacZ^{-} tumor cells (P815). Experiments were repeated 3 times with similar results.

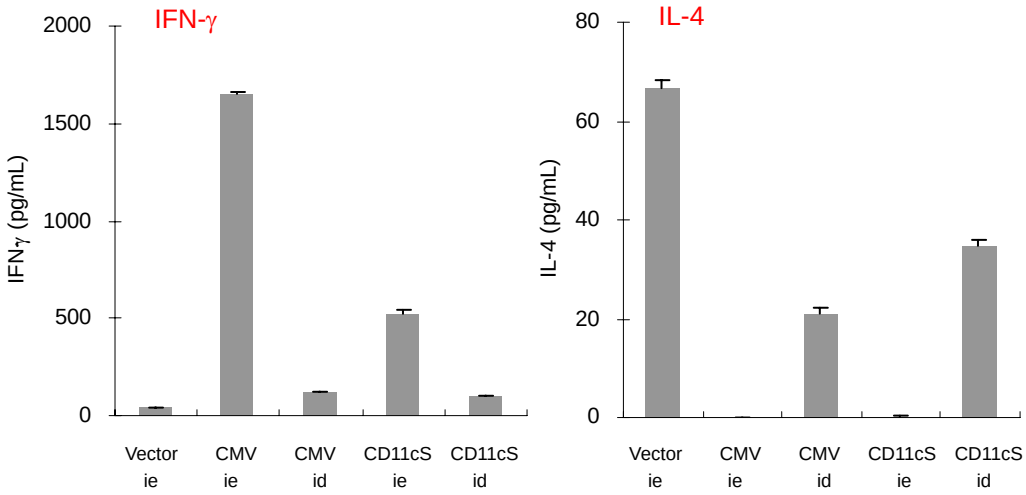

Figure 4.66 Cytokine production by DNA vaccines with the CD11cS promoter.

Supernatant from re-stimulated splenocytes (Figure 4.65) was collected and analyzed for IFN-γ (day 2 supernatant) and IL-4 (day 5 supernatant) ELISA. Experiments were repeated 3 times with similar results.

4.5.7 Prophylactic anti-tumor effect DC-targeting DNA vaccination

To determine if a DNA vaccine regulated by the CD11cS promoter can induce anti-tumor activity, we applied the CD11cS-lacZ plasmid (compared to CMV-lacZ and Vector) ie or id to immunocompetent mice with EP and challenged them 2 weeks later with highly metastatic ESb-lacZ cells (Figure 4.67a). All vaccinations with lacZ gene led to significantly inhibited tumor growth compared with the Vector control group (Figure 4.67b). DNA vaccine with the CMV promoter applied ie induced the best tumor inhibition. Median survival of the mice was also improved by all vaccinations compared to the Vector group (Table 4.6). Immunization by CD11cS-lacZ ie+EP (Median survival: 31 days) provided the best survival. These results demonstrated the efficiency of the CD11cS promoter for induction of anti-tumor activity *in vivo*.

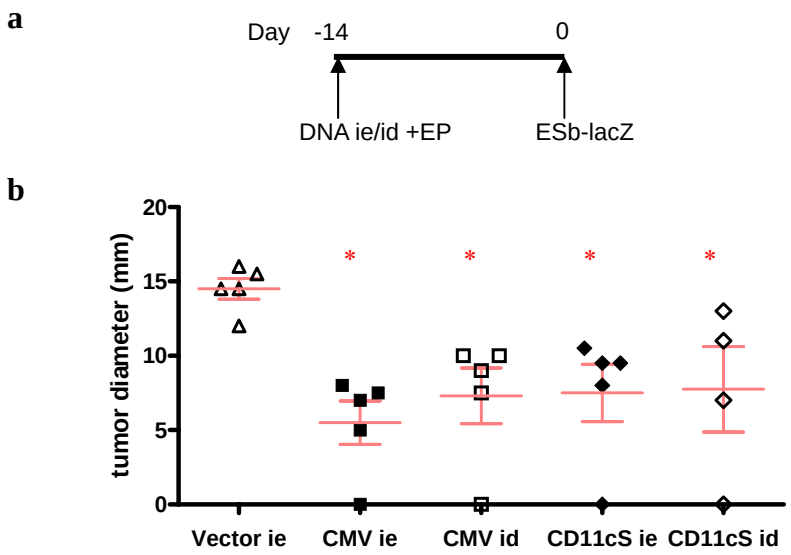

Figure 4.67 Prophylactic anti-tumor effects by DNA vaccines with CD11cS promoter.

DBA/2 mice (n=5/group) were immunized with CMV-lacZ, CD11cS-lacZ or Vector ie or id with EP. After 2 weeks, 2×10^5 ESb-lacZ lymphoma cells were injected sc to the flank. Tumor diameters at day 18 after tumor challenge were shown (because some mice died after this time point). * Compared to Vector group, $p<0.05$. Experiments were repeated 3 times with similar results.

Table 4.6 Median survival

Group	Median survival (day)
Vector ie	22
CMV ie	25
CMV id	29
CD11cS ie	31
CD11cS id	25

Median survival: the day 50% mice died

4.5.8 Therapeutic anti-tumor effect by DC-targeting DNA vaccination

Since bacterial β-gal only served as a surrogate tumor antigen, we next combined the CD11cS promoter to a DNA vaccine encoding human EpCAM. The mouse mammary carcinoma cell line DA3 transfected with the human EpCAM gene (DE) served as test tumor model. We applied the DNA vaccines by ie injection to the DE tumor therapy protocol and included DNA treatments for 4 times, weekly to tumor bearing mice 1 week after tumor inoculation (Figure 4.68a). Both CMV-EpCAM and CD11c-EpCAM plasmid DNA treatments had significant anti-tumor effect. With the help of EP, tumor regressions were seen by both treatments, especially by CD11cS-EpCAM +EP (Figure 4.68b). 60% tumor-free mice were found in the CMV-EpCAM group and 67% in the CD11c-EpCAM group at day 42 (2 weeks after the last treatment (Figure 4.68c). These results further corroborate the strong anti-tumor activity that can be induced by a DNA vaccine with the CD11cS promoter.

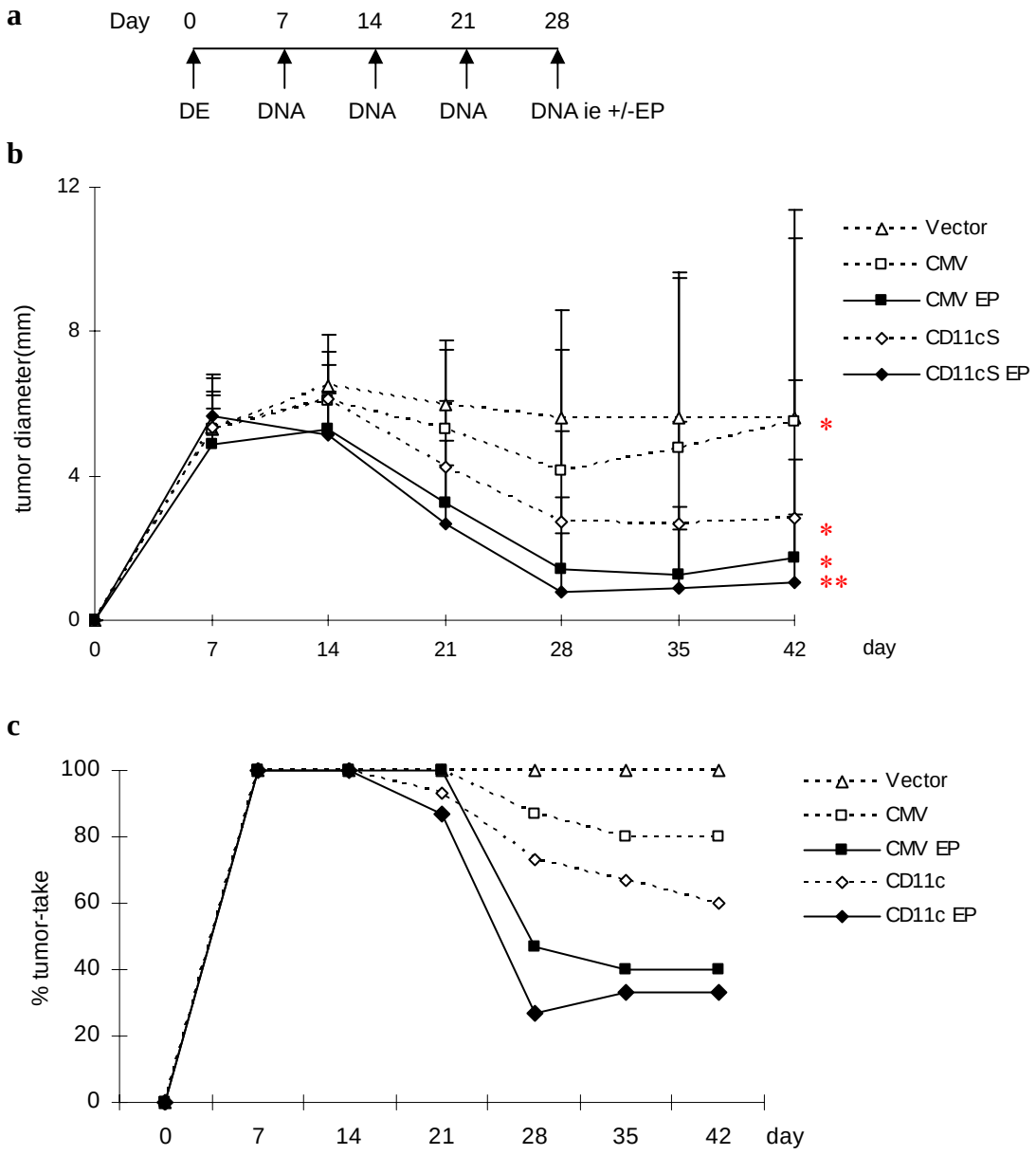

Figure 4.68 Therapeutic anti-tumor effects by DNA vaccines with the CD11cS promoter.

a. Strategy of DNA treatment. Balb/c mice (n=15/group) were inoculated sc with 1×10^7 DA3-EpCAM mammary carcinoma cells in the flank. DNA treatment was started after 1 week with 50μg/50μL CMV-EpCAM, CD11cS-EpCAM or Vector (pTandem1) for 1 treatment, with the total of 4 treatments. b. DE tumor growing curve. * Compared to the Vector group, $p<0.05$; ** Compared to the Vector group, $p\leq0.01$. c. % tumor-take (% of mice with palpable tumor at different time points).

5 Discussion

5.1 Improvement of DNA vaccine

DNA vaccine represents a promising new means of vaccination. *In vivo* gene transfer has been proven to be efficient for different applications. These include prophylactic and therapeutic vaccines for infectious diseases and cancer. In order to augment specific immunity, administration of cytokines and genes is possible. Application of DNA rather than protein has several advantages: 1) endogenous protein synthesis enables desirable protein folding and efficient antigen presentation; 2) induction of efficient humoral and cellular immunity, especially cell-mediated immunity which is difficult to induce by protein vaccine; 3) cost-effective construction and manufacturing, as well as ease of public application. In addition, DNA vaccines appear to be safer compared to live/attenuated microorganisms (29, 33, 36, 38, 129).

Because of those attractive advantages, DNA vaccine has been analyzed in a large number of disease systems in preclinical animal experiments and human clinical trials. Although efficient immune responses and protective & therapeutic immunity was achieved in some cases in small animals, weak performance was found in primates including humans. Various strategies have been tried to improve DNA vaccine, including adjuvant, different delivery methods, and optimized plasmid vectors (20, 56, 130). In this thesis, we included as a new possible adjuvant in the anti-tumoral plasmid vector the gene for hemagglutinin-neuraminidase (HN) molecule from Newcastle disease virus (NDV). We also tested a more efficient delivery system, electroporation (EP). Both strategies improved efficiency of DNA vaccination (Part 4.2, 4.3, and 4.4).

5.2 Cancer DNA vaccine

Cancer immunotherapy has made progress in recent years. Passive immunotherapy such as antibody treatment (e.g. anti-CD20 antibodies for B-cell leukemia (131, 132) and anti-HER2/neu antibodies for breast cancer) has been introduced for clinical treatment. Active immunotherapy via cancer vaccine aims at inducing or augmenting anti-cancer immune responses to eradicate tumor cells and at inducing long-term

immunological memory to maintain continuous immune surveillance against emergent cancer cells (4, 133). DNA vaccine is an attractive strategy for cancer vaccine development, because it can induce particularly efficient cellular immunity which is indispensible for anti-tumor effects, and persistent antigen expression which is required for durable immune responses. In addition, genetic strategies made it possible to combine different antigen/epitope sequences flexibly. This could help to establish a tumor therapy because of the complexity and the antigenic heterogeneity and escape mechanisms of tumors (36, 129, 134).

In this thesis, we applied DNA vaccines in different tumor models. In the prophylactic model with P815 mastocytoma cells, vaccination with the immunostimulating adjuvant NDV HN DNA protected 40% mice from tumor growth (Figure 4.10). In other prophylactic models with moderately aggressive Eb-lacZ lymphoma or DE (DA3-EpCAM) breast carcinoma cells, HN immunization slowed down tumor growth (Figure 4.14 and 4.18). Only vaccination with DNA encoding TAAs (tumor associated antigens; lacZ gene encoding β-gal protein was used as a model TAA, and EpCAM is a TAA) induced complete protection (100% tumor-free mice) (Figure 4.14 and 4.18). In the highly aggressive ESb-lacZ tumor model, prophylactic naked TAA DNA immunization without adjuvant showed only partially tumor inhibition (Figure 4.15). The ideal cancer vaccine would be applied therapeutically to late phase patients especially those with metastases (81). Therefore, it is more important to apply vaccines therapeutically to highly metastatic tumors as models. With the help of adjuvant HN or EP, prophylactic anti-tumor immunity was improved in the ESb-lacZ tumor (Figure 4.15). We then tested therapeutic vaccination strategies in the DE model. Tumor progression could be inhibited by TAA DNA immunization with the help of HN (Figure 4.24 and 4.28) or EP (Figure 4.50). Such immunizations even led to tumor regression in 60-70% of the mice.

5.3 Intra-pinna DNA immunization

A variety of routes of DNA administration have been studied, including intramuscular, intradermal (id), subcutaneous (sc), intravenous (iv), intraperitoneal (ip), oral, vaginal, and intranasal (in). Although muscle tissue was the first site for DNA immunization, other tissues were later proven to be similar or even better for induction of specific

immunity. The skin and mucous membranes are the first physiological front to encounter and protect against infection by exogenous organisms. These tissues are therefore expected to be efficient routes for immunization (135, 136). Id immunization is one of the most widely applied routes for DNA immunization because skin is rich in dendritic cells. Id immunization could be easily improved by gene-gun, electroporation and tattooing. All these methods have been shown to be efficient for improving antigen specific immunity induction (137-141).

Although in most cases in small animal experiments id immunization is applied to the abdominal or flank skin, ear pinna is an attractive alternative for DNA immunization. Ear pinna is a special site and form of skin. It contains two layers of epidermis and dermis (separated by cartilage), rich with DCs. Previous studies in our group showed that ear pinna is a better site than muscle tissue or flank skin for DNA immunization. Ie immunization of lacZ DNA (with a leukemia virus LTR driven BAG vector) induced earlier and stronger antigen expression at the local injection site compared to id and im injection. It was also superior with regard to induction of humoral and cellular immunity. Interestingly, a highly aggressive lymphoma cell line, ESb, did not grow in the ear pinna, although it induced very aggressive metastases when inoculated to other sites. ESb inoculation to the ear pinna quickly induced a Th1-type immune response, while ESb inoculation sc induced Th2-type cytokine production (74-76).

In this thesis, we proved again the superiority of antigen expression induced by DNA immunization to the ear pinna compared to the flank skin by following the kinetics of firefly luciferase expression (Figure 4.1). By using the IVIS100 *in vivo* imaging system, *in vivo* firefly luciferase expression could be visualized in live mice (142, 143). This strategy is superior to traditional methods of staining for antigen expression in situ in which case animals have to be sacrificed. *In vivo* imaging allows following the kinetics of antigen expression. We detected luciferase expression as early as 1 h after DNA injection in the ear pinna, compared to 2 h in the flank skin (Figure 4.63). Furthermore, the antigen expression level was much higher in the ear (~10 times higher, Figure 4.1) then in the flank skin, especially at early time points (~50-100 times higher in 1 h - 4 h after DNA injection, quantitative analysis of Figure 4.63, data not shown). Induced immune responses were also stronger by ie DNA (lacZ gene with a CMV promoter) injection compared to id (flank) injection, both for

antibody induction (Figure 4.2) and cytotoxicity (Figure 4.3). In addition, preferential IFN-γ induction by ie DNA immunization and IL-4 induction by id DNA immunization (Figure 4.4) indicated respectively skewed Th1 and Th2 responses at these two sites.

5.4 Immunostimulating adjuvant – HN of NDV

NDV has been shown to be nonpathogenic to humans. This avian paramyxovirus preferentially proliferates in tumor cells but not in normal cells (84, 86). Different strains of NDV have been developed for clinical cancer treatment including lytic or nonlytic strains. Lytic NDV strains induce necrosis or lysis upon infection of tumor cells (144-146). Nonlytic strains induce cell death by apoptosis (147). NDV can stimulate immune responses by inducing anti-viral proteins (148). One of the key cytokines is IFN-α, which is induced primarily by viral double-stranded RNA and the HN molecule expression at the cell surface (107-109, 115). HN expression is also related to T cell co-stimulation (108, 115). In this thesis, we corroborated that HN expression in cells *in vitro* could induce lymphocyte binding activity and IFN-α production (Figure 4.6 and 4.7). *In vivo*, HN expression by DNA immunization induced systemic IFN-α induction (Figure 4.9) and an adjuvant effect in the P815 tumor model (Figure 4.10). An *in vivo* adjuvant effect of an HN gene fused into a DNA vaccine encoding TAAs could be demonstrated in different tumor models both for prophylactic and therapeutic settings (Part 4.2 and 4.3).

Our results also revealed that the increased anti-tumor immunity from HN adjuvant is not due to antibody responses. HN adjuvant did not improve antibody level to TAA (Figure 4.30). Specific antibody levels were even higher in tumor-bearing compared to tumor-free mice after DNA treatment (Figure 4.26). However, HN adjuvant increased the IgG2a/IgG1 ratio by sc application (the best adjuvant effect was achieved by HN adjuvant sc injection), which indicated HN might privilege Th1 responses.

Although coexpression of HN together with β-gal improved β-gal specific cytotoxicity (Figure 4.31), HN sc injection failed to show such effect. Vector sc

injection improved β-gal specific cytotoxicity. HN DNA with the same plasmid backbone, however, did not induce any improvements of cytotoxicity. One possible explanation is that HN sc injection improves anti-tumor immunity by other factors such as innate immunity. Adoptive transfer of spleen cells from immunized mice to NOD/SCID mice did not transfer protective immunity (Figure 4.39). Perhaps this is due to the immune defect of NOD/SCID mice which lack many helpful immune factors. Further efforts are needed to reveal the detailed mechanisms of the adjuvant activity of HN.

Because type I IFN induction is one of the most important factors in innate immunity and closely related to NK cell activation, it is possible that HN is involved in NK cell activation. NK cells are important for innate immunity. They can rapidly recognize and eliminate pathogen infected cells as well as tumor cells (149, 150). They function by directed exocytosis of lytic granules (majorly granzymes and porferin) and the production of cytokines such as IFN-γ and TNF-α (151). In fact, the adjuvant effect of HN in $RAG2^{-/-}$ mice (Figure 4.40) suggested a crucial function of innate immunity for the HN mediated immunostimulating effect in anti-tumor immunity. Analysis of tumor infiltrating lymphocytes further supported this idea. Significantly increased NK-cell infiltration was observed in tumor (Figure 4.41). In addition, tumor mediated suppressive factors such as TGF-β (Figure 4.28) and myeloid derived suppressor cells (MDSCs) (Figure 4.40 and 4.41) were down-regulated by HN application.

Besides the potent tumor eradication activity of NK cells, cross-talk between activated NK cells and DCs is important for adaptive immunity (150, 152). Early stages of pathogen infections are associated with local recruitment and activation of dendritic cells (DC) and NK cells. For our vaccination, HN adjuvant as well as CpG motifs in the plasmid backbone might activate NK cells. NK cells are capable of inducing type 1 polarized "effector/memory" DC (DC1) that further translate NK cell-mediated helper signals for the development of Th1 immune responses. DC1s have an increased ability to produce IL-12p70, prime naive CD4 cells for high levels of IFN-gamma and low levels of IL-4 production, and induce Ag-specific CD8 T cell responses (153-161).

5.5 Electroporation

Application of DNA vaccine to large animals and humans poses new challenge for increasing the efficiency of this approach. A variety of delivery systems for DNA immunization were tried (41). The most efficient gene transfer has been achieved when DNA delivery was followed by the application of electrical pulses such as electroporation, gene-gun, and tattooing. *In vivo* electroporation of plasmid DNA is the simplest way without particular requirements for DNA preparation and injection. It has been tested for skin, skeletal muscle, cardiac muscle, liver, kidney, joints, spinal cord, brain, retina, cornea and the vasculature to induce long-term antigen expression in these tissues. In most reports, electroporation increased gene expression by 100- to 1000-fold compared to injection of naked plasmid DNA (31, 71, 137). The exact mechanism how EP enhances plasmid DNA delivery into cells is not fully understood. It is only clear now that membranes become effectively permeable by the formation of hydrophilic pores when a critical voltage has been applied, and subsequent plasmid-uptake by the cells would be more efficient.

We used the ELGEN1000 electroporation-based DNA delivery system from the Inovio Company. This system is designed for human applications by transferring small molecules including genetic materials and therapeutic drugs to certain tissues. Clinical trials (phase I/II) have proven the safety, tolerability and immunological reactions in human (162-165). The system consists of a pulse generator and a needle-electrode applicator that incorporates two syringes/needles. With the pressing of two buttons at the integrated applicator, the two needles are inserted into the selected tissue to the selected depth, DNA vaccine is injected, and electrical pulses are applied. Low-voltage electrical pulses are generated by the pulse generator and delivered through an attached electrical cord into the same selected tissue through the electrode-needle pair on the applicator, effectively co-localizing the DNA and the electrical field. For small animals like mice, EP could be applied to skin by a pedal and an electrode (as indicated in Figure 4.42).

Figure 5.1 ELGEN1000 electroporation -based DNA delivery system.

ELGEN1000 electroporation-based DNA delivery system (Inovio) contains a pulse generator and a needle-electrode applicator that incorporates two disposable syringes.
Image is obtained from: http://www.genetronics.com

By using this electroporation system, efficiency of *in vivo* DNA transfer was highly improved. Antigen expression was increased ~10 times in the ear pinna, and ~100 times in the flank skin by quantitative analysis of luciferase expression (Figure 4.44). Long-term antigen expression was achieved by this strategy. Stable and relatively strong (similar as the level by naked DNA injection at 24 h) gene expression was maintained for about 1 year (Figure 4.45). More importantly, both humoral and cellular immune responses, as well as anti-tumor immunity were dramatically improved (Figure 4.46-4.50). It is even more promising to use this strategy for the DC-targeted DNA vaccine with the CD11cS promoter. Although the antigen expression regulated by the CD11cS promoter was improved only ~1-5 times by EP in the ear (Figure 4.62), immune responses were much stronger (Figure 4.64-4.66) than those induced by naked DNA injection (undetectable by injection of 25μg DNA with the CD11cS promoter, data not shown). With the help of EP, significantly improved anti-tumor immunity could be induced by this DC-targeted DNA vaccine strategy in both the prophylactic and the therapeutic tumor models (Figure 4.67 and 4.68).

5.6 DCs in DNA vaccine

Dendritic cells (DCs) are the most potent professional antigen presenting cells (APCs) capable of priming naïve T cells. In DNA vaccination, they are efficient to present antigens by direct and cross-presentation. Adaptive immune responses are initiated in

secondary lymphoid organs, where naïve T cells encounter antigen-bearing DCs that have migrated there from the site of vaccination (70, 166).

The basic requirements for a DNA vaccine usually contain a bacterial plasmid vector containing a eukaryotic promoter, a cloning site, a transgene, a poly- adenylation sequence, an antibiotic selectable marker and a bacterial origin of replication (29). An efficient promoter may be required for optimal expression in mammalian cells. So far, most DNA vaccines have used viral promoters derived from cytomegalovirus (CMV) or simian virus 40 (SV40). Both promoters are strong and have no tissue-specificity. However, it was reported that CMV promoter induced cell death upon antigen overexpression (167). Restricting the site of gene expression should minimize the risks related to aberrant expression of an antigen. DCs are pivotal for antigen presentation, and directly transfected DCs have been reported to induce efficient immune responses by administration of relatively small numbers of cells (168-170). Furthermore, DC-targeted DNA vaccination preferentially induced cellular immune responses (171-173). Therefore, the idea of targeting antigen expression to DCs is promising for DNA vaccine development to lower the potential risk of unwanted side effects due to transgene expression in other cells (174). The development of a DNA plasmid vector with a DC-specific promoter would allow selective antigen expression in DCs and possibly increase the efficiency of the vector (175).

A 5.5-kb CD11c promoter is widely used for DC-specific gene expression (126-128, 176). Vaccination with such a promoter-regulating vector improved anti-tumor immune responses induced by TRP2hsp70 gene therapy (128). On the other hand, when using this promoter to regulate expression of the model antigen influenza hemagglutinin or ovalbumin, it turned out to be inefficient to induce protective humoral and cellular immunity following gene gun DNA vaccination (127). Furthermore, Lauterbach et al. claimed that expression of antigen in DCs by using the CD11c promoter induced antibody responses which were comparable to those induced by CMV promoter-driven constructs. They did not observe significant T cell responses after DNA gene gun immunization with their CD11c promoter plasmids (176). These previous studies revealed that gene expression by this promoter was restricted to DCs, but DNA vaccines with this promoter failed to induce efficient humoral and cellular immune responses following gene gun DNA immunization. This

might be due to the low level of antigen expression. *In vitro* transfection of DCs is difficult to achieve with high efficiency, especially with a long DNA sequence. Therefore, we tried to test if a short version of the CD11c promoter might be more appropriate for application *in vitro* and *in vivo*.

We constructed various short mouse CD11c promoter sequences (from 700-bp~5.5-kb). *In vitro* experiments revealed stronger promoter activity of CD11c promoters with 700-bp, 1.1-kb, or 2.4-kb than the 3.4-kb and 5.5-kb promoters (Figure 4.55). Since it is more convenient and more efficient to use a short promoter for *in vivo* experiments, we focused then on the 700-bp promoter (CD11cS) for further studies and compared it with the 5.5-kb CD11c promoter (CD11cL). Interestingly, the CD11cS had a stronger promoter activity than the long CD11cL promoter *in vitro* and *in vivo* (Figure 4.57 and 4.58). It was reported that a transcriptional enhancer element might be located in the region between -640 and -253 of the human CD11c promoter, while a negative regulatory element might exist between -960 and -640 (177). Although there were no similar studies related to the murine CD11c promoter, it is possible that the first few hundreds bases in the promoter region of murine CD11c gene are most important for gene regulation. It could be one of the explanations for the stronger activity of CD11cS than CD11cL. Furthermore, CD11cS appeared to be selectively active in DCs (Figure 4.59 and 4.60). With the help of electroporation, DNA vaccines encoding the lacZ gene coupled to the CD11cS promoter, when injected into the ear pinna, induced a weak humoral and a relatively strong cellular response (Figure 4.64-4.66). Prophylactic immunization under this protocol induced protective anti-tumor immunity upon challenge with the ESb-lacZ lymphoma cells and caused prolongation of survival (Figure 4.67). We also constructed a DNA vaccine in which the CD11cS promoter controlled expression of a natural tumor associated antigen (TAA), the human EpCAM. With this vaccine we could achieve even therapeutic immunization effects in mice bearing tumors expressing this TAA as transgene (Figure 4.68).

5.7 Innate immunity in vaccination

Generation of effective adaptive immunity is dependent on the initial stimulation of strong innate immunity. Similar with a natural infection which initiates innate

immunity immediately, DNA vaccines trigger innate immune responses very early (70). A central component of a DNA vaccine functions like an adjuvant (e.g. CpG motifs, or other immunostimulating molecules constructed into DNA vaccines). Such effect is important to enhance the magnitude and duration of immune responses induced by DCs and other innate immune cells (56). DCs exert a crucial connection function between innate and adaptive immunity, and translate information from pathogens or vaccines to T and B cells to regulate the quantity, quality and duration of the adaptive immune responses. DCs can sense microbes or adjuvants directly by TLRs; or indirectly by detecting inflammatory factors produced by NK cells, NKT cells, macrophages, mast cells and epithelial cells (178, 179).

Besides CpG motifs which are included in the vector backbone, we incorporated another immune stimulating molecule NDV viral HN to the DNA vaccine as an adjuvant. As we showed in Part 5.3, HN improved TAA DNA-mediated anti-tumor immunity primarily through stimulating innate immunity. Systemic IFN-α production and tumor infiltrating NK cells were increased by HN application. Although no significant improvements were found with respect to serum antibodies and cytotoxic activity, immune responses became skewed towards Th1 and anti-tumor activity was improved.

5.8 Tumor mediated immuno-suppression

Because of lack of co-stimulatory signals, cell mediated immune responses to TAAs become tolerated. Failures of tumor elimination might be due to the following factors: 1) Down-regulation of MHC class I molecules on tumor cells; 2) Loss or down-regulation of TAAs; 3) Physical barriers around the tumor; 4) Immuno-suppressive factors such as TGF-β, MDSCs, tumor-associated macrophages, tolerogenic DCs, regulatory T cells (Tregs); 5) T cell tolerance or anergy. Successful immunotherapy has to circumvent these suppressive mechanisms (123-125, 180-183).

5.8.1 MHC expression at the tumor cell-surface

Tumor cells can down-regulate expression of MHC I molecules and TAAs. This is one mechanism of tumor immune escape. NK cells are innate immune effectors that

can kill MHC class I deficient tumor cells *in vivo*. They can thus function when CTL cells can not. Therefore, it is important to induce both innate and adaptive immunity by a cancer vaccine (184-186).

We used tumor cell lines with high and low MHC I expression (Eb-lacZ/ESb-lacZ and DE/DA3/RMA-S, respectively). In the Eb-lacZ and ESb-lacZ tumor models which express MHC I molecules, improvement of anti-tumor activity induced by HN adjuvant or EP could be explained by increased cellular immunity and privileged Th1 responses. In the RMA-S (deficient in MHC I expression) tumor model, tumor growth might be inhibited mostly by NK cells. We found in this tumor model that tumor growth was reduced stronger in $RAG2^{-/-}$ mice than in wild-type mice after HN immunization (Figure 4.40). Improvement of IFN-α production in blood and NK-cell infiltration at the tumor site were also noticed after HN immunization

5.8.2 Tumor induced suppressive factors

Tumors can create a tolerogenic environment by secretion of suppressive cytokines such as TGF-β and IL-10 and by enhancing suppressive cell activity including MDSCs, tolerogenic DCs, tumor-associated macrophages and Tregs (128, 183, 187). We analyzed $Gr\text{-}1^{+}CD11b^{+}F4/80^{+}$ MDSCs in tumor-bearing mice, and found higher levels of these cells in advanced tumor stages. These cells contribute to immunosuppression by inhibiting the function of CD8 T cells and by promoting tumor angiogenesis. Combing HN or EP with TAA DNA vaccine could down-regulate TGF-β production in blood and MDSCs in both peripheral blood and tumor tissues. We also checked TGF-β secretion in a late tumor stage after re-challenge with DA3 tumor cells without observing any benefit from vaccination (data not shown). This might be due to the suppressive microenvironment induced by late phase tumor in all groups.

5.9 Safety of DNA vaccine

Accumulating data demonstrate the efficiency of DNA vaccine for infectious diseases and cancer in animal models as well as in human clinical trials. However, safety is of concern related to this strategy. The following possibilities are potential risks that

might occur: 1) integration into the host genome, so increasing the risk of tumor formation; 2) destruction of transfected cells, thereby inducing autoimmune disease; 3) induction of tolerance rather than immunity. Many efforts were taken to study these potential risks (29, 188). Although not all plasmids could be completely safe excluding integration into host genome (189), there are no reports of tumor induction related to DNA vaccine. Mutation rates induced by DNA integration into the host chromosome have been shown to be much lower than the spontaneous mutation rate. In addition, a modest induction of autoantibody has not led any autoimmune diseases (190). So far, DNA vaccines are reported to be well tolerated and have an excellent safety profile in human clinical trials. Therefore, more efforts are needed for the improvement of vaccine design and delivery system for human application. Understanding of the immune system and development of new delivery strategies will provide more possibilities to design optimal DNA vaccines suitable for clinical application.

6 References

1. Plotkin SA. 2008. Vaccines: correlates of vaccine-induced immunity. *Clin Infect Dis* 47: 401-9
2. Lambert PH, Siegrist CA. 1997. Science, medicine, and the future. Vaccines and vaccination. *Bmj* 315: 1595-8
3. Poland GA, Murray D, Bonilla-Guerrero R. 2002. New vaccine development. *Bmj* 324: 1315-9
4. Berzofsky JA, Terabe M, Oh S, Belyakov IM, Ahlers JD, Janik JE, Morris JC. 2004. Progress on new vaccine strategies for the immunotherapy and prevention of cancer. *J Clin Invest* 113: 1515-25
5. Berzofsky JA, Ahlers JD, Janik J, Morris J, Oh S, Terabe M, Belyakov IM. 2004. Progress on new vaccine strategies against chronic viral infections. *J Clin Invest* 114: 450-62
6. Girard MP, Steele D, Chaignat CL, Kieny MP. 2006. A review of vaccine research and development: human enteric infections. *Vaccine* 24: 2732-50
7. Girard MP, Cherian T, Pervikov Y, Kieny MP. 2005. A review of vaccine research and development: human acute respiratory infections. *Vaccine* 23: 5708-24
8. Abrahams BC, Kaufman DM. 2004. Anticipating smallpox and monkeypox outbreaks: complications of the smallpox vaccine. *Neurologist* 10: 265-74
9. Galazka AM, Robertson SE, Kraigher A. 1999. Mumps and mumps vaccine: a global review. *Bull World Health Organ* 77: 3-14
10. Teitelbaum MA, Franklin PC. 1994. Vaccine-preventable illness in U.S. children 1980-1992. *Stat Bull Metrop Insur Co* 75: 2-9
11. Jung MC, Gruner N, Zachoval R, Schraut W, Gerlach T, Diepolder H, Schirren CA, Page M, Bailey J, Birtles E, Whitehead E, Trojan J, Zeuzem S, Pape GR. 2002. Immunological monitoring during therapeutic vaccination as a prerequisite for the design of new effective therapies: induction of a vaccine-specific CD4+ T-cell proliferative response in chronic hepatitis B carriers. *Vaccine* 20: 3598-612
12. Webster G, Bertoletti A. 2001. Quantity and quality of virus-specific CD8 cell response: relevance to the design of a therapeutic vaccine for chronic HBV infection. *Mol Immunol* 38: 467-73
13. Brinkman JA, Hughes SH, Stone P, Caffrey AS, Muderspach LI, Roman LD, Weber JS, Kast WM. 2007. Therapeutic vaccination for HPV induced cervical cancers. *Dis Markers* 23: 337-52
14. Kaech SM, Wherry EJ, Ahmed R. 2002. Effector and memory T-cell differentiation: implications for vaccine development. *Nat Rev Immunol* 2: 251-62
15. Yewdell JW, Haeryfar SM. 2005. Understanding presentation of viral antigens to CD8+ T cells in vivo: the key to rational vaccine design. *Annu Rev Immunol* 23: 651-82
16. Janeway C. 2005. *Immunobiology: the immune system in health and disease*. New York: Garland Science
17. Savai R, Schermuly RT, Pullamsetti SS, Schneider M, Greschus S, Ghofrani HA, Traupe H, Grimminger F, Banat GA. 2007. A combination hybrid-based vaccination/adoptive cellular therapy to prevent tumor growth by involvement of T cells. *Cancer Res* 67: 5443-53
18. Leifert JA, Rodriguez-Carreno MP, Rodriguez F, Whitton JL. 2004. Targeting plasmid-encoded proteins to the antigen presentation pathways. *Immunol Rev* 199: 40-53
19. Golding B, Scott DE. 1995. Vaccine strategies: targeting helper T cell responses. *Ann N Y Acad Sci* 754: 126-37
20. Wang R, Doolan DL, Le TP, Hedstrom RC, Coonan KM, Charoenvit Y, Jones TR, Hobart P, Margalith M, Ng J, Weiss WR, Sedegah M, de Taisne C, Norman JA,

Hoffman SL. 1998. Induction of antigen-specific cytotoxic T lymphocytes in humans by a malaria DNA vaccine. *Science* 282: 476-80
21. Kaufmann SH, Hess J. 1999. Impact of intracellular location of and antigen display by intracellular bacteria: implications for vaccine development. *Immunol Lett* 65: 81-4
22. Rollenhagen C, Sorensen M, Rizos K, Hurvitz R, Bumann D. 2004. Antigen selection based on expression levels during infection facilitates vaccine development for an intracellular pathogen. *Proc Natl Acad Sci U S A* 101: 8739-44
23. Muller S. 2004. Avoiding deceptive imprinting of the immune response to HIV-1 infection in vaccine development. *Int Rev Immunol* 23: 423-36
24. Jeffrey Fessel W. 2005. A new approach to an AIDS vaccine: creating antibodies to HIV vif will enable apobec3G to turn HIV-infection into a benign problem. *Med Hypotheses* 64: 261-3
25. Igietseme JU, Eko FO, He Q, Black CM. 2004. Antibody regulation of Tcell immunity: implications for vaccine strategies against intracellular pathogens. *Expert Rev Vaccines* 3: 23-34
26. Schmader K, Gnann JW, Jr., Watson CP. 2008. The epidemiological, clinical, and pathological rationale for the herpes zoster vaccine. *J Infect Dis* 197 Suppl 2: S207-15
27. Guinovart C, Alonso PL. 2007. Methods for determining vaccine efficacy and effectiveness and the main barriers to developing a fully deployable malaria vaccine. *Am J Trop Med Hyg* 77: 276-81
28. Dobano C, Rogers WO, Gowda K, Doolan DL. 2007. Targeting antigen to MHC Class I and Class II antigen presentation pathways for malaria DNA vaccines. *Immunol Lett* 111: 92-102
29. Gurunathan S, Klinman DM, Seder RA. 2000. DNA vaccines: immunology, application, and optimization*. *Annu Rev Immunol* 18: 927-74
30. Donnelly JJ, Liu MA, Ulmer JB. 2000. Antigen presentation and DNA vaccines. *Am J Respir Crit Care Med* 162: S190-3
31. Wolff JA, Malone RW, Williams P, Chong W, Acsadi G, Jani A, Felgner PL. 1990. Direct gene transfer into mouse muscle in vivo. *Science* 247: 1465-8
32. Tang DC, DeVit M, Johnston SA. 1992. Genetic immunization is a simple method for eliciting an immune response. *Nature* 356: 152-4
33. Mor G. 1998. Plasmid DNA: a new era in vaccinology. *Biochem Pharmacol* 55: 1151-3
34. Whalen RG. 1996. DNA vaccines for emerging infectious diseases: what if? *Emerg Infect Dis* 2: 168-75
35. Feltquate DM. 1998. DNA vaccines: vector design, delivery, and antigen presentation. *J Cell Biochem Suppl* 30-31: 304-11
36. Rice J, Ottensmeier CH, Stevenson FK. 2008. DNA vaccines: precision tools for activating effective immunity against cancer. *Nat Rev Cancer* 8: 108-20
37. Shedlock DJ, Weiner DB. 2000. DNA vaccination: antigen presentation and the induction of immunity. *J Leukoc Biol* 68: 793-806
38. Donnelly JJ, Wahren B, Liu MA. 2005. DNA vaccines: progress and challenges. *J Immunol* 175: 633-9
39. Sasaki S, Tsuji T, Asakura Y, Fukushima J, Okuda K. 1998. The search for a potent DNA vaccine against AIDS: the enhancement of immunogenicity by chemical and genetic adjuvants. *Anticancer Res* 18: 3907-15
40. Sasaki S, Takeshita F, Xin KQ, Ishii N, Okuda K. 2003. Adjuvant formulations and delivery systems for DNA vaccines. *Methods* 31: 243-54
41. Patil SD, Rhodes DG, Burgess DJ. 2005. DNA-based therapeutics and DNA delivery systems: a comprehensive review. *Aaps J* 7: E61-77
42. Peachman KK, Rao M, Alving CR. 2003. Immunization with DNA through the skin. *Methods* 31: 232-42
43. Roos AK, Moreno S, Leder C, Pavlenko M, King A, Pisa P. 2006. Enhancement of

cellular immune response to a prostate cancer DNA vaccine by intradermal electroporation. *Mol Ther* 13: 320-7

44. Wu CJ, Lee SC, Huang HW, Tao MH. 2004. In vivo electroporation of skeletal muscles increases the efficacy of Japanese encephalitis virus DNA vaccine. *Vaccine* 22: 1457-64
45. Kent SJ, Zhao A, Best SJ, Chandler JD, Boyle DB, Ramshaw IA. 1998. Enhanced T-cell immunogenicity and protective efficacy of a human immunodeficiency virus type 1 vaccine regimen consisting of consecutive priming with DNA and boosting with recombinant fowlpox virus. *J Virol* 72: 10180-8
46. Alvarez D, Harder G, Fattouh R, Sun J, Goncharova S, Stampfli MR, Coyle AJ, Bramson JL, Jordana M. 2005. Cutaneous antigen priming via gene gun leads to skin-selective Th2 immune-inflammatory responses. *J Immunol* 174: 1664-74
47. Smorlesi A, Papalini F, Amici A, Orlando F, Pierpaoli S, Mancini C, Provinciali M. 2006. Evaluation of different plasmid DNA delivery systems for immunization against HER2/neu in a transgenic murine model of mammary carcinoma. *Vaccine* 24: 1766-75
48. Gronevik E, Mathiesen I, Lomo T. 2005. Early events of electroporation-mediated intramuscular DNA vaccination potentiate Th1-directed immune responses. *J Gene Med* 7: 1246-54
49. Marciani DJ. 2003. Vaccine adjuvants: role and mechanisms of action in vaccine immunogenicity. *Drug Discov Today* 8: 934-43
50. Pulendran B. 2004. Modulating vaccine responses with dendritic cells and Toll-like receptors. *Immunol Rev* 199: 227-50
51. Wack A, Rappuoli R. 2005. Vaccinology at the beginning of the 21st century. *Curr Opin Immunol* 17: 411-8
52. Haynes JR. 2004. Particle-mediated DNA vaccine delivery to the skin. *Expert Opin Biol Ther* 4: 889-900
53. Klinman DM. 2006. Adjuvant activity of CpG oligodeoxynucleotides. *Int Rev Immunol* 25: 135-54
54. Coban C, Ishii KJ, Gursel M, Klinman DM, Kumar N. 2005. Effect of plasmid backbone modification by different human CpG motifs on the immunogenicity of DNA vaccine vectors. *J Leukoc Biol* 78: 647-55
55. Stevenson FK. 2004. DNA vaccines and adjuvants. *Immunol Rev* 199: 5-8
56. Guy B. 2007. The perfect mix: recent progress in adjuvant research. *Nat Rev Microbiol* 5: 505-17
57. Mata-Haro V, Cekic C, Martin M, Chilton PM, Casella CR, Mitchell TC. 2007. The vaccine adjuvant monophosphoryl lipid A as a TRIF-biased agonist of TLR4. *Science* 316: 1628-32
58. Cui YL, He SY, Xue MF, Zhang J, Wang HX, Yao Y. 2008. Protective effect of a multiantigenic DNA vaccine against Toxoplasma gondii with co-delivery of IL-12 in mice. *Parasite Immunol* 30: 309-13
59. Su B, Wang J, Wang X, Jin H, Zhao G, Ding Z, Kang Y, Wang B. 2008. The effects of IL-6 and TNF-alpha as molecular adjuvants on immune responses to FMDV and maturation of dendritic cells by DNA vaccination. *Vaccine*
60. Sasaki S, Fukushima J, Hamajima K, Ishii N, Tsuji T, Xin KQ, Mohri H, Okuda K. 1998. Adjuvant effect of Ubenimex on a DNA vaccine for HIV-1. *Clin Exp Immunol* 111: 30-5
61. Kutzler MA, Weiner DB. 2004. Developing DNA vaccines that call to dendritic cells. *J Clin Invest* 114: 1241-4
62. Toka FN, Pack CD, Rouse BT. 2004. Molecular adjuvants for mucosal immunity. *Immunol Rev* 199: 100-12
63. Krieg AM, Davis HL. 2001. Enhancing vaccines with immune stimulatory CpG DNA. *Curr Opin Mol Ther* 3: 15-24
64. Krieg AM, Yi AK, Schorr J, Davis HL. 1998. The role of CpG dinucleotides in DNA vaccines. *Trends Microbiol* 6: 23-7

65. Bergmann-Leitner ES, Leitner WW, Tsokos GC. 2006. Complement 3d: from molecular adjuvant to target of immune escape mechanisms. *Clin Immunol* 121: 177-85
66. Hauser H, Chen SY. 2003. Augmentation of DNA vaccine potency through secretory heat shock protein-mediated antigen targeting. *Methods* 31: 225-31
67. Kojima Y, Jounai N, Takeshita F, Nakazawa M, Okuda K, Watabe S, Xin KQ, Okuda K. 2007. The degree of apoptosis as an immunostimulant for a DNA vaccine against HIV-1 infection. *Vaccine* 25: 438-45
68. Sasaki S, Amara RR, Yeow WS, Pitha PM, Robinson HL. 2002. Regulation of DNA-raised immune responses by cotransfected interferon regulatory factors. *J Virol* 76: 6652-9
69. Petrovsky N, Aguilar JC. 2004. Vaccine adjuvants: current state and future trends. *Immunol Cell Biol* 82: 488-96
70. Pulendran B, Ahmed R. 2006. Translating innate immunity into immunological memory: implications for vaccine development. *Cell* 124: 849-63
71. Liu J, Kjeken R, Mathiesen I, Barouch DH. 2008. Recruitment of antigen-presenting cells to the site of inoculation and augmentation of human immunodeficiency virus type 1 DNA vaccine immunogenicity by in vivo electroporation. *J Virol* 82: 5643-9
72. Stoecklinger A, Grieshuber I, Scheiblhofer S, Weiss R, Ritter U, Kissenpfennig A, Malissen B, Romani N, Koch F, Ferreira F, Thalhamer J, Hammerl P. 2007. Epidermal langerhans cells are dispensable for humoral and cell-mediated immunity elicited by gene gun immunization. *J Immunol* 179: 886-93
73. Stoitzner P, Tripp CH, Eberhart A, Price KM, Jung JY, Bursch L, Ronchese F, Romani N. 2006. Langerhans cells cross-present antigen derived from skin. *Proc Natl Acad Sci U S A* 103: 7783-8
74. Jurianz K, von Hoegen P, Schirrmacher V. 1998. Superiority of the ear pinna over a subcutaneous tumour inoculation site for induction of a Th1-type cytokine response. *Cancer Immunol Immunother* 45: 327-33
75. Forg P, von Hoegen P, Dalemans W, Schirrmacher V. 1998. Superiority of the ear pinna over muscle tissue as site for DNA vaccination. *Gene Ther* 5: 789-97
76. Schirmacher V, Forg P, Dalemans W, Chlichlia K, Zeng Y, Fournier P, von Hoegen P. 2000. Intra-pinna anti-tumor vaccination with self-replicating infectious RNA or with DNA encoding a model tumor antigen and a cytokine. *Gene Ther* 7: 1137-47
77. Jemal A, Siegel R, Ward E, Murray T, Xu J, Thun MJ. 2007. Cancer statistics, 2007. *CA Cancer J Clin* 57: 43-66
78. Bagley KC. 2008. Genetic adjuvant therapy for pancreatic cancer and other solid tumours. *Gut* 57: 289-91
79. Mkrtichyan M, Ghochikyan A, Loukinov D, Davtyan H, Ichim TE, Cribbs DH, Lobanenkov VV, Agadjanyan MG. 2008. DNA, but not protein vaccine based on mutated BORIS antigen significantly inhibits tumor growth and prolongs the survival of mice. *Gene Ther* 15: 61-4
80. Dalgleish AG. 2004. Cancer vaccines as a therapeutic strategy. *Expert Rev Vaccines* 3: 665-8
81. Hellstrom KE, Hellstrom I. 2003. Novel approaches to therapeutic cancer vaccines. *Expert Rev Vaccines* 2: 517-32
82. Hodge JW. 1996. Carcinoembryonic antigen as a target for cancer vaccines. *Cancer Immunol Immunother* 43: 127-34
83. Reinartz S, Wagner U. 2004. Current approaches in ovarian cancer vaccines. *Minerva Ginecol* 56: 515-27
84. Sinkovics JG, Horvath JC. 2000. Newcastle disease virus (NDV): brief history of its oncolytic strains. *J Clin Virol* 16: 1-15
85. Schirrmacher V, Schlag P, Liebrich W, Patel BT, Stoeck M. 1993. Specific immunotherapy of colorectal carcinoma with Newcastle-disease virus-modified autologous tumor cells prepared from resected liver metastases. *Ann N Y Acad Sci* 690: 364-6

86. Schirrmacher V, Griesbach A, Ahlert T. 2001. Antitumor effects of Newcastle Disease Virus in vivo: local versus systemic effects. *Int J Oncol* 18: 945-52
87. Bian H, Fournier P, Moormann R, Peeters B, Schirrmacher V. 2005. Selective gene transfer in vitro to tumor cells via recombinant Newcastle disease virus. *Cancer Gene Ther* 12: 295-303
88. Schirrmacher V. 2005. Clinical trials of antitumor vaccination with an autologous tumor cell vaccine modified by virus infection: improvement of patient survival based on improved antitumor immune memory. *Cancer Immunol Immunother* 54: 587-98
89. Schirrmacher V, Bai L, Umansky V, Yu L, Xing Y, Qian Z. 2000. Newcastle disease virus activates macrophages for anti-tumor activity. *Int J Oncol* 16: 363-73
90. Schirrmacher V, Haas C, Bonifer R, Ahlert T, Gerhards R, Ertel C. 1999. Human tumor cell modification by virus infection: an efficient and safe way to produce cancer vaccine with pleiotropic immune stimulatory properties when using Newcastle disease virus. *Gene Ther* 6: 63-73
91. Schirrmaker V. 2003. Improvements of survival in nine phase II clinical studies with different types of cancer upon anti-tumor vaccination with an autologous tumor cell vaccine modified by virus infection to introduce danger signals. *Adv Exp Med Biol* 532: 175-93
92. Liang W, Wang H, Sun TM, Yao WQ, Chen LL, Jin Y, Li CL, Meng FJ. 2003. Application of autologous tumor cell vaccine and NDV vaccine in treatment of tumors of digestive tract. *World J Gastroenterol* 9: 495-8
93. Batliwalla FM, Bateman BA, Serrano D, Murray D, Macphail S, Maino VC, Ansel JC, Gregersen PK, Armstrong CA. 1998. A 15-year follow-up of AJCC stage III malignant melanoma patients treated postsurgically with Newcastle disease virus (NDV) oncolysate and determination of alterations in the CD8 T cell repertoire. *Mol Med* 4: 783-94
94. Ockert D, Schirrmacher V, Beck N, Stoelben E, Ahlert T, Flechtenmacher J, Hagmuller E, Buchcik R, Nagel M, Saeger HD. 1996. Newcastle disease virus-infected intact autologous tumor cell vaccine for adjuvant active specific immunotherapy of resected colorectal carcinoma. *Clin Cancer Res* 2: 21-8
95. Ahlert T, Sauerbrei W, Bastert G, Ruhland S, Bartik B, Simiantonaki N, Schumacher J, Hacker B, Schumacher M, Schirrmacher V. 1997. Tumor-cell number and viability as quality and efficacy parameters of autologous virus-modified cancer vaccines in patients with breast or ovarian cancer. *J Clin Oncol* 15: 1354-66
96. Schirrmacher V, Ahlert T, Probstle T, Steiner HH, Herold-Mende C, Gerhards R, Hagmuller E, Steiner HH. 1998. Immunization with virus-modified tumor cells. *Semin Oncol* 25: 677-96
97. Martinez-Sobrido L, Gitiban N, Fernandez-Sesma A, Cros J, Mertz SE, Jewell NA, Hammond S, Flano E, Durbin RK, Garcia-Sastre A, Durbin JE. 2006. Protection against respiratory syncytial virus by a recombinant Newcastle disease virus vector. *J Virol* 80: 1130-9
98. Janke M, Peeters B, de Leeuw O, Moorman R, Arnold A, Fournier P, Schirrmacher V. 2007. Recombinant Newcastle disease virus (NDV) with inserted gene coding for GM-CSF as a new vector for cancer immunogene therapy. *Gene Ther* 14: 1639-49
99. Bian H, Wilden H, Fournier P, Peeters B, Schirrmacher V. 2006. In vivo efficacy of systemic tumor targeting of a viral RNA vector with oncolytic properties using a bispecific adapter protein. *Int J Oncol* 29: 1359-69
100. DiNapoli JM, Kotelkin A, Yang L, Elankumaran S, Murphy BR, Samal SK, Collins PL, Bukreyev A. 2007. Newcastle disease virus, a host range-restricted virus, as a vaccine vector for intranasal immunization against emerging pathogens. *Proc Natl Acad Sci U S A* 104: 9788-93
101. Ge J, Deng G, Wen Z, Tian G, Wang Y, Shi J, Wang X, Li Y, Hu S, Jiang Y, Yang C, Yu K, Bu Z, Chen H. 2007. Newcastle disease virus-based live attenuated vaccine completely protects chickens and mice from lethal challenge of homologous and heterologous H5N1 avian influenza viruses. *J Virol* 81: 150-8

102. Iorio RM, Glickman RL. 1992. Fusion mutants of Newcastle disease virus selected with monoclonal antibodies to the hemagglutinin-neuraminidase. *J Virol* 66: 6626-33
103. Iorio RM, Field GM, Sauvron JM, Mirza AM, Deng R, Mahon PJ, Langedijk JP. 2001. Structural and functional relationship between the receptor recognition and neuraminidase activities of the Newcastle disease virus hemagglutinin-neuraminidase protein: receptor recognition is dependent on neuraminidase activity. *J Virol* 75: 1918-27
104. Zeng J, Fournier P, Schirrmacher V. 2004. High cell surface expression of Newcastle disease virus proteins via replicon vectors demonstrates syncytia forming activity of F and fusion promotion activity of HN molecules. *Int J Oncol* 25: 293-302
105. Morrison TG. 2003. Structure and function of a paramyxovirus fusion protein. *Biochim Biophys Acta* 1614: 73-84
106. Nagai Y, Hamaguchi M, Toyoda T. 1989. Molecular biology of Newcastle disease virus. *Prog Vet Microbiol Immunol* 5: 16-64
107. Zeng J, Fournier P, Schirrmacher V. 2002. Induction of interferon-alpha and tumor necrosis factor-related apoptosis-inducing ligand in human blood mononuclear cells by hemagglutinin-neuraminidase but not F protein of Newcastle disease virus. *Virology* 297: 19-30
108. Zeng J, Fournier P, Schirrmacher V. 2002. Stimulation of human natural interferon-alpha response via paramyxovirus hemagglutinin lectin-cell interaction. *J Mol Med* 80: 443-51
109. Fournier P, Zeng J, Schirrmacher V. 2003. Two ways to induce innate immune responses in human PBMCs: paracrine stimulation of IFN-alpha responses by viral protein or dsRNA. *Int J Oncol* 23: 673-80
110. Arnon TI, Markel G, Mandelboim O. 2006. Tumor and viral recognition by natural killer cells receptors. *Semin Cancer Biol* 16: 348-58
111. Arnon TI, Achdout H, Lieberman N, Gazit R, Gonen-Gross T, Katz G, Bar-Ilan A, Bloushtain N, Lev M, Joseph A, Kedar E, Porgador A, Mandelboim O. 2004. The mechanisms controlling the recognition of tumor- and virus-infected cells by NKp46. *Blood* 103: 664-72
112. Jacobs B, Wuttke M, Papewalis C, Fenk R, Stussgen C, Baehring T, Schinner S, Raffel A, Seissler J, Schott M. 2008. Characterization of monocyte-derived IFNalpha-generated dendritic cells. *Horm Metab Res* 40: 117-21
113. Hershkovitz O, Jivov S, Bloushtain N, Zilka A, Landau G, Bar-Ilan A, Lichtenstein RG, Campbell KS, van Kuppevelt TH, Porgador A. 2007. Characterization of the recognition of tumor cells by the natural cytotoxicity receptor, NKp44. *Biochemistry* 46: 7426-36
114. Schirrmacher V, Haas C, Bonifer R, Ertel C. 1997. Virus potentiation of tumor vaccine T-cell stimulatory capacity requires cell surface binding but not infection. *Clin Cancer Res* 3: 1135-48
115. Fournier P, Zeng J, Von Der Lieth CW, Washburn B, Ahlert T, Schirrmacher V. 2004. Importance of serine 200 for functional activities of the hemagglutinin-neuraminidase protein of Newcastle Disease Virus. *Int J Oncol* 24: 623-34
116. Santini SM, Lapenta C, Logozzi M, Parlato S, Spada M, Di Pucchio T, Belardelli F. 2000. Type I interferon as a powerful adjuvant for monocyte-derived dendritic cell development and activity in vitro and in Hu-PBL-SCID mice. *J Exp Med* 191: 1777-88
117. Baeuerle PA, Gires O. 2007. EpCAM (CD326) finding its role in cancer. *Br J Cancer* 96: 417-23
118. Osta WA, Chen Y, Mikhitarian K, Mitas M, Salem M, Hannun YA, Cole DJ, Gillanders WE. 2004. EpCAM is overexpressed in breast cancer and is a potential target for breast cancer gene therapy. *Cancer Res* 64: 5818-24
119. Kirman I, Maydelman A, Asi Z, Whelan RL. 2003. Effect of surgical trauma on epithelial cell adhesion molecule (GA-733) vaccine-induced tumor resistance. *Surg Endosc* 17: 505-9

120. Oberneder R, Weckermann D, Ebner B, Quadt C, Kirchinger P, Raum T, Locher M, Prang N, Baeuerle PA, Leo E. 2006. A phase I study with adecatumumab, a human antibody directed against epithelial cell adhesion molecule, in hormone refractory prostate cancer patients. *Eur J Cancer* 42: 2530-8
121. Seligson DB, Pantuck AJ, Liu X, Huang Y, Horvath S, Bui MH, Han KR, Correa AJ, Eeva M, Tze S, Belldegrun AS, Figlin RA. 2004. Epithelial cell adhesion molecule (KSA) expression: pathobiology and its role as an independent predictor of survival in renal cell carcinoma. *Clin Cancer Res* 10: 2659-69
122. Went PT, Lugli A, Meier S, Bundi M, Mirlacher M, Sauter G, Dirnhofer S. 2004. Frequent EpCam protein expression in human carcinomas. *Hum Pathol* 35: 122-8
123. Quezada SA, Peggs KS, Curran MA, Allison JP. 2006. CTLA4 blockade and GM-CSF combination immunotherapy alters the intratumor balance of effector and regulatory T cells. *J Clin Invest* 116: 1935-45
124. Clark CE, Hingorani SR, Mick R, Combs C, Tuveson DA, Vonderheide RH. 2007. Dynamics of the immune reaction to pancreatic cancer from inception to invasion. *Cancer Res* 67: 9518-27
125. Gabrilovich D. 2004. Mechanisms and functional significance of tumour-induced dendritic-cell defects. *Nat Rev Immunol* 4: 941-52
126. Brocker T, Riedinger M, Karjalainen K. 1997. Targeted expression of major histocompatibility complex (MHC) class II molecules demonstrates that dendritic cells can induce negative but not positive selection of thymocytes in vivo. *J Exp Med* 185: 541-50
127. Hon H, Oran A, Brocker T, Jacob J. 2005. B lymphocytes participate in cross-presentation of antigen following gene gun vaccination. *J Immunol* 174: 5233-42
128. Kim R, Emi M, Tanabe K. 2005. Cancer cell immune escape and tumor progression by exploitation of anti-inflammatory and pro-inflammatory responses. *Cancer Biol Ther* 4: 924-33
129. Stevenson FK, Ottensmeier CH, Johnson P, Zhu D, Buchan SL, McCann KJ, Roddick JS, King AT, McNicholl F, Savelyeva N, Rice J. 2004. DNA vaccines to attack cancer. *Proc Natl Acad Sci U S A* 101 Suppl 2: 14646-52
130. Scheerlinck JY. 2001. Genetic adjuvants for DNA vaccines. *Vaccine* 19: 2647-56
131. Beum PV, Lindorfer MA, Beurskens F, Stukenberg PT, Lokhorst HM, Pawluczkowycz AW, Parren PW, van de Winkel JG, Taylor RP. 2008. Complement activation on B lymphocytes opsonized with rituximab or ofatumumab produces substantial changes in membrane structure preceding cell lysis. *J Immunol* 181: 822-32
132. Silverman GJ, Boyle DL. 2008. Understanding the mechanistic basis in rheumatoid arthritis for clinical response to anti-CD20 therapy: the B-cell roadblock hypothesis. *Immunol Rev* 223: 175-85
133. Pardoll DM. 1998. Cancer vaccines. *Nat Med* 4: 525-31
134. Chlichlia KS, V; Sandaltzopoulos, R. 2005. Cancer Immunotherapy: Battling Tumors with Gene Vaccines. *Current Medicinal Chemistry - Anti-Inflammatory & Anti-Allergy Agents* 4: 353-65
135. Pfutzner W, Vogel JC. 2000. Advances in skin gene therapy. *Expert Opin Investig Drugs* 9: 2069-83
136. Holmgren J, Adamsson J, Anjuere F, Clemens J, Czerkinsky C, Eriksson K, Flach CF, George-Chandy A, Harandi AM, Lebens M, Lehner T, Lindblad M, Nygren E, Raghavan S, Sanchez J, Stanford M, Sun JB, Svennerholm AM, Tengvall S. 2005. Mucosal adjuvants and anti-infection and anti-immunopathology vaccines based on cholera toxin, cholera toxin B subunit and CpG DNA. *Immunol Lett* 97: 181-8
137. Hirao LA, Wu L, Khan AS, Satishchandran A, Draghia-Akli R, Weiner DB. 2008. Intradermal/subcutaneous immunization by electroporation improves plasmid vaccine delivery and potency in pigs and rhesus macaques. *Vaccine* 26: 440-8
138. Capone S, Zampaglione I, Vitelli A, Pezzanera M, Kierstead L, Burns J, Ruggeri L,

Arcuri M, Cappelletti M, Meola A, Ercole BB, Tafi R, Santini C, Luzzago A, Fu TM, Colloca S, Ciliberto G, Cortese R, Nicosia A, Fattori E, Folgori A. 2006. Modulation of the immune response induced by gene electrotransfer of a hepatitis C virus DNA vaccine in nonhuman primates. *J Immunol* 177: 7462-71

139. Verstrepen BE, Bins AD, Rollier CS, Mooij P, Koopman G, Sheppard NC, Sattentau Q, Wagner R, Wolf H, Schumacher TN, Heeney JL, Haanen JB. 2008. Improved HIV-1 specific T-cell responses by short-interval DNA tattooing as compared to intramuscular immunization in non-human primates. *Vaccine* 26: 3346-51
140. Pokorna D, Rubio I, Muller M. 2008. DNA-vaccination via tattooing induces stronger humoral and cellular immune responses than intramuscular delivery supported by molecular adjuvants. *Genet Vaccines Ther* 6: 4
141. Kim D, Hoory T, Monie A, Ting JP, Hung CF, Wu TC. 2008. Enhancement of DNA vaccine potency through coadministration of CIITA DNA with DNA vaccines via gene gun. *J Immunol* 180: 7019-27
142. Bins AD, Jorritsma A, Wolkers MC, Hung CF, Wu TC, Schumacher TN, Haanen JB. 2005. A rapid and potent DNA vaccination strategy defined by in vivo monitoring of antigen expression. *Nat Med* 11: 899-904
143. Jeon YH, Choi Y, Kang JH, Chung JK, Lee YJ, Kim CW, Jeong JM, Lee DS, Lee MC. 2006. In vivo monitoring of DNA vaccine gene expression using firefly luciferase as a naked DNA. *Vaccine* 24: 3057-62
144. Lorence RM, Roberts MS, O'Neil JD, Groene WS, Miller JA, Mueller SN, Bamat MK. 2007. Phase 1 clinical experience using intravenous administration of PV701, an oncolytic Newcastle disease virus. *Curr Cancer Drug Targets* 7: 157-67
145. Freeman AI, Zakay-Rones Z, Gomori JM, Linetsky E, Rasooly L, Greenbaum E, Rozenman-Yair S, Panet A, Libson E, Irving CS, Galun E, Siegal T. 2006. Phase I/II trial of intravenous NDV-HUJ oncolytic virus in recurrent glioblastoma multiforme. *Mol Ther* 13: 221-8
146. Csatary LK, Gosztonyi G, Szeberenyi J, Fabian Z, Liszka V, Bodey B, Csatary CM. 2004. MTH-68/H oncolytic viral treatment in human high-grade gliomas. *J Neurooncol* 67: 83-93
147. Fabian Z, Csatary CM, Szeberenyi J, Csatary LK. 2007. p53-independent endoplasmic reticulum stress-mediated cytotoxicity of a Newcastle disease virus strain in tumor cell lines. *J Virol* 81: 2817-30
148. Fiola C, Peeters B, Fournier P, Arnold A, Bucur M, Schirrmacher V. 2006. Tumor selective replication of Newcastle disease virus: association with defects of tumor cells in antiviral defence. *Int J Cancer* 119: 328-38
149. Ljunggren HG, Malmberg KJ. 2007. Prospects for the use of NK cells in immunotherapy of human cancer. *Nat Rev Immunol* 7: 329-39
150. Robbins SH, Bessou G, Cornillon A, Zucchini N, Rupp B, Ruzsics Z, Sacher T, Tomasello E, Vivier E, Koszinowski UH, Dalod M. 2007. Natural killer cells promote early CD8 T cell responses against cytomegalovirus. *PLoS Pathog* 3: e123
151. Vivier E, Tomasello E, Baratin M, Walzer T, Ugolini S. 2008. Functions of natural killer cells. *Nat Immunol* 9: 503-10
152. Strowig T, Brilot F, Munz C. 2008. Noncytotoxic functions of NK cells: direct pathogen restriction and assistance to adaptive immunity. *J Immunol* 180: 7785-91
153. Mailliard RB, Son YI, Redlinger R, Coates PT, Giermasz A, Morel PA, Storkus WJ, Kalinski P. 2003. Dendritic cells mediate NK cell help for Th1 and CTL responses: two-signal requirement for the induction of NK cell helper function. *J Immunol* 171: 2366-73
154. Meller B, Frohn C, Brand JM, Lauer I, Schelper LF, von Hof K, Kirchner H, Richter E, Baehre M. 2004. Monitoring of a new approach of immunotherapy with allogenic (111)In-labelled NK cells in patients with renal cell carcinoma. *Eur J Nucl Med Mol Imaging* 31: 403-7
155. Morales A, Pang AS. 1986. Experimental immunotherapy with NK-like cells. A preliminary report. *Cancer Immunol Immunother* 21: 156-60

156. Nakazawa M. 1985. [Immunological response in cryo-immunotherapy of malignant tumors--the mechanism of the rise and fall of NK activity and cytotoxic T lymphocytes after inoculation of Cryo-destructed Meth A cells]. *Osaka Daigaku Shigaku Zasshi* 30: 60-86
157. Nielsen B, Hokland P, Ellegaard J, Hasselbalch H, Hokland M. 1989. Whole blood assay for NK activity in splenectomized and non-splenectomized hairy cell leukemia patients during IFN-alpha-2b treatment. *Leuk Res* 13: 451-6
158. Ogmundsdottir HM, Thorsteinsson L, Sigfusson A, Sveinsdottir S, Bjornsson S, Eyjolfsson G, Johannesson GM, Jensson O. 1992. Natural killer cell function and malignant cell phenotype in hairy cell leukaemia. *Apmis* 100: 10-20
159. Orleans-Lindsay JK, Barber LD, Prentice HG, Lowdell MW. 2001. Acute myeloid leukaemia cells secrete a soluble factor that inhibits T and NK cell proliferation but not cytolytic function--implications for the adoptive immunotherapy of leukaemia. *Clin Exp Immunol* 126: 403-11
160. Orraca ZM, Rios-Olivares E, Carrasco-Canales JA, Aquino E, Marchand AM, Colon JI. 1989. Characterization of the antitumor activity of a polyantigenic immunomodulator (PAI): II--Involvement of NK cells and adoptive immunotherapy. *Bol Asoc Med P R* 81: 254-8
161. Reschner A, Hubert P, Delvenne P, Boniver J, Jacobs N. 2008. Innate lymphocyte and dendritic cell cross-talk: a key factor in the regulation of the immune response. *Clin Exp Immunol* 152: 219-26
162. Gronevik E, von Steyern FV, Kalhovde JM, Tjelle TE, Mathiesen I. 2005. Gene expression and immune response kinetics using electroporation-mediated DNA delivery to muscle. *J Gene Med* 7: 218-27
163. Rabussay D. 2008. Applicator and electrode design for in vivo DNA delivery by electroporation. *Methods Mol Biol* 423: 35-59
164. Tjelle TE, Rabussay D, Ottensmeier C, Mathiesen I, Kjeken R. 2008. Taking electroporation-based delivery of DNA vaccination into humans: a generic clinical protocol. *Methods Mol Biol* 423: 497-507
165. Tjelle TE, Salte R, Mathiesen I, Kjeken R. 2006. A novel electroporation device for gene delivery in large animals and humans. *Vaccine* 24: 4667-70
166. Banchereau J, Steinman RM. 1998. Dendritic cells and the control of immunity. *Nature* 392: 245-52
167. Garmory HS, Brown KA, Titball RW. 2003. DNA vaccines: improving expression of antigens. *Genet Vaccines Ther* 1: 2
168. Tuting T, Wilson CC, Martin DM, Baar J, DeLeo A, Lotze MT, Storkus WJ. 1998. DNA vaccines targeting dendritic cells for the immunotherapy of cancer. *Adv Exp Med Biol* 451: 295-304
169. Tuting T, DeLeo AB, Lotze MT, Storkus WJ. 1997. Genetically modified bone marrow-derived dendritic cells expressing tumor-associated viral or "self" antigens induce antitumor immunity in vivo. *Eur J Immunol* 27: 2702-7
170. Timares L, Takashima A, Johnston SA. 1998. Quantitative analysis of the immunopotency of genetically transfected dendritic cells. *Proc Natl Acad Sci U S A* 95: 13147-52
171. Steitz J, Bruck J, Knop J, Tuting T. 2001. Adenovirus-transduced dendritic cells stimulate cellular immunity to melanoma via a CD4(+) T cell-dependent mechanism. *Gene Ther* 8: 1255-63
172. Ross R, Sudowe S, Beisner J, Ross XL, Ludwig-Portugall I, Steitz J, Tuting T, Knop J, Reske-Kunz AB. 2003. Transcriptional targeting of dendritic cells for gene therapy using the promoter of the cytoskeletal protein fascin. *Gene Ther* 10: 1035-40
173. Morita A, Ariizumi K, Ritter R, 3rd, Jester JV, Kumamoto T, Johnston SA, Takashima A. 2001. Development of a Langerhans cell-targeted gene therapy format using a dendritic cell-specific promoter. *Gene Ther* 8: 1729-37
174. Nchinda G, Kuroiwa J, Oks M, Trumpfheller C, Park CG, Huang Y, Hannaman D, Schlesinger SJ, Mizenina O, Nussenzweig MC, Uberla K, Steinman RM. 2008. The

efficacy of DNA vaccination is enhanced in mice by targeting the encoded protein to dendritic cells. *J Clin Invest* 118: 1427-36

175. Gruber A, Chalmers AS, Rasmussen RA, Ong H, Popov S, Andersen J, Hu SL, Ruprecht RM. 2007. Dendritic cell-based vaccine strategy against human immunodeficiency virus clade C: skewing the immune response toward a helper T cell type 2 profile. *Viral Immunol* 20: 160-9
176. Lauterbach H, Gruber A, Ried C, Cheminay C, Brocker T. 2006. Insufficient APC capacities of dendritic cells in gene gun-mediated DNA vaccination. *J Immunol* 176: 4600-7
177. Lopez-Cabrera M, Nueda A, Vara A, Garcia-Aguilar J, Tugores A, Corbi AL. 1993. Characterization of the p150,95 leukocyte integrin alpha subunit (CD11c) gene promoter. Identification of cis-acting elements. *J Biol Chem* 268: 1187-93
178. Wen H, Schaller MA, Dou Y, Hogaboam CM, Kunkel SL. 2008. Dendritic cells at the interface of innate and acquired immunity: the role for epigenetic changes. *J Leukoc Biol* 83: 439-46
179. Kwissa M, Amara RR, Robinson HL, Moss B, Alkan S, Jabbar A, Villinger F, Pulendran B. 2007. Adjuvanting a DNA vaccine with a TLR9 ligand plus Flt3 ligand results in enhanced cellular immunity against the simian immunodeficiency virus. *J Exp Med* 204: 2733-46
180. Enk AH. 2005. Dendritic cells in tolerance induction. *Immunol Lett* 99: 8-11
181. Enk AH. 2006. DCs and cytokines cooperate for the induction of tregs. *Ernst Schering Res Found Workshop*: 97-106
182. Frumento G, Piazza T, Di Carlo E, Ferrini S. 2006. Targeting tumor-related immunosuppression for cancer immunotherapy. *Endocr Metab Immune Disord Drug Targets* 6: 233-7
183. Gajewski TF, Meng Y, Harlin H. 2006. Immune suppression in the tumor microenvironment. *J Immunother* 29: 233-40
184. Smyth MJ, Godfrey DI. 2000. NKT cells and tumor immunity--a double-edged sword. *Nat Immunol* 1: 459-60
185. Smyth MJ, Thia KY, Street SE, Cretney E, Trapani JA, Taniguchi M, Kawano T, Pelikan SB, Crowe NY, Godfrey DI. 2000. Differential tumor surveillance by natural killer (NK) and NKT cells. *J Exp Med* 191: 661-8
186. Karre K, Ljunggren HG, Piontek G, Kiessling R. 1986. Selective rejection of H-2-deficient lymphoma variants suggests alternative immune defence strategy. *Nature* 319: 675-8
187. Movahedi K, Guilliams M, Van den Bossche J, Van den Bergh R, Gysemans C, Beschin A, De Baetselier P, Van Ginderachter JA. 2008. Identification of discrete tumor-induced myeloid-derived suppressor cell subpopulations with distinct T cell-suppressive activity. *Blood* 111: 4233-44
188. Klinman DM, Takeno M, Ichino M, Gu M, Yamshchikov G, Mor G, Conover J. 1997. DNA vaccines: safety and efficacy issues. *Springer Semin Immunopathol* 19: 245-56
189. Martin T, Parker SE, Hedstrom R, Le T, Hoffman SL, Norman J, Hobart P, Lew D. 1999. Plasmid DNA malaria vaccine: the potential for genomic integration after intramuscular injection. *Hum Gene Ther* 10: 759-68
190. Mor G, Singla M, Steinberg AD, Hoffman SL, Okuda K, Klinman DM. 1997. Do DNA vaccines induce autoimmune disease? *Hum Gene Ther* 8: 293-300

7 Appendix

7.1 Titration of hygromycin sensitivity of different cell lines

To generate stable gene expression in mammary cell lines, we used pcDNA3-hygro vector encoding interested genes. Cells with the gene expression can be selected by hygromycin. We first titrated hygromycin sensitivity of different cell lines. **Table 7.1** shows percentage of cells resistant to hygromycin with different concentration. Concentration of hygromycin for selection of stable transfection for different cell lines is outlined in **table 7.2**.

Table 7.1 Hygromycin resistance titration (% of resistant cells)

Cell line	Time (day)	Hygromycin (μg/mL)			
		800	400	200	0
BHK21	**2**	<5%	30%	80%	100%
	4	0	0	30%	100%
	6	0	0	0	100%
	7	0	0	0	100%
DE	**2**	<5%	30%	50%	100%
	4	0	0	0	100%
	6	0	0	0	100%
	7	0	0	0	100%
ESb	**2**	50%	70%	80%	100%
	4	50%	60%	80%	100%
	6	10%	50%	70%	100%
	7	0	20%	50%	100%

Table 7.2 Hygromycin for stable transfection (conc.)

Cell line	Cell origin	Hygromycin (μg/mL)
BHK21	Fibroblast/Hamster kidney	100-200
DE	Epithelial cells/Mouse mammary carcinoma	100-150
ESb	Lymphcytes/Mouse lymphoma	600-800

7.2 Dendritic cell depletion from ear in CD11c-DTR-tg mice

Diphtheria toxin-based CD11c-DTR transgenic mice were used to deplete DCs *in vivo*. Those mice carry a transgene encoding a simian DTR-GFP fusion protein under control of the murine CD11c promoter (Figure 7.1a) (Jung 2002). By systemic DT injection (ip), $CD11c^+$ DCs could be depleted in spleen, lymph node, lung, liver and lamina propria tissues (as described by The Jackson Laboratory). We depleted DCs in the ear skin by applying DT either by ip injection (systemically) or ie injection (locally) to these mice. $CD11c^+$ cells isolated from ear skin (both epidermis and dermis) of the CD11c-DTR-tg mice express low level of GFP as reported (11). By DT ip administration, 80% DCs were depleted in the ear after 24 h, compared to 90% depletion by DT ie local injection (Figure 7.1b). No influences of $CD11c^+$ DCs in the ear were induced by DT application in wild-type C57BL/6 mice. These results showed the possibility to deplete DCs in the ear skin in CD11c-DTR-tg mice.

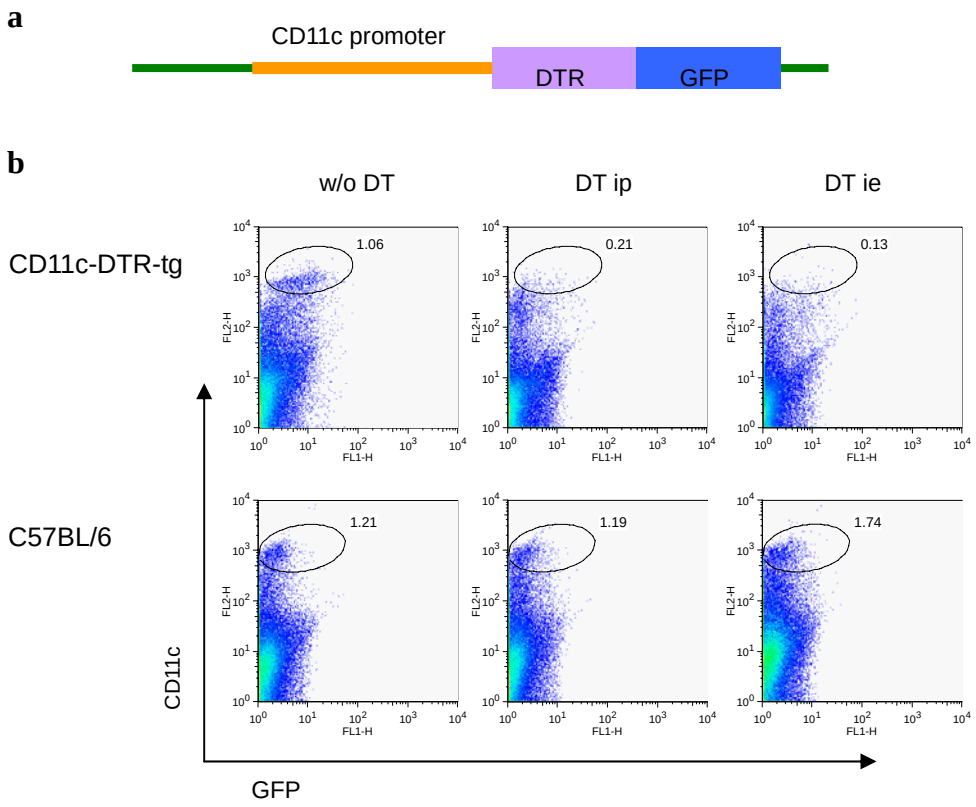

Figure 7.1 Depletion of DCs in the ear skin.

a. Schematic representation of the DTR/GFP transgene in CD11c-DTR-tg mice. b. FACS analysis of CD11c+GFP+ DCs in the ear skin. Single cell suspension was prepared from the epidermis and dermis of ear skin 24 h after DT injection in CD11c-DTR-tg mice and C57BL/6 mice. Cells were analysis by FACS after staining with CD11c-PE antibody.

7.3 Comparison of gene expression by ie and im DNA immunization

Intra-pinna (ie) DNA immunization was also compared to intramuscular (im) DNA injection for gene expression. *In vivo* luciferase expression revealed that earlier and stronger antigen expression was detected in the ear by naked DNA injection (Figure 7.2a). No visible expression was found in the muscle at 4 h by naked DNA injection (left ear and quadriceps). This pattern lasted for about 2 weeks, and then antigen expression dropped in the ear while maintained the same level in the muscle till 1 month. After 2 month, luciferase expression decreased about 10 times in both sides. However, with the help of EP (right side), im DNA injection benefited more than ie injection for antigen expression. From 24 h till 56 d, antigen expression maintained a stable high level (Figure 7.2b). These results showed that ie naked DNA injection could induce better antigen expression than im injection; while EP improved antigen expression in the muscle much more than that in the ear. Im DNA injection is particularly superior for long-term antigen expression.

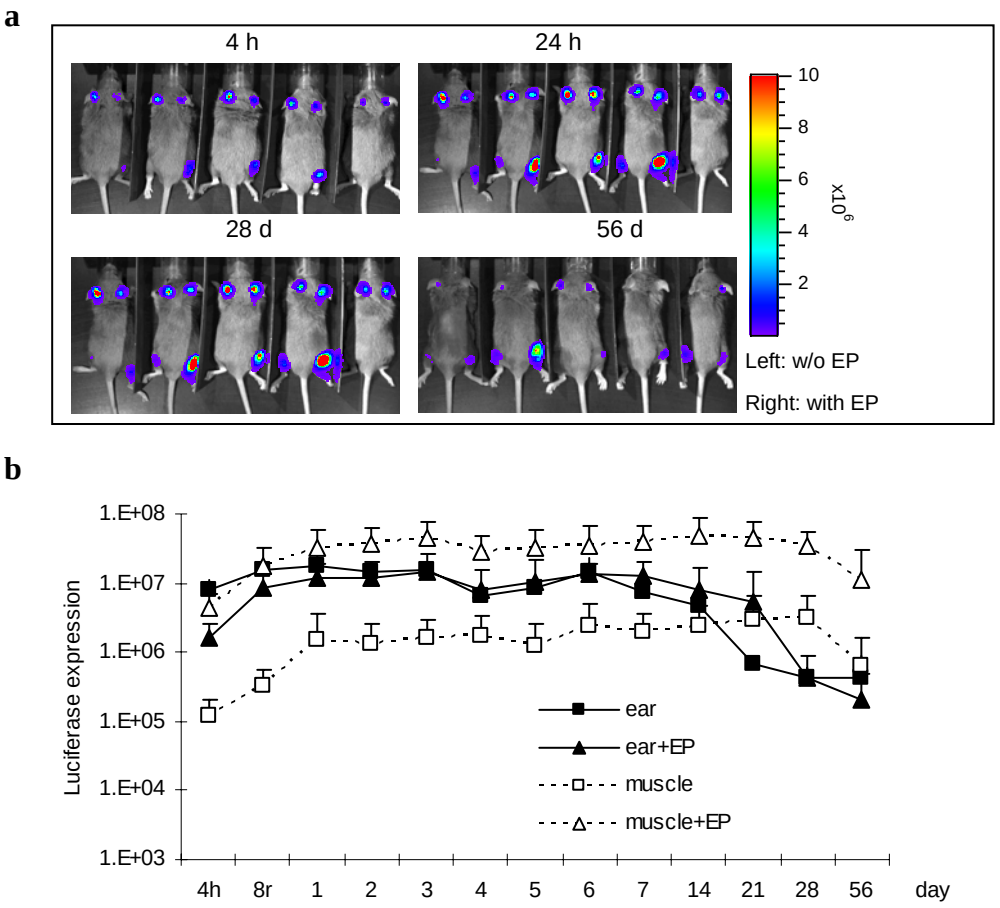

Figure 7.2 CD11cS-luc expression in skin compared to muscle.

CMV-luc plasmid (25μg/50μL) was injected ie and im without (left side) or with electroporation (right side) to the ear and muscle (DBA/2 mice, n=5). Mice were imaged for firefly luciferase expression at different time points with 1 min exposure time. Experiments were repeated 3 times with similar results.

7.4 Comparison of activities of tissue specific promoters

Tissue specific promoters are helpful tools for gene therapy by which gene expression can be restricted to specific tissues. Besides CD11c promoters, we also analyzed murine fascine promoter (specific for mature DCs) and keratin 14 promoter (specific for keratinocytes).

7.4.1 *In vitro* activity

DNA constructs encoding firefly luciferase gene under control of fascin or keratin 14 promoters were transfected to B16 (fascin positive cell line) and HaCaT (keratin positive cell line, human keratinocytes), compared to CMV and CD11c promoters. As it is indicated in Figure 7.3, fascin promoter induced better luciferase expression in B16 cells than other promoters (similar with CD11cS promoter), while keratin 14 promoter induced better luciferase expression in HaCaT cells.

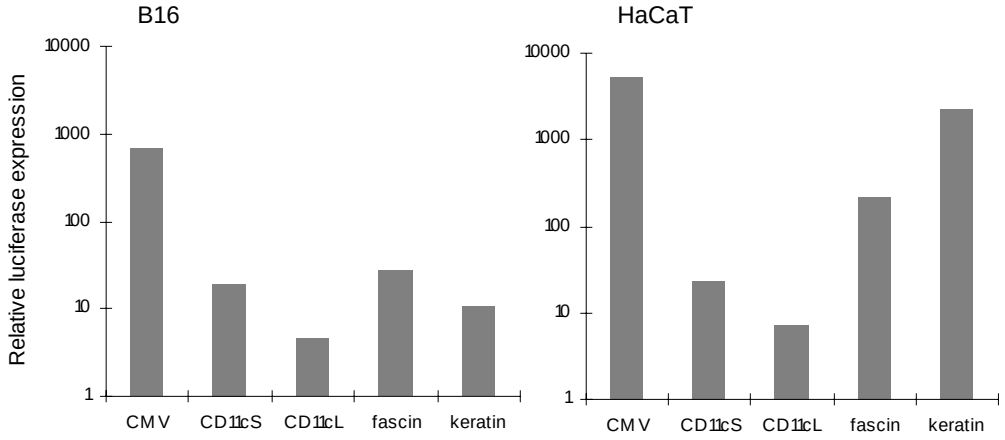

Figure 7.3 *In vitro* luciferase expression regulated by different promoters.

Cells were transfected with DNA vectors (encoding firefly luciferase) under control of different promoters, as well as pGL3-Basic (negative control). A vector CMV-Ruc encoding renilla luciferase was used for co-transfection (1:25) to control the transfection efficiency. Promoter activity is expressed relative to the luciferase activity produced by the promoterless plasmid, pGL3-Basic, after correction for transfection efficiency by Renilla luciferase. Transfections were made by triplicate, and repeated for 3 times.

7.4.2 *In vivo* activity

Fascin and keratin 14 promoter induced cell specific antigen expression *in vitro* (Figure 7.3). To further analyze their activity *in vivo*, we injected those DNA constructs into the mice ie and id. EP was applied (the right side) to improve antigen expression. All the tissue/cell specific promoters are much weaker than CMV promoter. Between these tissue specific promoters, CD11cS induced earliest and strongest antigen expression. This indicates CD11cS might be also superior to other promoters for cancer DNA vaccine development which might need superior antigen expression.

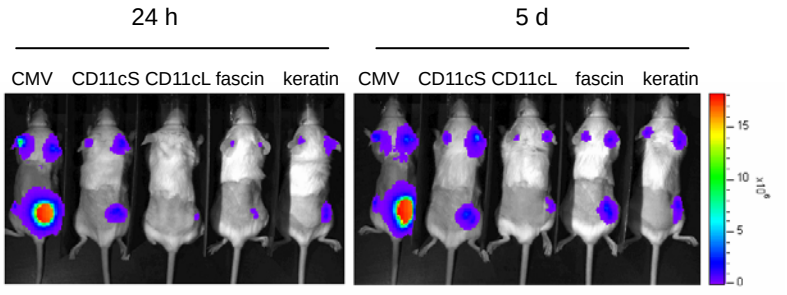

Figure 7.4 *In vivo* luciferase expression regulated by different promoters in ear and flank skin.

DNA plasmid (25μg/50μL) encoding firefly luciferase gene under control of different promoters was injected ie and id without (left side) or with electroporation (right side) to the ear and flank skin (Balb/c mice). Mice were imaged for firefly luciferase expression at different time points with 1 min exposure time. Experiments were repeated 3 times with similar results.